SPIS TREŚCI

Nauka i Technika

NECHVAL K.N., NECHVAL N.A., BERZINS G., PURGAILIS M.: **Probabilistic assessment of the fatigue reliability**; EiN 3/2007, s. 3-6.
The prediction of stochastic crack growth accumulation is important for the reliability analysis of structures as well as the scheduling of inspection and repair/replacement maintenance. Because the initial crack size, the stress, the material properties and other factors that may affect the fatigue crack growth are statistically distributed, the first-order second-moment technique is often adopted to calculate the fatigue reliability of industrial structures. In this paper, a second-order third-moment technique is presented and a three-parameter Weibull distribution is adopted to reflect the influences of skewness of the probability density function. The second-order third-moment technique that has more characteristics of those random variables that are concerned in reliability analysis is obviously more accurate than the traditional first-order second-moment technique.

CZAPLICKI J.M.: **On the system: truck – workshop in the queue theory terms**; EiN 3/2007, s. 7-10.
There are a lot of technical systems in engineering world that apply tire haulage as significant component of their structure. It is quite obvious that in order to maintain a haulage fleet in proper conditions the system must possess a preservative subsystem to meet planned maintenance and repair requirements. A suitable organization of this subsystem determines the number of transport units accomplishing the given transportation task.
In the paper the problem of proper mathematical description of the system: truck – workshop is being considered employing models taken from the queue theory. The main characteristic that is obtained is the probability distribution of a number of failed trucks as the function of several parameters such as the fleet size and possession of a reserve, reliability indices of machines and parameters characterizing intensity of realized repairs and number of repair stands.

RADKOWSKI S.: **Use of vibroacoustical signal in detecting early stages of failures**; EiN 3/2007, s. 11-18.
An understanding of vibroacoustic signal is required for the robust and more effective detection of early stage failure. In the paper the possibility and method of time varying vibration decomposition are discussed. It is shown that analysing the coupling between the structure's components changes from linear to nonlinear or to other kind of nonlinearity together with intermodulation phenomena can be used as measure in structural health monitoring. In addition on an analytical connection is investigated between the tracking method and the physics of the kinematic contact process based on the idea of higher-order spectra analysis, bispectral analysis specially.

KALINCSÁK Z., TAKÁCS J., SÓLYOMVÁRI K., GÖNDÖCS B., NAGY G.Cs.: **Local laser marking – new technology in the identification of steel parts**; EiN 3/2007, s. 19-22.
The importance of identification of machines in the field of maintenance becomes more and more significant. In the field of mechanical maintenance or especially in large-scale production serious difficulties cause to identify various metal parts which have similar form and/or size during technological process. The paper based and printed barcode seemed a safe resolution to this purpose. Unfortunately during the repairing or renewal process the paper based barcodes of steel parts very often were destroyed or damaged, the currently applied paper based and painted codes can cause data losses. This is the fact which indicated the research of steel marking system. In this type of marking the material contains the signs. Other advantage of this system is the readability beneath from painted layer.

WERBINSKA S.: **The availability model of logistic support system with time redundancy**; EiN 3/2007, s. 23-29.
Any operational system, in order to successfully accomplish its intended mission, must rely on logistic support that will be available when required. According to this, unlike traditional approaches to availability development, the paper indicates on the problem of integration between two systems – operational and its supporting system into one 'system of systems'. Moreover, in many systems undesired event (system failure) occurs later than components failure, and only if repair is not completed within a defined period of time. The time dependency is a convenient approach for definition of interactions between the above systems. Thus, the paper considers the time dependent system of systems where the system total task must be executed during constrained time resource. For the developed model, there are derived general equations for the evaluation of system of systems availability function and steady-state availability ratio. The model solution is obtained based on analytical method. Furthermore, the mathematical expressions for the mean availability ratio are derived when the all probability density functions are to be exponential.

WĘGRZYN T., HADRYŚ D., MIROS M.: **Optimization of operational properties of steel welded structures**; EiN 3/2007, s. 30-33.
Safety and exploitation conditions of steel welded structure depend on many factors. The main role of that conditions is connected with materials, welding technology, state of stress and temperature. Because of that very important is good selection of steel and welding method for proper steel structure. For responsible steel structure are used low carbon and low alloy steel, very often with small amount of carbon and the amount of alloy elements such as Ni, Mn, Mo, Cr and V in low alloy steel and their welds. In the terms of the kind of steel it is used a proper welding method and adequate filler materials. In the present paper it was tested and optimized the chemical composition of metal weld deposit on the operational properties of steel welded structures.

GRENČÍK J., LEGÁT V.: **Maintenance audit and benchmarking - search for evaluation criteria on global scale**; EiN 3/2007, s. 34-39.
Maintenance strategy and concept of management are very important for proper execution of maintenance of physical assets in different organizations. Authors present main objectives for maintenance and define maintenance strategy and concept. The key benefit of the paper is a methodology of strategy maintenance development. The methodology is based on input data definition and on proposed procedure of data processing. Proper developed maintenance strategy is a presumption of excellent maintenance effectiveness. The paper presents use of audit and benchmarking methods for development the maintenance strategies.

RUSIN A., WOJACZEK A.: **Selection of maintenance range for power machines and equipment in consideration of risk**; EiN 3/2007, s. 40-43.
The operational safety of power units depends upon many factors, including the methods of their operation, their working conditions, age, regularity and range of maintenance. The scope of the paper is the analysis of maintenance options for power machines and equipment. The assumed criterion for the selection of the range of repair works is the level of technical risk posed by a given facility below the accepted allowable level. Detailed discussion is focused on the water and steam system of the boiler. The influence of the maintenance on the probability of failure of certain components is described on the grounds of Kijima's model. For the assumed maintenance periods minimal sets of equipment were determined, the repair of which should secure the operation of the water-steam system for a successive interval with the risk level lower than the allowable one.

KOSMAN G., ŁUKOWICZ H., NAWRAT K., KOSMAN W.: **Assessment of the effects of the operation of power unitson sliding-pressure**; EiN 3/2007, s. 44-48.
In the article the results of an analysis of the performance of a unit operated with incomplete sliding-pressure and with full sliding-pressure adjusted each time to a specific load are shown. The article also presents the gain obtained from the use of full sliding-pressure resulting from the reduction of thermodynamic loss in the system and the reduction of the unit's own needs. The measurements of the condensation-heating turbo set operated with incomplete sliding-pressure was used in the analysis.

PIASECZNY L., ROGOWSKI K.: **Modelling the mechanical properties of screw propellers for selection of the technology of their repairs**; EiN 3/2007, s. 49-51.
During repairing screw propellers by welding and plastic deformation it is indispensable to know their material features and strength properties relative to the propeller part subject to repair. The authors have conducted statistical and empirical research aimed at determining those features depending on the propeller's chemical composition and blade thickness.

SKROBACKI Z.: **Selected methods for the estimation of the logistic function parameters**; EiN 3/2007, s. 52-56.
The logistic function can be employed as a model of record for a number of processes occurring in the management of technical objects and in logistics. The methods used for function parameter estimation include the analytical methods by Hotelling and Tinter and the numerical procedure of optimization in Excel with the Theil index as the optimization criterion.

ANTOSZEWSKI B.: **A non-conventional method for the improvement of the functional properties of sliding pairs**; EiN 3/2007, s. 57-61.
One of the ways to improve the functional properties of sliding friction pairs is to apply heterogeneous rubbing surfaces. Although this approach is still under investigation, heterogeneous surfaces are commonly employed in friction pairs under extreme lubrication conditions. The paper is concerned with the modeling of the friction process of flat textured sliding surfaces.

OLEJNIK K.: **The use of the additional lighting of the semi trailers for their safety exploatation**; EiN 3/2007, s. 62-64.
The report has pointed out the need to provide the truck driver with a semi trailer, the ability to see the contour of the semi trailer and road illumination in the insufficient lighting conditions. The need for equipping the vehicle with additional contour light and lamps illuminating the section of the road overrun by the semi trailer wheels has been assessed.

CHŁOPEK Z.: **Ecological aspects of using bioethanol fuel to power combustion engines**; EiN 3/2007, s. 65-68.
Out of many ways of lowering harmful effects of motorism on the environment, more and more attention is being paid to popularising the use of biofuels. Using bioethanol enables combustion engines to run on fuels containing high content of biocomponent. They are E95 fuels for the self ignition engines, E85 and in the foreseeable future, E100 for the spark ignition engines. Engines running on ethanol fuel are especially adapted for that, with spark ignition engines being multi–fuel ones able to run on a mixture of ethanol fuel with petrol in any proportion. The use of bioethanol fuels makes it possible to lower the emission of harmful pollutants, such as, nitrogen oxides , or – in case of self ignition engines – particulate matter, and also global reduction of carbon dioxide emission. Paper presents results of pollutants emission studies, from the engines powered by bioethanol fuel.

TOMASZEK H., ŻUREK J., JASZTAL M.: **A method of evaluating fatigue life of some selected structural components at a given spectrum of loads – an outline**; EiN 3/2007, s. 69-71.
The paper has been intended to introduce a method of evaluating the damage hazard and fatigue life of a structural component of an aircraft for: a given spectrum of loading the component; the Paris formula with the range of values of the material constant – differentiated.
Fatigue crack growth while the aircraft is operated shows random nature. To describe the dynamics of the crack propagation as a random process, a difference equation was used to arrive at a partial differential equation of the Fokker-Planck type. Having solved this equation enables the density function of growth in the crack length to be found. With the density function of the crack length and the boundary value thereof, probability of exceeding the boundary condition has been determined.

DROŻYNER P., MIKOŁAJCZAK P.: **Assessment of the effectiveness of machine and device operation**; EiN 3/2007, s. 72-75.
In effectively managed companies, the answer to the question of whether employees should be perceived as cost or as investment, is obvious. Investment should be made in human resources as this allows for reducing the cost of company's activities, increasing its effectiveness, efficiency, etc. A similar question can be put for machine operation, but here the answer is not so straightforward. The conflict between production managers and machine maintenance managers still exists; it is usually settled with the production side winning. This paper is an attempt to assess the effectiveness of machine operation and the effectiveness of the whole company based on an analysis of so called OEE (Overall Equipment Effectiveness) index, calculated from a timekeeping study of a big food producing company.

NECHVAL K.N., NECHVAL N.A., BERZINS G., PURGAILIS M.: **Planning inspections in service of fatigue-sensitive aircraft structure components for initial crack detection**; EiN 3/2007, s. 76-80.
Based on a random sample from the Weibull distribution with unknown shape and scale parameters, lower and upper prediction limits on a set of m future observations from the same distribution are constructed. The procedures, which arise from considering the distribution of future observations given the observed value of an ancillary statistic, do not require the construction of any tables, and are applicable whether the data are complete or Type II censored. The results have direct application in reliability theory, where the time until the first failure in a group of m items in service provides a measure regarding the operation of the items, as well as in service of fatigue-sensitive aircraft structures to construct strategies of inspections of these structures; examples of applications are given.

MARECKA–CHŁOPEK E., CHŁOPEK Z.: **Pollutants emission problems from the combustion engines of other applications than motor cars**; EiN 3/2007, s. 81-85.
Following motor car combustion engines, more and more significance is being attached to the pollutants emissions from the engines other than used in motor cars. The scale and variety of applications of such engines are considerable. At present these engines are less modern than those from motor cars, and requirements posed for them are not as restrictive with regards environmental protection, as in the case of motorism. This paper analyzes assessment procedures for the pollutant emissions from the combustion engines of other applications than in motor cars. Influence of the engine operating conditions on the pollutants emission has been evaluated.

Konstantin N. NECHVAL
Nicholas A. NECHVAL
Gundars BERZINS
Maris PURGAILIS

PROBABILISTIC ASSESSMENT OF THE FATIGUE RELIABILITY

The prediction of stochastic crack growth accumulation is important for the reliability analysis of structures as well as the scheduling of inspection and repair/replacement maintenance. Because the initial crack size, the stress, the material properties and other factors that may affect the fatigue crack growth are statistically distributed, the first-order second-moment technique is often adopted to calculate the fatigue reliability of industrial structures. In this paper, a second-order third-moment technique is presented and a three-parameter Weibull distribution is adopted to reflect the influences of skewness of the probability density function. The second-order third-moment technique that has more characteristics of those random variables that are concerned in reliability analysis is obviously more accurate than the traditional first-order second-moment technique.

Keywords*: Paris–Erdogan law, fatigue reliability, Weibull distribution.*

1. Introduction

The prediction of stochastic crack growth accumulation is important in the reliability and durability analyses of fatigue critical components. Stochastic crack growth analysis is useful for scheduling inspection and repair/replacement maintenance of structures. Various stochastic crack growth models have been proposed and studied in the literature for metallic materials and superalloys. No attempt is made herein to review the literature in this important subject area.

In practical applications of the stochastic crack growth analysis, either one of the following two distribution functions is needed: *the distribution of the crack size at any service time or the distribution of the service time to reach any given crack size*. Unfortunately, when the crack growth rate is modeled as a stochastic process, these two distribution functions are not amenable to analytical solutions, because the solution is equivalent to that of the first passage time problem. As a result, numerical simulation procedures have been used to obtain accurate results. The simulation approach is a very powerful tool, in particular with modem high-speed computers. However, in some situations, such as the preliminary analysis or design, simple approximate analytical solutions are very useful. The accuracy of such solutions depends on the sophistication of the approximation. Among attractive features of such an approximation are as follows: (i) it is mathematically simple to obtain the analytical solution for the distribution of the crack size at any service time; (ii) it is conservative in predicting the stochastic crack growth damage accumulation; (iii) it can account for the effects of variations in material crack growth resistance, usage severity and other random phenomena; and (iv) it can be implemented using a deterministic crack growth computer program.

The purpose of this paper is to present a more accurate stochastic crack growth analysis technique that is obviously more accurate than the traditional first-order second-moment technique [3] which only considers the means and variances of random variables. But probabilistic fracture mechanics problems generally involve non-normal distributions such as the lognormal, the exponential or the Weibull distribution. The skewness of a probability density function is sometimes used to measure the asymmetry of a probability density function about the mean. The second-order third-moment technique considers not only the mean and variance of a probability density function, but also the influence of skewness (which is represented by the third moment) of a probabilistic distribution. Because more characteristics of random variables are concerned with reliability analysis, the precision of reliability analysis can be increased. Particularly when random variables are not normally distributed. It is very important for industrial structures with high reliability requirement.

2. Paris-Erdogan crack growth law as a starting point

The analysis of fatigue crack growth is one of the most important tasks in the design and life prediction of aircraft fatigue-sensitive structures and their components. Failures of any high speed rotating components (jet engine rotors, centrifuges, high speed fans, etc.) can be very dangerous to surrounding equipment and personnel (see Fig. 1), and must always be avoided.

Several models based on the principles of fracture mechanics for the prediction of fatigue crack growth in components and structures under dynamic loads have been proposed, one of the best known is the Paris–Erdogan law [1],

$$\frac{da}{dN} = C(\Delta K)^{\upsilon} = C\vartheta^{\upsilon} S^{\upsilon} a^{\upsilon/2} \tag{1}$$

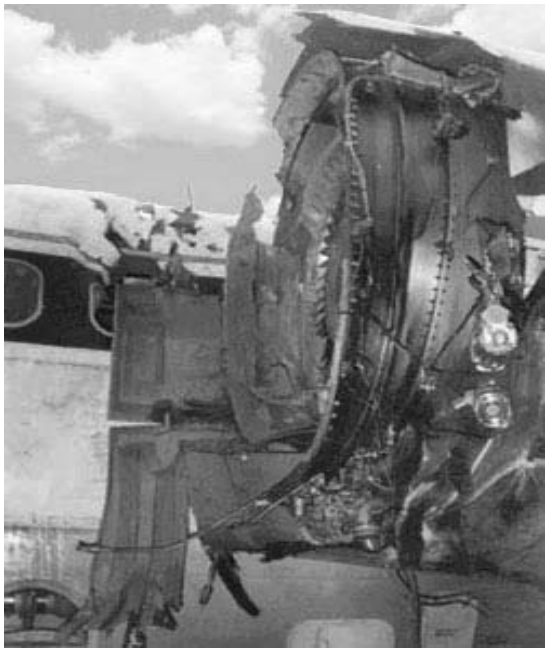

Fig. 1. Jet engine fan section failure

where da/dN is the crack growth rate, $\Delta K = \vartheta S\sqrt{a}$, the range of the stress intensity factor, S, the stress range, ϑ, a constant that depends on the type of load and geometry of the crack, C and υ are material constants.

If we assume all parameters in Eq. (1) are constants and deterministic, then the crack length, *a(N)*, after N cycles of stress can be obtained directly from Eq. (1). Integrating Eq. (1) from a deterministic initial crack size, *a(0)*, to crack size *a(N)*, one obtains:

$$a(N) = \left([a(0)]^{1-\upsilon/2} + (1-\upsilon/2) C \vartheta^{\upsilon} S^{\upsilon} N \right)^{1/(1-\upsilon/2)} \qquad \upsilon \neq 2 \tag{2}$$

$$a(N) = a(0) \exp\left(C \vartheta^2 S^2 N \right) \qquad (\upsilon \neq 2) \tag{3}$$

However, *a(0)*, C, ϑ and S may be all random variables with prescribed probability density functions in probabilistic fracture mechanics analysis. In practical applications of the stochastic crack growth analysis, either one of the following two distribution functions is needed: the distribution of the crack size at any given number of load cycles or the distribution of the number of load cycles to reach any given crack size.

3. Approximation technique

Let us assume that the random variable Y is the function of several mutually independent random variables, $X_1, X_2, \ldots, X_n$, as follows:

$$Y = f(X_1, X_2, \ldots, X_n) \tag{4}$$

where vector $\mu=(\mu_1, \mu_2, \ldots, \mu_n)$ denotes the mean of vector $X=(X_1, X_2, \ldots, X_n)$, namely μ_i is the mean of random variable X_i.

To obtain a better approximation, Y is expanded about μ to second order

$$Y = f(\mu_1, \mu_2, \ldots, \mu_n) + \sum_{i=1}^{n} \left(\frac{\partial Y}{\partial X_i} \right)_{\boldsymbol{\mu}} (X_i - \mu_i) + \frac{1}{2} \sum_{i,j=1}^{n} \left(\frac{\partial^2 Y}{\partial X_i \partial X_j} \right)_{\boldsymbol{\mu}} (X_i - \mu_i)(X_j - \mu_j) \tag{5}$$

Taking the first, the second and the third moment of both sides of Eq. (5) respectively, one obtains:

$$\mu_Y = f(\mu_1, \mu_2, \ldots, \mu_n) + \frac{1}{2} \sum_{i=1}^{n} \left(\frac{\partial^2 Y}{\partial X_i^2} \right)_{\boldsymbol{\mu}} \sigma_i^2 \tag{6}$$

$$\sigma_Y^2 = f^2(\mu_1, \mu_2, \ldots, \mu_n) + \sum_{i=1}^{n} \left[\left(\frac{\partial Y}{\partial X_i} \right)^2 + Y \frac{\partial^2 Y}{\partial X_i^2} \right]_{\boldsymbol{\mu}} \sigma_i^2 + \sum_{i=1}^{n} \left(\frac{\partial Y}{\partial X_i} \frac{\partial^2 Y}{\partial X_i^2} \right)_{\boldsymbol{\mu}} \gamma_i - \mu_Y^2 \tag{7}$$

$$\gamma_Y = f^3(\mu_1, \mu_2, \ldots, \mu_n) + \frac{3}{2} \sum_{i=1}^{n} \left[2Y \left(\frac{\partial Y}{\partial X_i} \right)^2 + Y^2 \frac{\partial^2 Y}{\partial X_i^2} \right]_{\boldsymbol{\mu}} \sigma_i^2 + \sum_{i=1}^{n} \left[\left(\frac{\partial Y}{\partial X_i} \right)^3 + 3Y \frac{\partial Y}{\partial X_i} \frac{\partial^2 Y}{\partial X_i^2} \right]_{\boldsymbol{\mu}} \gamma_i - \mu_Y^3 - 3\mu_Y \sigma_Y^2 \tag{8}$$

where μ_Y and σ_Y^2 are the mean and variance of the random variable Y, and γ_Y is the third moment of the random variable Y, which measures the amount of skewness of the distribution, σ_i^2 is the variance of the random variable X_i and γ_i is the third moment of the random variable X_i. When $\gamma > 0$, the distribution is skewed to the right such as the lognormal and exponential distributions. When $\gamma < 0$, the distribution is skewed to the left. When $\gamma = 0$, the distribution is a symmetrical distribution such as the normal distribution.

In this paper, Y may denote the crack length *a(N)*, and X_1, X_2, X_3 and X_4 may denote *a(0)*, C, ϑ and S, respectively.

4. Finding a probabilistic assessment of the fatigue reliability

The Weibull distribution is one of the most widely used distributions in reliability calculations. The great versatility of the Weibull distribution stems from the possibility to adjust to fit many cases where the hazard rate either increases or decreases. Further, of all statistical distributions that are available the Weibull distribution can be regarded as the most valuable because through the appropriate choice of parameters (the location parameter, the shape parameter and the scale parameter), a variety of shapes of probability density function can be modeled [2] which include the cases of $\gamma > 0$, $\gamma = 0$ and $\gamma < 0$.

The three-parameter Weibull distribution pertains to a continuous variable Y that may assume any value $\mu < y < \infty$, and is defined in terms of its density function or distribution function as follows:

$$f(y) = \frac{\delta}{\sigma} (y-\mu)^{\delta-1} \exp\left[-(y-\mu)^{\delta} / \sigma \right] \quad (y \geq \mu) \tag{9}$$

$$Pr\{Y \leq y^*\} = 1 - \exp\left[-(y^* - \mu)^{\delta} / \sigma \right] \tag{10}$$

where μ is the location parameter, δ and σ are the shape parameter and the scale parameter respectively; δ, σ and μ are related to the mean value μ_Y, the variance σ_Y^2 and third moment γ_Y through the following:

$$\mu_Y = \sigma^{1/\delta}\Gamma\left(1+\frac{1}{\delta}\right)+\mu \tag{11}$$

$$\sigma_Y^2 = \sigma^{2/\delta}\left[\Gamma\left(1+\frac{2}{\delta}\right)-\Gamma^2\left(1+\frac{1}{\delta}\right)\right] \tag{12}$$

$$\gamma_Y = \sigma^{3/\delta}\left[\Gamma\left(1+\frac{3}{\delta}\right)-3\Gamma\left(1+\frac{2}{\delta}\right)\Gamma\left(1+\frac{1}{\delta}\right)+2\Gamma^3\left(1+\frac{1}{\delta}\right)\right] \tag{13}$$

where $\Gamma(\cdot)$ is the gamma function.

If a variable X is normally distributed, the third moment of the random variable X is $\gamma_X = 0$ and its density function is:

$$f(x) = \frac{1}{\sigma\sqrt{2\pi}}exp\left[-(x-\mu)^2/(2\sigma^2)\right] \tag{14}$$

Then the mean and variance of the random variable X are given by:

$$\mu_X = \mu \tag{15}$$

$$\sigma_X^2 = \sigma^2 \tag{16}$$

If a variable X is exponentially distributed and its density function is given by:

$$f(x) = \sigma^{-1}exp\left[-(x-\mu)/\sigma\right] \tag{17}$$

then the mean, the variance and the third moment of the variable is given by:

$$\mu_X = \mu+\sigma \tag{18}$$

$$\sigma_X^2 = \sigma^2 \tag{19}$$

$$\gamma_X = 2\sigma^3 \tag{20}$$

If a variable X is lognormally distributed and its density function is given by

$$f(x) = \frac{1}{\sigma x\sqrt{2\pi}}exp\left[-(ln\,x-\mu)^2/(2\sigma^2)\right] \tag{21}$$

then the mean, the variance and the third moment of the variable is given by:

$$\mu_X = exp(\mu+0.5\sigma^2) \tag{22}$$

$$\sigma_X^2 = exp(2\mu+\sigma^2)\left[exp(\sigma^2)-1\right] \tag{23}$$

$$\gamma_X = exp(3\mu+4.5\sigma^2)-3exp(3\mu+2.5\sigma^2)+2exp(3\mu+1.5\sigma^2) \tag{24}$$

If a variable X follows the Weibull distribution and its density function is defined by Eq. (9), then the mean, the variance and the third moment of the variable X is calculated from Eqs. (11)–(13).

Thus, procedure for finding a probabilistic assessment of the fatigue reliability can be summarized as follows. If, a(0), C, ϑ and S in Eqs. (2) and (3) may be all random variables with prescribed probability density functions such as the normal, the lognormal, the exponential and the Weibull distributions, in which the means, the variances and the third moments can be calculated from Eqs. (14)–(24) (the Weibull distribution calculated from Eqs. (11)–(13)). Then the mean, the variance and the third moment of the crack length *a(N)* at any given N cycles of stress can be calculated from Eqs. (6)–(8). The parameters δ, σ and μ of the Weibull distribution are solved from Eqs. (11)–(13) and the reliability of the cracked structure after N cycles of stress is obtained from Eq. (10).

5. Numerical example

Let us assume that a cracked structure with the fatigue crack growth rates $da/dN = 5\times10^{-5}$ mm/cycle is researched. The probability density function of the initial crack size *a(0)* is exponential distribution function,

$$f(x)=exp[-(x-2)] \tag{25}$$

The critical crack length is $a^{\bullet}$=10 mm. The reliability of the cracked structure after N=10^5 cycles of stress is obtained as follows:

(i) Suppose that the constant of the Paris–Erdogan law is υ=0 and only *a(0)* is random variable. From Eq. (2), one can obtain the crack size after N=10^5 cycles of stress:

$$a(N) = a(0)+5\times10^{-5}N = a(0)+5 \text{ (mm)} \tag{26}$$

(ii) From Eqs. (17)–(20), the mean, the variance and the third moment of the initial crack size *a(0)* is calculated in which σ=1, μ=2 mm. Then from Eqs. (6)–(8), one can obtain the mean, the variance and the third moment of the crack size a after N=10^5 cycles of stress as follows:

$$\mu_{a(N)} = 8.0,\quad \sigma_{a(N)}^2 = 1.0,\quad \gamma_{a(N)} = 2.0 \tag{27}$$

(iii) Substituting $\mu_{a(N)}$, $\sigma_{a(N)}^2$, and $\gamma_{a(N)}$ into Eq. (11), Eq. (12) and Eq. (13), respectively, these simultaneous equations for δ, σ and μ can be solved to obtain three parameters of the Weibull distribution as follows:

$$\delta=1.0,\quad \sigma=1.0,\quad \mu=7.0. \tag{28}$$

(iv) As the density distribution of the crack length *a(N)* is defined as Eq. (9), the reliability of the cracked structure after N=10^5 cycles of stress is calculated by Eq. (10) as follows:

$$Pr\{a(N)\le a^{\bullet}\} = 1-exp\left[-(a^{\bullet}-\mu)^{\delta}/\sigma\right] = 1-exp[-(10-7)] = 0.95. \tag{29}$$

Let us assume that we use the above technique to calculate the reliability of the cracked structure, where only the mean $\mu_{a(N)} = 8.0$ and the variance $\sigma_{a(N)}^2 = 1.0$ of the crack size *a(N)* are considered. The distribution of the crack size *a(N)* is assumed to be a normal distribution. One can obtain:

$$Pr\{a(N)\le a^{\bullet}\} = \Phi\left(\frac{10-8}{1}\right) = \Phi(2) = 0.9772 \tag{30}$$

where $\Phi(\cdot)$ is the standard normal distribution function.

Actually the problem discussed has an analytical solution, which is given as follows:

$$Pr\{a(N) \le a^{\bullet}\} = Pr\{a(0) + 5 \le 10\} = Pr\{a(0) \le 5\} = \\ = \int_{2.}^{5.} exp\left[-(x-2)\right]dx = 1 - exp\left[-(5-2)\right] = 0.95 \quad (31)$$

where the result is the same as the one of (29).

6. Conclusions

From the case discussed above, the second-order third-moment technique is obviously more accurate than the traditional first-order second-moment technique.

7. References

[1] Paris P.C., Erdogan F.: *Critical analysis of propagation laws*. J. Basic Eng. Trans. ASME Ser. D 55, 1963, p. 528–534.
[2] Provan J.W.: *Probabilistic Fracture Mechanics and Reliability*. Dordrecht: Martinus Nijhoff, 1987.
[3] Yang J.N., Manning S.D.: *A simple second order approximation for stochastic crack growth analysis*. Engineering Fracture Mechanics vol. 53, 1996, p. 677-686.

Dr. sc. Konstantin N. NECHVAL
Applied Mathematics Department
Transport and Telecommunication Institute
Lomonosov Street 1, LV-1019 Riga, Latvia
konstan@tsi.lv

Dr. habil. sc. Nicholas A. NECHVAL
Dr. sc. Gundars BERZINS
Dr. sc. Maris PURGAILIS
Mathematical Statistics Department
University of Latvia
Raina Blvd 19, LV-1050 Riga, Latvia
nechval@junik.lv

Jacek M. CZAPLICKI

ON THE SYSTEM: TRUCK – WORKSHOP IN THE QUEUE THEORY TERMS

There are a lot of technical systems in engineering world that apply tire haulage as significant component of their structure. It is quite obvious that in order to maintain a haulage fleet in proper conditions the system must possess a preservative subsystem to meet planned maintenance and repair requirements. A suitable organization of this subsystem determines the number of transport units accomplishing the given transportation task.
In the paper the problem of proper mathematical description of the system: truck – workshop is being considered employing models taken from the queue theory. The main characteristic that is obtained is the probability distribution of a number of failed trucks as the function of several parameters such as the fleet size and possession of a reserve, reliability indices of machines and parameters characterizing intensity of realized repairs and number of repair stands.

Keywords: *Marjanovitch model, Sivazlian and Wang model, heavy traffic situation.*

1. Introduction

The system that comprises trucks and workshop is widely employed in the engineering world. Civil engineering, mining, earthmoving, ordinary transporting firms are – among the other things – examples of scope of application of that system.

In some areas of applications, the system is the only one, self-dependant. In some areas the system is only a certain component of larger system e.g. in surface mining. But there is no doubt that its characteristics determine the whole systems' character.

It is quite astonishing that the main point of interest for the system that comprises tire transportation units was and still is the system: loading units – transporting machines. And nothing but that. The preserving subsystem that is obviously needed was usually considered taking into account planned maintenance and possible preventive actions for carrying devices. Mathematical identification of the generated stream of machines for repair was considered reluctantly, usually assuming the Poisson character of it, rarely presuming more general nature of this process.

In Polish literature the above statements can be easily proved making a review of more important papers that have occurred in last fifty years in this regard. Almost all papers neglected the problem of mathematical determination of number of repair stands for the maintenance shop.

Before the publication [10] made by Takács in 1962 where the mathematical description of model *M/G/1/m* was done, application of Palm's system was used exclusively, i.e. the incoming stream of clients was identified as Poisson one and the service was described by exponential distribution. Some years later Kopocińska in article [5] considered employment of Takács model for the system: loading shovel – transporting trucks for proper organization of the system applied in the gravel mine. The system comprised of one loading machine and a certain number of trucks. All machines were totally reliable therefore a workshop was not needed. Mathematicians considering properties of the real system were aware of the fact that the employed model was significantly simplified versus reality. Therefore Huk and Łukasiewicz published article [3] making some small steps towards generalizations, mainly by application of the simulation technique. A year later Kapliński in paper [4] considered optimization of technological system employing model M/M/1+m for analysis of selected problem in the civil engineering. A few years later Stryszewski in paper [9] described a queue model for the system: shovels – trucks – crusher assuming Poisson character of incoming process and exponential time of service. Again, all machines were totally reliable and the repair shop obviously did not exist. It should be added that even in textbook [1] published just recently – where machines were considered unreliable – the problem of the workshop has not arisen. However, one of the models presented in this work was suitable for modeling the system with repair stands. Finally, last year occurred the dissertation [2] in which the problem: trucks - workshop is well thought-out for proper organization of machinery system in the surface mining field.

The goal of this paper is to present some important outcomes of the cited dissertation that should be interested for engineers from different areas as well as to show some extensions in those considerations, results obtained just recently.

2. The system considered and mathematical model applied

The general model that can be applied to analyze the problem of operation of trucks – workshop system is Sivazlian and Wang one, remembering that the exploitation situation should fulfill *the heavy traffic situation* [8]. The operating scheme of the system can be illustrated as it is shown in Fig. 1.

This system can be described as follows. There are m trucks given to accomplish the transportation task and r trucks are in reserve (cold one). Working machines can fail with intensity δ and repair is being realized with intensity of γ. The number of repair stands is k. The standard deviations of random variables – work time between failures and repair time – are known and are identified as σ_p and σ_n respectively.

Let us neglect here the problem of proper selection of the reserve size. As it was proved in dissertation [2] three system parameters must be selected simultaneously: $< m, r, k >$. But here we assume that these three parameters have been determined in a proper way for the system. If so, basing on the procedure given in cited dissertation, we are able to construct the probability distribution of number of trucks in failure P_j.

At first we have to specify relationship between the number of repair stands and the reserve size because this relation determines the set of patterns that should be taken into consideration [8].

Usually, in practice the following inequalities hold: $r < k < m$.

If, additionally, we check that the condition determining heavy traffic situation, is fulfilled:

$$k \le \frac{m}{0.75}\frac{1-A_w}{A_w} \tag{1}$$

where A_w is the truck long run availability, we are able to select the suitable set of patterns.

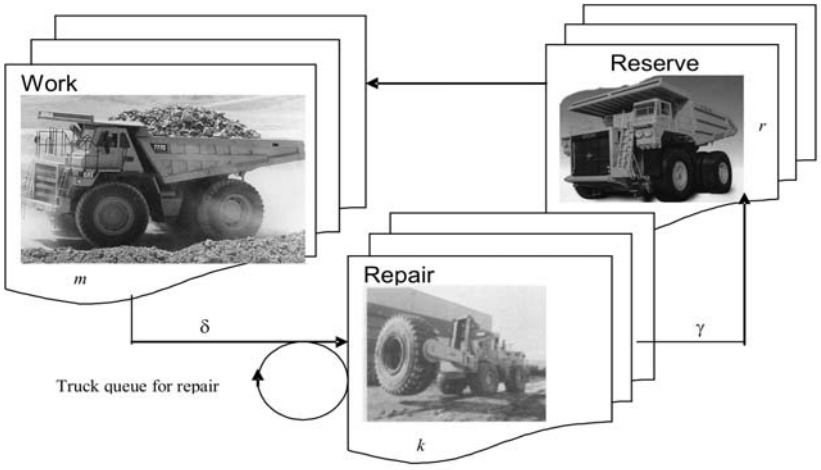

Fig. 1. Operating scheme of truck – workshop system

Here is the procedure that allows finding this distribution in such a way that is convenient for a pc application.

- Determination of power exponents:

$$\beta_1 = 2m\xi\frac{C_M + C_R}{(C_R)^2} \qquad \beta_5 = 2(m+r)\xi\frac{C_M + C_R}{(C_R - \xi C_M)^2}$$
$$\beta_3 = \frac{2k}{\xi C_M}\left(1 + \frac{C_R}{C_M}\right) \tag{2}$$

where:

$$C_M = (\delta\sigma_p)^2, \qquad C_R = (\gamma\sigma_n)^2, \qquad \xi = \delta/\gamma; \tag{3}$$

- Construction of functions:

$$g_4(x) = \frac{1}{m\xi C_M + xC_R}\left(\frac{m\xi C_M + xC_R}{m\xi C_M}\right)^{\beta_1} exp\left(\frac{-2x}{C_R}\right)$$

$$g_5(x) = \frac{1}{(m+r)\xi C_M + xC_R}\left(\frac{(m+r)\xi C_M + xC_R}{m\xi C_M + rC_R}\right)^{\beta_5} exp\left(\frac{-2(\xi+1)(x-r)}{\xi C_M - C_R}\right) \tag{4}$$

$$g_6(x) = \frac{1}{(m+r)\xi C_M + kC_R}\left(\frac{(m+r-x)\xi C_M + kC_R}{(m+r-k)\xi C_M + kC_R}\right)^{\beta_3} exp\left(\frac{2(x-k)}{C_M}\right)$$

- Two conditions to assure function continuity:

$$\alpha_1 = \frac{g_6(k)}{g_5(k)} \qquad \alpha_2 = \frac{g_5(r)}{g_4(r)} \tag{5}$$

- Three constants to close probability to unity:

$$K_6 = \left(\alpha_1\alpha_2\int_0^r g_4(x)dx + \alpha_1\int_r^k g_5(x)dx + \int_k^{m+r} g_6(x)dx\right)^{-1}$$
$$K_5 = \alpha_1 K_6 \qquad K_4 = \alpha_1\alpha_2 K_6 \tag{6}$$

- The probability distribution of number of trucks in failure P_j is given by:

$$P_0 = \int_0^{0,5} K_4 g_4(x)dx$$

$$P_j = \int_{j-0,5}^{j+0,5} K_4 g_4(x)dx \qquad \text{for } j = 1, 2, ..., r-1;$$

$$P_r = \int_{r-0,5}^{r} K_4 g_4(x)dx + \int_{r}^{r+0,5} K_5 g_5(x)dx$$

$$P_j = \int_{j-0,5}^{j+0,5} K_5 g_5(x)dx \qquad \text{for } j = r+1, ..., k-1;$$

$$P_k = \int_{k-0,5}^{k} K_5 g_5(x)dx + \int_{k}^{k+0,5} K_6 g_6(x)dx$$

$$P_j = \int_{j-0,5}^{j+0,5} K_6 g_6(x)dx \qquad \text{for } j = k+1, ..., m+r-1;$$

$$P_{m+r} = \int_{m+r-0,5}^{m+r} K_6 g_6(x)dx \tag{7}$$

The above probability distribution is a function of seven variables: m, r, k, δ, γ, σ_p, σ_n.

Depending on the data system, i.e. values of these seven parameters, we are now able to analyze and – in the next step – we are able to find directions for improvement of the system considered. This can be achieved by tracing changes in the basic system operation parameters as the result of changes in values of the variables. Two additional parameters could be pieces of important information for the system.

- The mean time that truck spends in a queue waiting for repair:

$$T_{ow} = \gamma^{-1}\sum_{j=k+1}^{m+r}(j-k)K_6\int_{j-0,5}^{j+0,5} g_6(x)dx \tag{8}$$

- The mean truck time spent in failure, i.e. the sum of two means: that one determined by pattern (8) plus the mean time of truck repair T_n:

$$T_{ns} = T_n(1 + \phi)$$
$$\phi = K_6\int_{k+0,5}^{m+r} g_6(x)dx\sum_{j=k+1}^{m+r}(j-k)K_6\int_{j-0,5}^{j+0,5} g_6(x)dx \tag{9}$$

3. The problem of service saturation

It is obvious that parameter T_{ow} is a measure of system imperfection. The greater value of the parameter, the greater losses in production/truck service. The best solution that can be achieved in this field is when the number of repair stands equals the total number of trucks in the system. In such a case, we can say that the system is of full service saturation – no losses due to machines in failure without service.

From the theoretical point of view such a case was considered by Marjanovitch under the assumption that the machine work time between failures can be described by the exponential distribution (comp.[6]). Marjanovitch model is identified according to the Kendall system of notation as: *M/G/m+r/r*. Fortunately, in a lot of cases this exponential assumption is acceptable for operating trucks, Therefore the Marjanovitch model has been applied widely before Sivazlian and Wang model was developed.

It was proved (comp. [6]) that the probability distribution of number of machines in repair in the Marjanovitch model is given by:

$$P_k^{(n)} = \begin{cases} P_0^{(n)}(\kappa^k / k!)m^k & for \quad 1,2,...,r \\ P_0^{(n)}(\kappa^k / k!)m^r m(m-1)...(m-k+r+1) & for \quad k = r+1,...,m+r \end{cases} \tag{10}$$

where: $\kappa = (1-A_w)/A_w$ and obviously $\sum_{k=0}^{m+r} P_k^{(n)} = 1$.

Thus, if we consider Sivazlian and Wang model and we are going to increase the number k of repair stands we are moving towards Marjanovitch solution.

Let us notice that very often the probability of occurrence of event that all machines are down is very small, especially for larger system and/or for trucks of high reliability. So, it is of high interest to find such a number of repair stands for which the mean time in which a truck spends in failure waiting for repair is negligible. We presume speculatively that this number could be smaller than the total number of machines in the system. And it is true in reality. As it was shown by calculation [2] – considering truck system for open pit mining – it is enough when the number of repair stands equals approximately 1/3 of the total number of trucks in the system. For lower reliability of machines this fraction is smaller. Fig. 2 shows general relationship between the mean number of trucks in failure E_u versus the number of repair stands k.

Generally, the following regularities have been identified:

- for trucks of high reliability the function $E_u(k)$ runs quickly towards the asymptote defined by Marjanovitch model; conclusion: the required number of repair stands for the shop is significantly smaller than the total number of trucks in the system,
- for trucks of low reliability the function $E_u(k)$ runs slowly towards the asymptote; the required number of repair stands for the shop is smaller than the total number of trucks in the system, but usually high enough to generate significant cost,
- considerations associated with this problem are of special value for large systems.

Interesting properties posses also the standard deviation function *S(X)* of random variable – number of trucks in failure. Fig. 3 illustrates three plots of this function obtained analyzing the system operating in one of southern African open pits.

4. The probability distribution of number of trucks in work state

Our hitherto consideration was generally directed to find such a number of repair stands to reduce losses connected with the truck state in which this unit waits idly for repair. This problem was interested due to the fact that we would like to extend the work time of transporting means.

Having specified the probability distribution of machines in failure we are able to determine the probability distribution in work state. Denoting by $P_{wm}^{(p)}$ probability that machine is in work state, we can define:

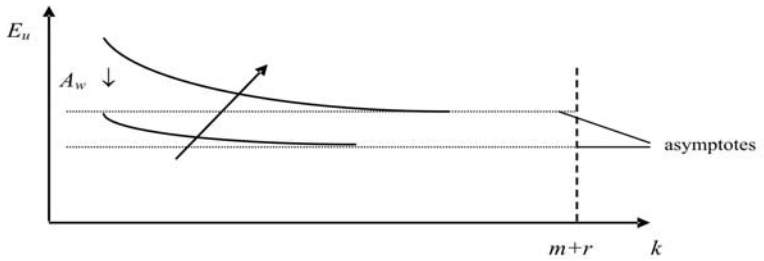

Fig. 2. The mean number of trucks in failure E_u as a function of number of repair stands k for different values of truck availability A_w

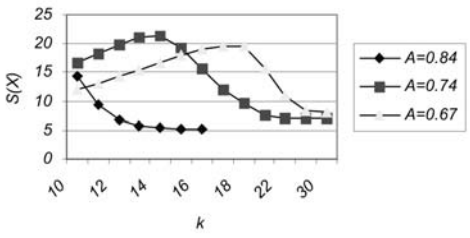

Fig. 3. The function of standard deviation of number of trucks in failure versus number k of repair stands for different levels of truck availability A_w

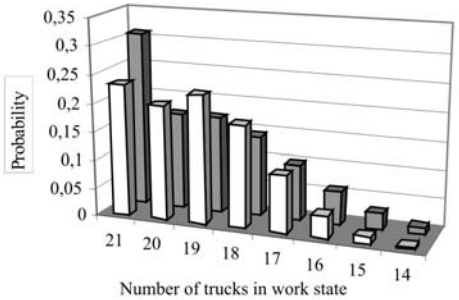

Fig. 4. The probability distribution of number of trucks in work state for two different systems with different reserve

$$\begin{cases} P_{wm}^{(p)} = \sum_{j=0}^{r} P_j \\ P_{w(m-j)}^{(p)} = P_{r+j} \qquad for \quad j = 1+2,...,m \end{cases} \tag{11}$$

The typical feature of this probability distribution is the accumulation of the mass of probability in point *m* because of the reserve. If in a system there are no spare units such regularity does not exist. The greater number of machines in reserve, the greater accumulation of the probability mass. Fig. 4 shows typical distributions for two different machinery systems having different size of reserve.

The probabilistic function (11) is the essential tool to compute the system output. In some modeling procedures, this is only a certain item being the information input to obtain the analyzed system important characteristics how it was shown in dissertation [2].

5. Final remarks

There are two important problems connected with the above considerations, namely:

- selection of three basic system parameters <*m, r, k*>,
- repair stands can fail.

The first problem is of great significance. Selection of these parameters has influence on the amount of money spent to purchase transportation units (in some cases one truck can cost more than 3 billion US$ and we need more than 100 such units [1, 2]) and to arrange a maintenance bay (further 3 to 4 billion of US$). Sometimes one hour of operation of a truck can reach several hundreds of US$. It is easy to calculate what amount of money is involved in such a business. Therefore the selection of these three parameters can result in great money savings or great money losses. Generally, these parameters should be chosen to accomplish a transportation task formulated in a proper way. This mission should be attained in the cheapest way, assuring proper level of safety. Sometimes it is impossible to find the best economic solution, but fortunately, we are usually able to formulate optimizing criterion in a different way, not moving far from a financially viable key. Such a case was considered in monograph [2].

The second problem requires randomization of parameter *k*. At first glance, the problem looks simple. Usually it is assumed that repair stands operate independently on each other, all units are of the same nature and the workshop system consists of *k* such elements. Nevertheless, even in such case construction of the probability distribution of number of trucks in failure can make some troubles. It is connected with areas of validity of sets of patterns determined by values of basic system parameters. Situation becomes much more complicated when the assumption that all stands are of the same nature must be rejected. Immediately the problem of sequences of repair stands for a given type of repair comes together with the probability of their occurrence. For the time being it is much better to consider a particular system in this regard than to find general solutions.

6. Preferences

[1] Czaplicki J. M.: *Elementy teorii i praktyki systemów cyklicznych w zagadnieniach górniczych i robót ziemnych*. Wydawnictwo Politechniki Śląskiej, Gliwice 2004.

[2] Czaplicki J. M.: *Modelowanie procesu eksploatacji systemu koparki – wywrotki*. Zeszyty Naukowe Politechniki Śląskiej nr 1740, Gliwice 2006.

[3] Huk J., Łukasiewicz J.: *Cykliczne systemy obsługi masowej*. Matematyka Stosowana, seria III, I, 1973. s. 85-104.

[4] Kapliński O.: *Zastosowanie teorii kolejek do optymalizacji ciągu technologicznego*. Przegląd Statystyczny R. XXI. z. 4. 1974. s. 631-646.

[5] Kopocińska I.: *Matematyczne modele kolejek cyklicznych*. Inwestycje i budownictwo. 18, nr 12, 1968. s. 22-25.

[6] Kopociński B.: *Zarys teorii odnowy i niezawodności*. WNT, Warszawa 1973.

[7] Sivazlian B. D., Wang K.-H.: *System characteristics and economic analysis of the G/G/k machine repair problem with warm standbys using diffusion approximation*. Microelectronics & Reliability, 29, 5, 1989, pp. 829-848.

[8] Stryszewski M.: *Ocena pracy i sterowanie wydajnością ciągu technologicznego koparka – samochód – kruszarka z zastosowaniem teorii kolejek*. AGH Zeszyty Naukowe, Górnictwo. Rok.5, z. 2, 1981. s.157-169.

[9] Takács L.: *Introduction to the theory of queues*. Oxford University Press, New York 1962.

Dr hab. inż. Jacek M. CZAPLICKI

Mining Mechanization Institute
Silesian University of Technology
Akademicka 2, 44-100 Gliwice, Poland
E-mail: jacek.czaplicki@polsl.pl

Stanisław RADKOWSKI

USE OF VIBROACOUSTICAL SIGNAL IN DETECTING EARLY STAGES OF FAILURES

An understanding of vibroacoustic signal is required for the robust and more effective detection of early stage failure. In the paper the possibility and method of time varying vibration decomposition are discussed. It is shown that analysing the coupling between the structure's components changes from linear to nonlinear or to other kind of nonlinearity together with intermodulation phenomena can be used as measure in structural health monitoring. In addition on an analytical connection is investigated between the tracking method and the physics of the kinematic contact process based on the idea of higher-order spectra analysis, bispectral analysis specially.

Keywords: *Vibroacoustic diagnostics, modulation phenomena, bispectrum, time-frequency representation.*

1. Introduction

Half a century ago, when solving the issue of dealing with effects of failures in machines and devices as well as the task of lubrication of important kinematic pairs, attention was drawn to the fact of relevant organization of operation and maintenance units and introduction of new operational methods. However the need for cost reduction as well as increasing mechanization and complexity of devices and the associated growth of loss in a situation of a failure pointed to the importance of maintenance and repair activities. As a result, procedures were introduced in the years 1950-1970 which defined the scope and the time of scheduled maintenance-and-repair inspections.

The next stage of development, associated with 1970's, was the inclusion of elements of prediction in the existing, essentially preventive methods. This direction of development was to a great extent stimulated by the introduction of "Just – in – Time" manufacturing system which put a lot of focus on minimizing the warehouse stock. The present stage of development, which has continued developing since the beginning of 1980's, is determined by high automation of equipment and development of technologies on the one hand and putting stress on relevant security of operated systems and the need for reducing the threat to the environment on the other. Hence the enormous interest in the procedures of identification and forecasting of emergency situations as well as growth of credibility of reliability assessment related to monitored machines and devices.

This results from the fact that a system which has been designed while accounting for the possibilities of technical condition monitoring (CM) enables us to avoid the loss associated with forced downtimes, reduces the cost of unnecessary storage of spare parts as well as the costs associated with occurrence of unforeseen failures. Thus production cost is reduced by avoiding the need to pay the crew for readiness to work during downtimes.

In such circumstances it is natural to adopt Condition Based Maintenance (CBM), which means introduction of a system of evaluating the technical condition based on the collected data related to the parameters of a machine's operation and the parameters of residual processes as well as performance of preventive maintenance based on the forecasted damage (failure) occurrence, which we could term as "just – in – time" maintenance. The right selection and implementation of a diagnostic system and the relevant training of the diagnostic team who, based on the examination of trends of defect occurrence and development, would able to determine the time to failure and assess the actual, longer operating time are the factors conditioning the ability to accomplish the goals assumed for such an operation process.

One of the basic elements of such a strategy is the use of diagnostic systems for monitoring of technical condition of systems or accordingly process monitoring systems in order to detect and identify the defect development phase and prevent the occurrence of dangerous disturbance of functioning of critical elements and units of a system. This often calls for the need of solving the issue of diagnostic inspection optimization according to the criteria defined by RBI (Risk Based Inspection) and RBM (Risk Based Maintenance) methods. In accordance with the propositions found the publications on the topic [3,16] the basic tasks of advanced security monitoring include: defining the scope of monitoring and the method of limiting the scope and presenting the information related to emergency conditions and values; selection of methods and means enabling monitoring and on-line inference in a manner enabling early detection of growing disturbance and extraction of features characteristic for developing defects from general signals pointing to operating anomalies; controlling the defects and taking corrective actions by the operator so as to minimize, and in particular avoid, the occurrence of undesirable events which are accompanied by extensive consequences; development of a method of forecasting future events based on the current observations and registered, lasting changes of parameters that have been detected during measurements' analyses as well as examination of the results found in the database. The last item is particularly important when monitoring the condition of elements and units subject to degradation and fatigue-related wear in whose case the identification of early stages of defect development may prevent the occurrence of the catastrophic phase of a defect and consequently destruction of the entire system.

Taking this into account, the possibilities of applying vibroacoustics in technical systems, including the issues of vibroacoustic diagnosis of units and elements, inspire increasing interest among engineers and technicians involved in the organization and planning of [machine] operations in companies.

Early detection of defects and determination of their causes occupies a special place among the vibroacoustic diagnosis methods. Let us note that the process of defect formation can lead both to intensification of non-linear phenomena as well as to occurrence of non-stationary effects even if in the early stages the intensity of defects is small while the growth of the level of vibration and noise is negligible in contrast with emergency situations. Here let us only note that the emergence of defects and the low-energy phases of their development are most often accompanied by local disturbance of the signal's run, which may result in tangible changes of the signal's frequency structure that are additionally variable in time. Such a situation inclines one to formulate the diagnosis of origin of defects while relying on

the diagnostic information carried by non-stationary disturbance and non-linear effects.

Let us note that the analysis of low-energy pulse-type disturbance, causing broadband response with small amplitude, calls for accounting for not only the information on the changes of the signal's power but also on its phase, which points to the need for reaching beyond the information contained in the second-order process. This is so because even though the correlation function provides a sufficient description of the Gauss process with the mean value equal zero, still in the case of non-Gauss distributions of probability it is accordingly the correlation function of the power spectrum that provides partial information on the process.

For example the information on emergence of a defect can be contained in the low-energy components of the signal that are carried across the structure of a machine from the measurement source as a result of modulation of a relevant carrier function. Thus when examining signals attention is particularly devoted to the analysis of amplitude-and-phase modulation of a signal and occurrence of non-linear and non-stationary effects.

The actual signal can contain both, the component generated by the diagnosed kinematic pair as well as by the components transmitted over structure of the examined object which are generated by other kinematic nodes. This brings us to the necessity of solving the issue of relevant separation of diagnostically-useful information. It is connected with the issue of developing a relevant procedure which could be a part of the algorithm for diagnosing the low-energy phases of defect development

As has been demonstrated by to-date research [10], significant diagnostic information is contained the higher order moments, which underscores the significance of non-linear phenomena in the detection of defect development. Such possibilities are not offered by the analysis of power spectrum which relies on the assumption of mutual independence of respective frequency components, which is a consequence of adopting the linearity and the superposition in the applied methods of power spectrum determination. In majority of cases the development of low-energy defects cannot be adequately presented by means of linear models. An example confirming this situation is the phenomenon of transformation of a harmonic function in which the additional frequency components are coupled. Similarly, the transition through a non-linear phenomenon with a square component of a signal consisting of two harmonics with various frequencies and various initial phases will lead to the emergence among the additional components, at the output points of system, also of components which maintain the same relationships between the original frequencies and phases as those found in the input signal. This phenomenon is called in publications [8] as quadratic-phase coupling.

The above presented introduction points to the need of broader reference to the methods of signal analysis that enable detection of phase relationships between the harmonics and the modulation, inter-modulation and mutual modulation effects which enable examination of resultant multi-dimensional signals.

Treating the diagnosed object as an operator which transforms the parameters of a technical condition of $\boldsymbol{X''}$ into parameters of vibroacoustic signal $\boldsymbol{Z}$, we will obtain the solution of the problem of general diagnosis of state in the form of a inverse task:

$$\boldsymbol{Z} = \boldsymbol{AX} \Rightarrow \boldsymbol{X} = \boldsymbol{A}^{-1}\boldsymbol{Z} \qquad (1)$$

where A – system matrix.

Solution of equation (1) for the general case is difficult. Thus the problem of general diagnosis of object's state is in its essence reduced to selection of such subset of diagnostic parameters so that the changes of the values of the technical state parameters are accompanied by changes of one diagnostic parameter (symptom). In such case the quantitative relationships can be established on the basis of analysis of the models of defect symptom generation.

With such approach, the subset of $\boldsymbol{X'}$, the elements of which are states that ensure the realization of the object's functional tasks, is disregarded.

Assuming that transition from one state to another within the subset of $\boldsymbol{X'}$ is caused by appearance of defects which do not have direct influence upon decrease of the object's functional value, we are faced with a diagnostic problem that is new in terms of its characteristics.

In this case we are interested in making of a diagnosis of state and forecast of transition into a given state from the subset of $\boldsymbol{X''}$. In order to carry out this type of diagnosis on the basis of the character and intensity of the changes connected with the degree of object's readiness for work, it is necessary to analyze the relationships between the degradation and wear and tear processes that take place in the functionally essential (kinematic) pairs, and the related changes of the vibroacoustic processes properties. This implies a necessity of defining of such a set of diagnostic parameters whose elements will be sensitive to slight changes of technical parameters and which can be used for location and identification of origins and development of low energy stages of defects. Let us note that similarly as in the case of general diagnosis, also in this case the fundamental problem is the structure and the analysis of the relationships and cause and effect relations, and creation of an adequate set of diagnostic parameters. Let us consider this problem in more detail.

2. Diagnostic model in detection of low-energy defects

While attempting to develop a model oriented on such defects one should on the one hand consider the issue of examining the signal's parameters from the point of view of their sensitivity of to low-energy changes of the signal and, on the other, the issue of quantification of energetic disturbances occurring in the case of defect initiation.

Let us assume that the degree of damage D is the dissipated variable that covers the changes of the structure's condition due wear and tear:

$$dE_d(\Theta, D_0) = \frac{\partial E_d(\Theta, D_0)}{\partial D} dD + \frac{\partial E_d(\Theta, D_0)}{\partial \Theta} d\Theta \qquad (2)$$

where: $dE_d = \frac{df(D,\Theta,\gamma(\Theta))}{d\Theta}$, $\gamma(\Theta)$ - the parameter describing how big a part of the dissipated energy dE_d is responsible for structural changes, Θ - operating time.

Bearing in mind the possibility of diagnosis of the origin and the development of low-energy phases of defect formation, when the extent of the original defect can be different in each case, let us analyze this issue more precisely.

To examine this problem let us recall here the two-parameter isothermal energy dissipation model proposed by Najar [8] where:

$$dE_{d_s} = dE_d - dE_{dq} = Tds = \sigma_\Theta dD \qquad (3)$$

where: dE_{d_q} - energy transformed into heat, dE_{d_s} - energy responsible for internal structural changes, T - temperature, ds - growth of entropy.

The expression (3) shows that the growth of the dissipated variable D is attributable to the dE_{d_s} part of energy, which is the dissipated part of dE_d energy, that causes the growth of entropy *ds*.

The role of the multiplier determining the relation between the increments of dissipated variable and the entropy is played by the dissipation stress σ_Θ.

The assumption of T=constans results in independence of dissipation-related loss $dE_{d_s} = dE_{\Theta_s}$, thus following integration the expression (3) takes the following form:

$$E_{d_s} = T\Delta s \tag{4}$$

The derivative of defect development energy related to *D*, when $E_f(D_0) \le \frac{1}{2}E\varepsilon^2$, means the boundary value of deformation energy and takes the following form:

$$\frac{dE_{d_s}}{dD} = \frac{E_f(D_0)(1-D_f)(1-k)D^{-k}}{D_f^{1-k} - D_0^{1-k}} \tag{5}$$

For a defined initial defect of D_0 and for a defect leading to damage D_f, relationship (5) will have the following form:

$$\frac{dE_{d_s}(D)}{dD} = (1-k)E_{D_0,f}(k)D^{-k} \tag{6}$$

Let us note that parameter $E_{D_0,f}$ is an exponential function of power *k*, similarly as the whole derivative. While referring to the second rule of thermodynamics for irreversible processes we will assume the following in the contemplated model:

$$\frac{dE_{d_s}(D)}{dD} \ge 0 \tag{7}$$

Thus for the assumed model to be able to fulfil condition (7), the exponent must meet the requirement of $k \le 1$. In addition, while referring to the rule of minimization of dissipated energy, the conditions of permissible wear process [8] show that the change of exponent k is possible as the defect develops.

To examine this problem let us assume that the exponent shows a straight line dependence on the extent of damage:

$$k(D) = a + bD \tag{8}$$

For damage of small magnitude the linear approximation seems to be sufficient and enables description of defects whose emergence is characterized by small growth of defect energy (see Figure 1).

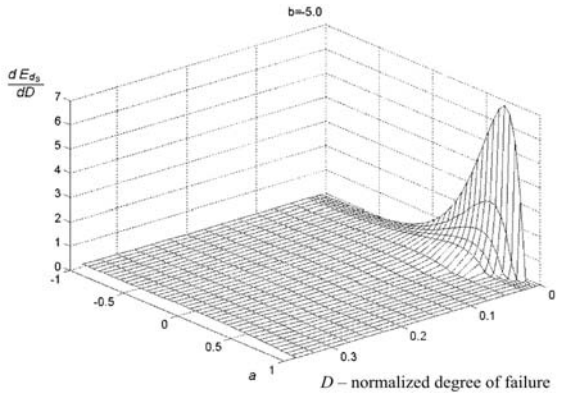

Fig. 1. Change of energy of defect development for small D

Thus while defining the set of diagnostic parameters we should pay attention to the need for selecting such a criterion so that it will be possible to identify defects whose emergence is characterized by small growth of defect-related energy.

While contemplating this issue let us assume that vibroacoustic signal is real and meets the cause-and-effect requirement, which means that it can be the base for creating an analytical signal.

In accordance with the theory of analytical functions, the real and the imaginary components are the functions of two variables and meet Cauchy-Riemann requirements.

While contemplating this issue let us assume that vibroacoustic signal is real and meets the cause-and-effect requirement, which means that it can be the base for creating an analytical signal.

In accordance with the theory of analytical functions, the real and the imaginary components are the functions of two variables and meet Cauchy-Riemann requirements.

Please be reminded that the analysis of the run of the analytical signal will be conducted while relying on the observation of changes of the length of vector *A* and phase angle φ:

$$z(x,y) + jv(x,y) = A(\cos\varphi + j\sin\varphi) \tag{9}$$

Thus,

$$z\big(x(\tau),y(\tau)\big) = A(\tau)\cos\varphi(\tau) \qquad v\big((x(\tau),y(\tau)\big) = A(\tau)\sin\varphi(\tau) \tag{10}$$

means that the signal measured is the orthogonal projection of vector *A* on real axis.

Ultimately, while exploiting the Cauchy-Riemann conditions for variables $A(\tau)$ and $\varphi(\tau)$ we will obtain:

$$\frac{dz}{d\tau} = \frac{dA}{d\tau}\cos\varphi - A\sin\varphi\frac{d\varphi}{d\tau} \tag{11}$$

As we expected the obtained relationship presents an equation that enables the analysis of the measured signal while observing *A* and φ. At the same time it should be noted that for low-energy processes, when we can neglect the changes of the vector's length and assume $A \cong const$, the whole information on the changes of the measured signal is contained in the phase angle, or more precisely in the run of momentary angular velocity.

While accounting for the obtained results of the analysis of the process of low-energy defect emergence and detection of diagnostic information associated with the changes of momentary values of amplitude and angular velocity, let us analyze the conditions that must be fulfilled by a diagnostic model intended to enable observation of the influence of such disturbance on the form of the system's dynamic response.

Occurrence of errors can lead to change of the conditions of contact in kinematic node, including: the qualitative change of the process of coming into / out of contact, disturbance of the linearity which as a result lead to non-linear changes of the system's parameters, in particular of rigidity and damping. This has essential impact upon the frequency structure of generated vibration. To make this problem more familiar, let us note that if we assume that the function $y: C \to C_0$ is holomorphic in the neighbourhood of a set point t_0, then Taylor's expansion defines $y(t)$ for points close to t_0 with any arbitrarily selected precision. The first term of this expansion shows linear changes of $y(t)$ which depend upon $(t - t_0)$. In points at which the first derivative $y'(t_0)$ disappears, it is only the analysis of the second derivative, responsible for second order increments, that gives us information about the way the function behaves around point t_0. This simple observation turns our attention to the models in which the $x(t)$ signal is processed according to the following pattern:

$$y(t) = h_0(t) + h_1(t) * x(t) + h_2(t) * x(t) * x(t) + \ldots \tag{12}$$

and the Fourier transform will respectively assume the following form:

$$Y(\omega) = Y_0(\omega) + H_1(\omega)X(\omega) + H_2(\omega)X^2(\omega) + \ldots \quad (13)$$

This entails the necessity of analysis of non-linear signals, and particularly of examination and modelling of linear and bilinear components.

In comparison to input signals, the bilinear component will be characterised by additional frequencies having the form of sums and differences of frequencies found at the input point. Let us note that similar disturbance will be caused by the phenomenon of amplitude and phase modulation. Referring to the presented model of generation process, let us assume that the bilinear part of the signal is transmitted to the measuring point by a linear transmission channel. Then, after including the linear part of the signal and the non-linear one, which in accordance with the procedure proposed by Eykhoff [4] will be presented in the form of a process containing linear elements and multiplying terms, we shall obtain the following relationship:

$$z(t) = \int_0^t h_1(\tau_1)x(t-\tau_1)d\tau_1 + \int_0^t\int_0^t h_2(\tau_1,\tau_2)x(t-\tau_1)x(t-\tau_2)d\tau_1 d\tau_2 \quad (14)$$

where:

$$h_1(\tau_1) = h_{Q_1}(\tau_1) * h_{p_1}(\tau_1) \quad (15)$$

$$h_2(\tau_1,\tau_2) = h_{Q_{22}}(\tau_1-\tau_3)\cdot h_{Q_{21}}(\tau_2-\tau_3) * h_{p2}(\tau_3) \quad (16)$$

Let us note that the complex mechanism of the influence of non-linearity on the system's response was brought down to generation of a signal by a system with components that are relatively simple, which refers back to the model in the form of a Volterra series [13].

3. Detection of non-linear disturbance

Let us note that low-energy impulse disturbances cause broad-band response with small amplitude and that is why typical spectral analysis of averaged power spectrum in the domain of frequency, as well as the correlation function in the domain of time can contain information of second order process. For example, a sufficient characteristic of a Gauss process with an average value equal to zero is its covariance function. However, in the case of process with non-Gauss distribution of probability, respectively the correlation function or the power spectrum supplies only partial information about the process. Analysis of higher-order spectra, properly defining the non-linear effects, is required to obtain a more precise description. This observation pointed to the need for the analysis of the frequency structure of a signal in the plane defined by time and frequency [9].

Additionally, in many cases it becomes necessary to increase the resolution in order to detect the diagnostic information, which most often leads to the increase of the size of the data block and to extending of the required calculation time. Since the analysis of the effects of amplitude and phase modulation of a vibroacoustic signal requires examination of the distribution of the signal's power, both in time and with respect to individual frequency components, then apart from the fulfilment of the resolution-related requirements it also calls for the necessity to define the frequency of sampling. Let us note that conducting of such signal processing is justified in a situation when the general structure of a signal is known and when it is possible, without losing any essential diagnostic information, to select such parameters of a sample so as to obtain a locally stationary signal. Further investigation can be then conducted with the use of the known methods of stationary process analysis, e.g. Fourier transform:

$$S(\varpi) = \int_{-\infty}^{\infty} s(t)e^{-j\varpi t}dt \quad (17)$$

Assuming that the above mentioned assumptions regarding the stationary character of a signal can be implemented by selecting the parameters of a time window which will be moved with respect to a non-stationary signal, we will achieve the possibility to create a spectrogram picturing the frequency curve in the domain of time:

$$S(t,\varpi) = \int_{-\infty}^{\infty} s(\tau)w(\tau-t)e^{-j\varpi\tau}d\tau \quad (18)$$

In practice it is synonymous with dividing the signal into many brief samples by means of a rectangular time window and with the related discontinuity at the ends of the records thus created, as well as with an essential drop in terms of resolution. In work [1], devoted to the analysis of non-stationary character of the signals generated by the heart, we point to the necessity of fulfilment of a compromise criterion of selection of the time window which ensures that the requirements of the sample's stationary character and proper spectrum resolution will be maintained. Wang and McFadden [15], while presenting the possibility of using spectrograms in the tasks related to the identification of damage in toothed gears, stress the importance of the proper function of a window. What we have in mind here is particularly such a function of a window, which will prevent the appearance of additional rolling and the unwelcome Wigner-Ville complication [7]:

$$W_{f_z}(t,\varpi) = \int_{-\infty}^{\infty} f\left(t+\frac{\tau}{2}\right)f^*\left(t-\frac{\tau}{2}\right)e^{-j\varpi\tau}d\tau \quad (19)$$

This transform gives the possibility of differentiating between the phenomena of amplitude and phase modulation. Kumar and Carrol [5], who pointed to the possibility of using the Wigner-Ville distribution for analysing the signals, compare this method to an analysis performed with the use of a two-dimensional cross correlation function. Starting from an assumption that the change of the technical parameters leads to specific changes of the spectral picture, they proposed the evaluation of the status by comparing the obtained distribution with the characteristics of the reference picture. Such an approach enables us for example to define the carrier frequencies and the modulated bands, build a relevant analytical signal, and carry out further analysis on this basis, in particular the quantitative evaluation of the parameters of amplitude and phase modulation. To carry out the proposed procedure it is necessary to apply the Hilbert's transform [10]:

$$\hat{a}(t) = \frac{1}{\pi}\int_{-\infty}^{\infty}\frac{a(\tau)}{t-\tau}d\tau = a(t) * \left(\frac{1}{\pi t}\right) \quad (20)$$

which allows for the creation of an analytical signal:

$$\tilde{a}(t) = a(t) + j\hat{a}(t) \quad (21)$$

The discussed methods of generating the time and frequency power distributions, while taking into account relevant selection of the windows, turn out to be generally usable in the analysis of signals in which the diagnostically-essential features have similar time scale. On the other hand, their effectiveness drops significantly when examining signals, which contain features with various scales. In this case, as is shown for example in [1,15], much better results can be achieved by applying wavelet analysis:

$$W(t,\alpha) = \frac{1}{-\sqrt{a}} \int_{-\infty}^{\infty} x(\tau) g^* \left(\frac{\tau - t}{a} \right) d\tau, \qquad a(>0) \qquad (22)$$

where respectively:

x(t) is the signal analysed, a is the scale parameter which decreases as the frequency increases, while function *g(t)* describes a variable size window, which allows for selecting the proper sampling frequency while maintaining the expected resolution.

Let us note that in contrast with the Fourier transformation, where the base for decomposing the signal is constituted by the harmonic functions, in this case the choice of the shape of the function's base may account for both, the disturbances and the requirements of the digital processing [14]. Such a manner of analysis is particularly essential in a situation when for a series of modulated bands around the defined carrier frequencies it is necessary to define the type and size of modulation on the basis of the analysis of envelope and phase functions.

On the other hand, the attempt of modelling non-linear effects and generating a disturbed vibroacoustic signal requires accounting for additional effects, e.g. in the form of consecutive carrier frequency. Let us note that in these cases it is the multi-dimensional analysis in the domain of frequency that becomes particularly significant.

Some of these, and in particular the spectrogram, multi-dimension Fourier transform, Wigner-Ville distribution, and bispectral analysis were discussed in [9], in the context of their usability to examine the modulated vibroacoustic signals. Let us note at this place that as a result of signal modulation additional components will appear in the spectrum, respectively in the form of sums and differences of carrier frequencies and modulating frequencies in the case of modulation by a harmonic function. This points to the significance of the bispectrum, which is responsible for "third-order information". If the generally accepted interpretation of the spectrum of vibroacoustic signal's power does not raise any objections, the attempts to interpret the information found in the higher-order spectrum are not so clear. From the interesting to us point of view of using the time and frequency representation to analyse the phenomena of modulation of a signal generated by disturbance of the meshing and contact conditions, it was assumed that time and frequency distribution represents the momentary power spectrum – Wigner distribution:

$$W_{2,x}(t,f) = \int C_{2,x}(t,\tau) e^{-j2\pi f\tau} d\tau \qquad (23)$$

where: $C_{2,x}(t,\tau)$ - local autocorrelation function, second order cumulant.

Let us note that in this way, by using $C_{3,x}(t,\tau_1,\tau_2)$ - a third order cumulant it is possible to present a relationship defining the bispectral Wigner distribution:

$$W_{3,x}(t,f_1,f_2) = \iint C_{3,x}(t,\tau_1,\tau_2) e^{-j2\pi(f_1\tau_1 + f_2\tau_2)} d\tau_1 d\tau_2 \qquad (24)$$

With the assumption of relevant stationary character of a signal in accordance with Gerr's proposal [15], the relationship is in force for a bispectrum and for a bispectral Wigner's distribution:

$$E\left[W_{3,x}(t,f_1,f_2)\right] = \int W_{3,x}(t,f_1,f_2) dt = S_{3,x}(f_1,f_2) \qquad (25)$$

Thus a question appears, can more data be also obtained, both quality and quantity related data concerning the type and the extent of signal's modulation, by using the bispectral Wigner's distribution. Taking into account the fact that multiparameter modulation phenomenon, and the related additional complication of the spectrum's structure appear in a toothed gear, obtaining of a positive answer can have essential application significance.

4. Intermodulation and mutual modulation phenomena

Thus the occurrence of a defect and development of its low-energy phases are accompanied by a disturbance of the operation of kinematic node leading to change of power distribution between the spectrum components. The shares of respective components will be determined by multi-parameter modulation processes of four different modulated functions whose carrier frequencies correspond to the basic frequencies of harmonics appearing in the solution.

Let us note that the presented models showing the influence of defect origin and development are clearly associated with the development of the phenomenon of modulation of the signal's parameters. This is only partly confirmed by the results of analyses of the spectra generated by defective gears. Another effect that should be in addition taken into account is the occurrence of non-linear effects. For that reason the vibroacoustic signal generated by a defect should presented as a higher order components, which includes cases of non-linearity of the second, third or even fourth order:

$$y(t) = x(t) + \varepsilon\left(x(t)\right)^2 + \sigma\left(x(t)\right)^3 + \delta\left(x(t)\right)^4 \qquad (26)$$

It is sufficient in the case of systems or sets of machines with not so complex dynamic and kinematic structure. Let the results of simulation, as presented in [2], be an example of the fact that such a model of signal generation is unable to explain in a sufficient degree the spectrum's change in connection with a developing defect.

Figures 2-3 present the example of evolution of the spectrum simulated by the model of non-defective and defective two-stage toothed gear.

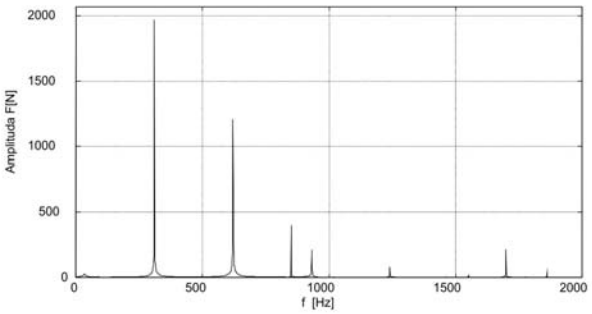

Fig. 2. Amplitude spectra of simulated response of bearings in an "ideal" toothed gear

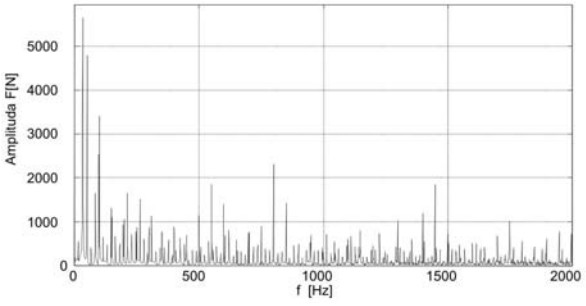

Fig. 3. Amplitude spectra of simulated response of bearings in a toothed gear with 2nd degree pitch error the pinion

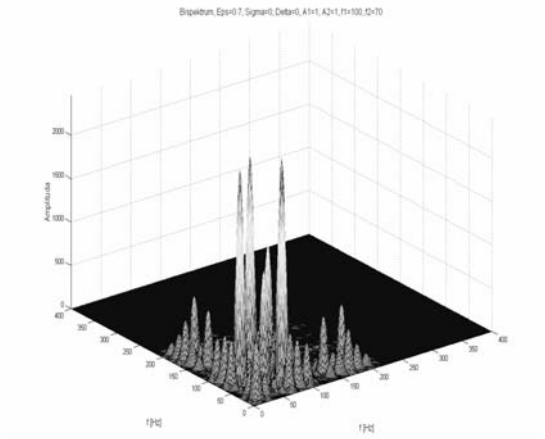

Fig. 4. Bispectrum of a signal with mutual modulation and squared non-linearity

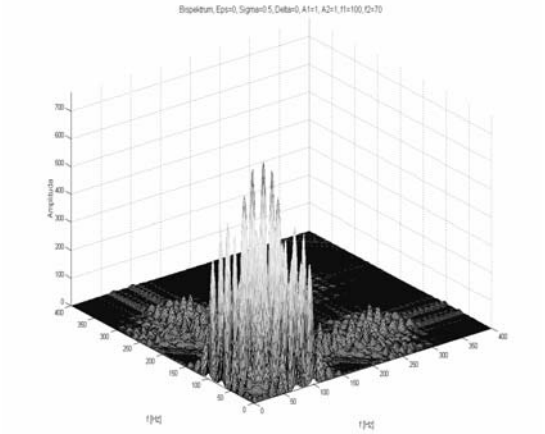

Fig. 5. Bispectrum of a signal with mutual modulation and non-linearity of the third order

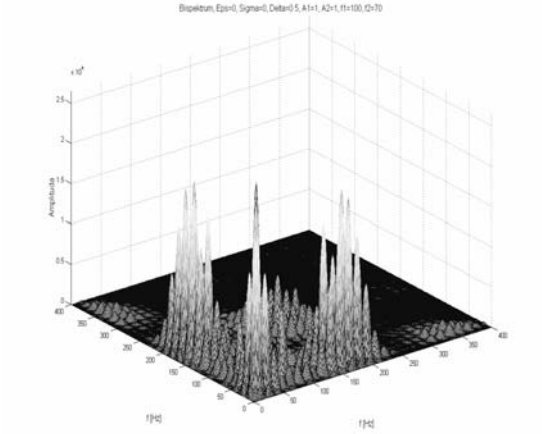

Fig. 6. Bispectrum of a signal with mutual modulation and non-linearity of the fourth order

While explaining the problem let us note that by taking into account the two-stage toothed gear, we as result are able to follow the vibroacoustic signal generated by two pairs of toothed wheels, that is by two sources. This means that the measured vibroacoustic signal is the sum of the minimum values from the two signals whose complexity, in this case the modulation of the parameters, depends on defect development. Bearing in mind the associated developing impact of non-linear effects one should expect coincidence of the influence of both phenomena. Thus one should include the phenomena of mutual modulation and inter-modulation in the description of changes of the frequency structure of the signal generated by the defective two-stage toothed gear [11].

Let us note that the phenomena of inter-modulation and mutual modulation enable, on the one hand, the explanation of the mechanism of emergence of additional components in the spectrum, and on the other they constitute interesting basis for diagnostic inference. Above all thanks to the analysis of the relations between the emerging defect and the developing modulation effect we can observe the growing role of mutual modulation in shaping the frequency structure of a vibroacoustic signal.

Assuming that numerous components are related to each other due to phase coupling, one should expect that significantly better results of diagnostic inference will be brought by applying multi-dimensional spectra, especially the bi-spectrum.

The relevant results of analyses are presented in Figures 4÷6. What is worth noting is the extension of the frequency band as the degree of non-linearity increases. Also the structure of bands which are characteristic for a square phase coupling can be a distinctive feature for a given type of non-linearity.

5. Applying of symbolic time series

One of problems conditioning the effective and reliable diagnostic-and-programming inference is the possibility of defining and building a relevant, well-defined functional model of such environment. It enables us to correctly determine the physical values and to select the relevant measurement and registration devices, which will enable proper measurement.

The awareness that we are not always able to construct a well-defined dynamic diagnostic model which is characterized by controlled uncertainty, directs the attention of people responsible for diagnosis towards direct utilization of the time series that are variable in time for the purpose of constructing such models.

The results we have obtained to date confirm that the right choice of relevant parameters of signal analysis, including the range of equipment dynamics, sampling frequencies and the ratio of useful signal to noise have significant impact on the credibility of results.

Thus there is increasing focus on the analytical methods which apply relevant weights to the structure of the experimental data set, particularly in the context of establishing or detecting the physical relations and links between the results of measurements and the occurring phenomena which result from or are associated with the processes taking place during operations. Such methods include the symbolic analysis of a time series, which has attracted a lot of attention in recent publications related to experimental data analysis.

The symbolic analysis of a time series is strictly connected with symbolic dynamics, which has developed together with the examination of complex dynamic systems. The closest to experimental research use of symbolic dynamics is presented in [6, 8].

While looking from our point of view we should stress that there exist no general rules of creation of measurement signal partitions that contain random noise.

The awareness of the limitations associated with symbolic dynamics leads to a situation that the selection of parameters in

the symbolic analysis of a time series takes place on the basis of arbitrary decisions or experience in conducting experimental data analysis.

An essential element of symbolic analysis is the determination of sequences of symbolic values selected from a predefined set of symbols. The sequencing procedure by assumption contains a kind of a diagnostic model having the form of a template with a defined length which, when moved step by step in time, sets a different sequence each time. Each of such models of sequences is a new expression of the symbolic time series. Let us note that such a method of construction of symbolic sequences can be compared to immersion in a multi-dimensional space generated by a relevant time lag. In reality no such analogy exists and thus it is hard to expect that symbolic time series will have the same information value as a series obtained as a result of the immersion procedure.

Let us note that for a defined dynamic system and observed process the length of a symbolic sequence is correlated with the selection of sampling frequency on the one hand and the models of the observed phenomenon on the other. Too high sampling frequency can cause the effect of redundancy of information while too small frequency leads to loss of essential diagnostic information and impossibility of accomplishing the assumed diagnostic goal. Various methods are applied to evaluate the adopted sampling method, including the mutual information function:

$$I(\tau) = \sum p_{ij}(\tau)\frac{p_{ij}(\tau)}{p_i p_j} \tag{27}$$

where τ – the lag resulting from the assumed symbol of digitization of measurement results.

Thus, in the case of analysis of results of measurements of complex systems with complex dynamics we can use symbolic transformation which enables transformation of original measurement results into a limited set of discrete symbols.

In the simplest case, when we apply a series composed of binary symbols and while assuming a 3-element sequence, we have the possibility of analyzing 2^3=8 various sequences and examining of dynamics while using a histogram of symbol sequences. For the same binary series and expression length D=2 we will get a four-element set of conditions {00, 01, 10, 11} for which the transitional matrix shall take the form of [12]:

	00	01	10	11
00	P_{00}	$1\text{-}P_{00}$	0	0
01	0	0	P_{01}	$1\text{-}P_{01}$
10	P_{10}	$1\text{-}P_{10}$	0	0
11	0	0	$1\text{-}P_{11}$	P_{11}

While using the measure in the form of a matrix norm**(?)** or applying the method of state equations for Markov models, we can detect the occurrence of a defect. Let us note that in such a case our k nowledge about the occurring phenomenon is based on the analysis of results of observation.

6. Conclusions

Progress in technical diagnosis, in combination with development of micro technology and sensorics, offers the possibility of developing new methods which enable formulation of more reliable forecasts of technical condition changes, thus reducing the uncertainty in the process of operational decisions. At the same time the cost of such systems enable their application in technical objects which present smaller threats for the environment and are characterized by relatively low prices, e.g. general purpose toothed gears.

Due to this an item which is of particular interest is the possibility of forecasting the fatigue-related destruction while relying on the analysis of vibroacoustic signal's structure. This is particularly related to examination of the process of generation and transmission of diagnostic information during the early stages of defect development.

Generally attention is drawn to the fact that defects of contact surfaces, corrosive and erosive wear, emergence of cracks and chipping are the reasons of occurrence of amplitude, phase and multi-parameter modulation of vibroacoustic signals. As a result, apart from accounting for the changes in power distribution for a defined harmonic or between harmonics, the model should distinguish the modulating and modulated functions and it should also describe the occurring modulation phenomena. Additional difficulty is that, as has been proven, along with the development of defects, the set of modulating and carrier functions that contain diagnostic information can change. If in parallel we account for the difficulties occurring during analysis of evolution of signals modulated by many parameters and caused by non-linear effects, then the unsatisfactory, till now, effectiveness of such models in diagnosis of defect development process becomes more comprehensible. On the other hand the low level of the useful signal vs. the noise and the need for applying the relevant selection of signal features make the selection of diagnostic signals with high information content the central issue.

While accounting for the natural feature of vibroacoustic diagnosis, which results from the possibility of registration of big number of vibration runs (leading to excessive information that is most often not fully utilized), the paper presents the issues of data compression and useful diagnostic information selection. In the case of multi-dimensional diagnostic signals the information of defect development is often contained not in the variability of absolute values of respective variables' measures but in the changes of relations between the variables which describe the course of a given phenomenon.

The set of main components, obtained thanks to the applied transformation and reduced in terms of dimensions, can enable extraction of a hidden structure of variables which serve as the basis for diagnostic models. Such a model combines the information on the course of operation and the accompanying wear and tear as well as degradation processes with the information on permitted boundary values for emergency/failure states. On the one hand the projection of the hidden structure enables the reduction of the dimensionality in measurement data and the vector of observed technical state, while on the other hand it enables defining the set of the most correlated components of the diagnostic vector and the technical condition vector, thus enabling not only the explanation of changes in the symptom vector but also ensuring the possibly most effective prediction of technical condition.

****
Scentific research project financed from the scientific research for years 2005÷2007.
****

7. References:

[1] Barschdorff D., Femmer U.: *Signal Processing and Pattern Recognition Methods for Biomedical Sound Analysis*. 2nd International Symposium Acoustical and Vibratory Surveillance Methods and Diagnostic Techniques, ″, pp. 279÷290.
[2] Chudzikiewicz A., Radkowski S.: *Failure – oriented procedure of vibroacoustic signal analysis*. Proceedings of the Third European Workshop Structural Health Monitoring 2006. Juli 5-7 2006. pp. 1300÷1307.
[3] Drożynek P., Veith E.: (2002) *Risk Based Inspection Methodology Overview*; Diagnostyka Vol. 27, 2002. pp. 82÷88.
[4] Eykhoff P.: *Identification in Dynamic Systems*, Warszawa, 1980, (in Polish).
[5] Kumar B. U. K. V., Carroll C. W.: *Effects of Sampling on Signal Detection Using the Cross-Wigner Distribution Function*. Applied Optics, 23/22 4090÷4094.
[6] Mendel J.M.: *Tutorial on Higher-Order Statistics (Spectra) in Signal Processing and System Theory*: Theoretical Results and Some Applications. Proc. of the IEEE, Vol.79 No 3, 1991, pp. 278÷305.
[7] Meng Q., Qu L.: *Rotating Machinery Fault Diagnosis Using Wigner Distribution*. Mechanical Systems and Signal Processing, 5 (3), 1991, pp. 155÷166.
[8] Najar, J.: *Continuous damage of in: Continuum damage mechanics theory and applications*. Editors: Krajcinovic D., Lemaitre J. International Centre for Mechanical Sciences Courses and Lectures, 295, 1991, pp. 234÷293.
[9] Nikias Ch. L., Petropulu A. P.: *Higher-Order Spectral Analysis*, PTR Patience Hall, New Jersey 1993.
[10] Radkowski S.: *Vibroacoustic Diagnostics of Low-energy Failures*, ITE Radkom, 2002, (in Polish).
[11] Radkowski S.: *Nonlinearity and Intermodulation Phenomena Tracking as a Method for Detecting Early Stages of Gear Failures*. Proceedings of the Second World Congress on Engineering Asset Management, WCEAM'2007.
[12] Ray A.: *Symbolic Dynamic analysis of complex systems for anomaly detection*. Signal Processing, Vol. 84, 2004, pp. 1115÷1130.
[13] Schetzen M.: *The Volterra and Wiener Theories of Non-linear Systems*, John Willey & Sons, New York, 1980.
[14] Staszewski W. J.,. Tomlinson G. R.: *Application of the Wavelet Transform to Fault Detection in Spur Gear*. Mechanical Systems and Signal Processing, 8 (3), 1994, pp. 289÷307.
[15] Wang W. J., McFadden P. D.: *Early Detection of Gear Failure by Vibration Analysis-I. Calculation of the Time-Frequency Distribution.* Mechanical Systems and Signal Processing, 7(3), 1993, pp. 193÷203.
[16] Yatomi M. ai all.: *Application of Risk-Based Maintenance on Materials Handling Systems*, IHI Engineering Review, vol. 37, No 2, 2004, pp. 52÷58.

Prof. dr hab. inż. Stanisław RADKOWSKI
Institute of Machine Design Fundamentals
Warsaw University of Technology
Narbutta 84 , 02-524 Warsaw, Poland
E-mail: ras@simr.pw.edu.pl

Zoltán KALINCSÁK
János Gábor TAKÁCS
Károly SÓLYOMVÁRI
Balázs GÖNDÖCS
Géza Cs. NAGY

LOCAL LASER MARKING – NEW TECHNOLOGY IN THE IDENTIFICATION OF STEEL PARTS

The importance of identification of machines in the field of maintenance becomes more and more significant. In the field of mechanical maintenance or especially in large-scale production serious difficulties cause to identify various metal parts which have similar form and/or size during technological process. The paper based and printed barcode seemed a safe resolution to this purpose. Unfortunately during the repairing or renewal process the paper based barcodes of steel parts very often were destroyed or damaged, the currently applied paper based and painted codes can cause data losses. This is the fact which indicated the research of steel marking system. In this type of marking the material contains the signs. Other advantage of this system is the readability beneath from painted layer.

Keywords: *Advanced materials, laser beam induced transformation, low carbon steel, barcode, eddy current loss, Fluxset sensor.*

1. Introduction

In this paper some new results of laser marking will be presented obtained during CO_2 laser irradiation. This type of marking is considered to apply as barcode for identification in industry and production logistics. The physical basis of the marker evolution is a local phase transformation in the vicinity of the surface in a low and high carbon steel occurring as a consequence of rapid heating and cooling process. A special Fluxset sensor [1] was applied for the read out which is based on eddy current measurements. The spatial resolution of the marker density will be determined from the point of view of applied sensor. The codes can be successfully detected using this sensor, even beneath the 1 mm painted layer. The markings are thermally stable enough to use them as barcodes in the field of maintenance.

The productions of laser marking on the surfaces of rails have been described in [2]. This type of marking is considered to apply for the detection of thermal induced stresses, as well as to produce bar codes as signals on low carbon steel surfaces for production logistics. The thermal stability of markings has of a primary importance for any application (particularly in the case of magnetic reading out technique like (i.e. using Barkhausen effect, eddy current testing). The fitting of the scribing parameters (power density, scanning rate, distance between the individual marks) are also important requirement for the point of view the reading out.

The physical basis of the reading out is the local phase transformations and the local modifications in the stress field around the individual markers. It is caused by the rapid heating and cooling processes during the laser-metal interaction.

The appropriate reading out is usually based on magnetic or classical eddy-current measurements. In our measurements a special sensor was used to reading out. It was found, that markers produced in 100-300 W power ranges with the 6 mm distance between them are successfully detectable using this sensor. The markings are thermally stable enough to use them as barcodes in production logistic and car industry to mark the car body sheets (Fig. 1). Magnetization processes are also involved in the development of eddy current losses therefore the local modification of the domain structure is also important in the process. Therefore, the direct observation of magnetic properties (domain structure in the surface layer) can also be important from point of view reading out. Some results associated with the outlined topics will be presented in this paper.

2. Experimental details

2.1 Materials

Samples are prepared from cold rolled low carbon steel sheets (C content 0.1 Wt%; Si 0.34 Wt%; Ti 0.06 Wt%; Mn 0.85 Wt%;). The sheets were covered with 0,01 mm thick phosphate layer. As the carbon content is low, the investigated sheets can be regarded

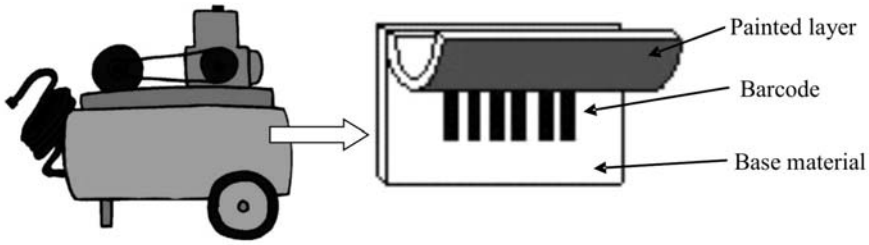

Fig.1.Identification of machines

as soft magnetic. The Fig. 2 shows schematically the local laser treating process and modal structure of laser beam. The applied diameter of laser spot was 1 mm and the movement speed was 1200 mm/min.

2.2 Principle and device for the reading out

The ECT probe

The principle of the applied readout device is described in [3]. The sensor consists of a magnetic field detector (i.e. Fluxset sensor, see in Fig. 3a) and pancake shaped exciting coil, which generates alternating magnetic field perpendicular to the specimen surface. This exciting field induces eddy current in the inspected conductive plate. The magnetic detector measures one of the horizontal (i.e. surface parallel) component of the field only, and it is located exactly in the axes of the exciting coil between the coil bottom and the specimen surface(see in Fig. 3a and b). The Fluxset magnetic sensor based on ECT (eddy current testing) is working at 20 kHz excitation frequency trough 1 mm thick plastic insulation (i.e. probe lift-off, the "*a*" parameter in Fig. 3b).

The described ECT method has two particular advantages for the laser scribing application. It is based on alternating magnetic field excitation despite of any constant (DC) methods such as the leaking flux technique. That means, it does not relay on the previous magnetic state of the inspected specimen or it does not require the magnetisation or demagnetisation in its whole volume prior to the measurement. On other hand, the probe is based on high sensitivity Fluxset sensor, which has high spatial resolution as well. The separation of the excitation and the sensing in the probe makes possible to increase the probe resolution, therefore the density of markers as well, without any risk of degradation in the sensitivity of probe. It can be observed well that even the effect of the lowest energy produced markers are clearly detectable. As a consequence, this arrangement is sensitive exclusively for magnetic field perturbations caused by the asymmetric distribution of the eddy currents in the presence of any localised changes of the magnetic material property inherited from the effect of the laser scribing

To detect the local changes of the conductivity as well as of the magnetic property in steels is traditional task for ECT methods. The ECT also offers contact free operation, which makes us possible to detect the existence of the transformed volume of alloy caused by the scribing even below the protective coating (like the painting). The transformed area, which is produced by using varying power density laser beams in which the magnetic behaviour differs from the untouched surrounding areas due to this treatment, can be made visible by help of the ECT technique.

2.3 The physical background of marker formation obtained by laser scribing

The laser scribing represents rapid local heating and subsequent rapid cooling in the vicinity of the surface of irradiated sheet. The Fig. 4 shows the markers on the surface of a low carbon steel. In Fig. 5 the photomicrograph on the cross-section of transformed zone can be seen. The resolution of micrograph is too low, consequently the structural changes are not visible in Fig. 5. As a consequence of the entrapped C atoms (metastabil solid solution formation) together with the heat shock induced stresses arising from the misfit between the heat affected and unaffected zones causes a local resistance increase in the sheet. This is the basis of the reading out.

The control of energy density is necessary in order to avoid the local surface melting (overheating effect). On the order hand the energy input should be high enough to rise the local temperature for the enhancement of solution of carbon in the austenite phase.

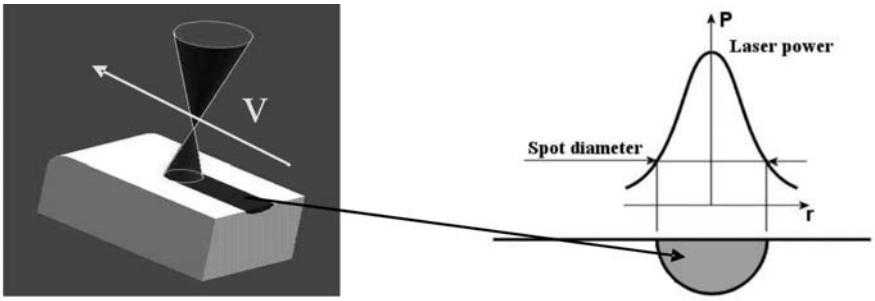

Fig. 2. Process of laser scribing and modal structure

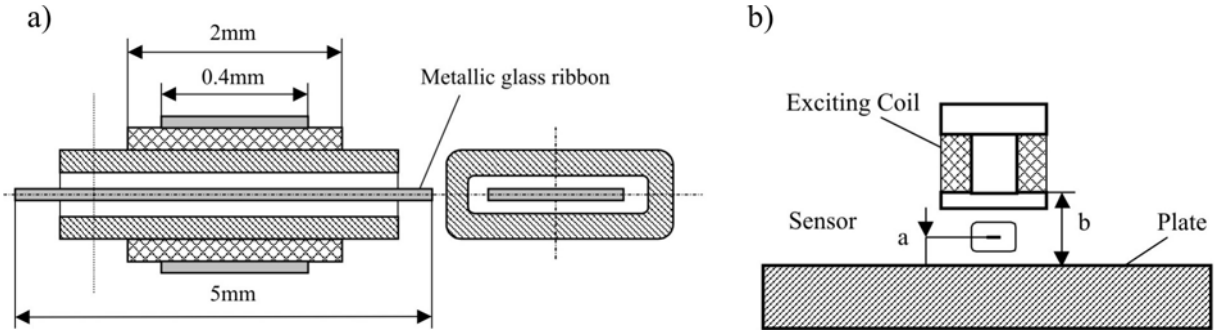

Fig. 3. a) Fluxset sensor geometry b) Probe set-up

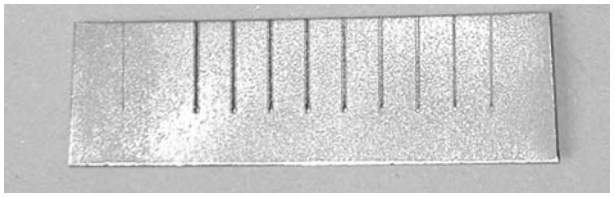

Fig. 4. Laser scribed low carbon steel sheets applying various laser power (100-300 W) and constant distance between marks

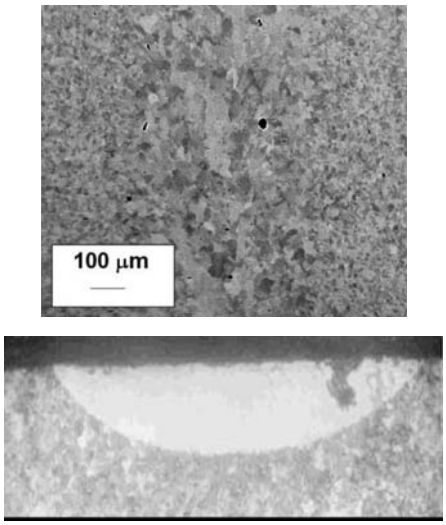

Fig. 5. Photomicrograph of laser marked sheets. Left: low carbon steel (0.1 C%); right: high carbon steel (0.6 C%)

2.4 Marker stability and the resolution of reading out

Fig. 6 does supply a qualification of the laser scribed markers. The position of periodic markings versus of the distance are plotted here. Distance between marks was 6 mm, the applied laser density is changed between 100 W to 300 W (raised by 25 W). The physical position of marks are at around of the inflectional points of signal curves. In this figure the influence of long time heat treatment on the shape of signal curves is also illustrated. It is obvious that the amplitude of the signal curve increases due to the subsequent heat treatment. Meanwhile no change in the position of maxima can be detected. These facts do confirm the sufficient thermal stability of markers from the point of view read out.

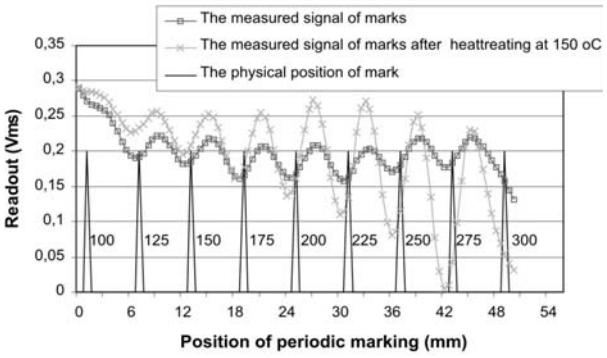

Fig. 6. Readout on laser scribed steel sheets using various laser density

The information density can be increased by lowering the distance between the individual markers. Therefore, the distance between the markers is also important factore from point of wiev of reading out. In principle, the density of markers can be technically also increased by applying the same laser power density as it is illustrated in Fig. 7. In this experiment the distance between the markers was gradually decreased using constant power density (see Fig.7). Fig. 6 shows the concrate arrengements of signs. The beginning overlap between the heat affected zones associated with the individual markers represents the limit of spatial resolution which can be attained with a given set of scribing-readout system.

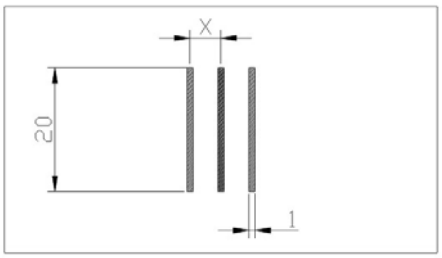

Fig. 7. The marking arrangement produced by constant (150 W) laser power density and spot diameter (1 mm) and various distance between marks

For example, the power density was 150 W, and the distance between markers was narrowed. The power density in a surface unit:

$$A = (d^2 * \pi)/4 = (l^2 * \pi)/4 = 0.7854 \text{ mm}^2 \quad (1)$$

$$Pd = P/A = 150\text{W} / 0.7854 \text{ mm}^2 = 190.98 \text{ W/mm}^2$$

Pd: power density in a surface unit [W/mm^2], *P* : applied laser power [W], *d* : diameter of laser spot [mm], *A*: area of laser spot [mm^2].

The results of readout obtained by the same Fluxset sensor is completely differ in the case of applied markers distance as the Fig. 8 shows. In this Fig. can be seen the results of reading out, when the distance between marks was diferent. The sensor can detect the individual marks when the distance between marks is relatively high. The arised heat affected zone around the marks influence the reading out.

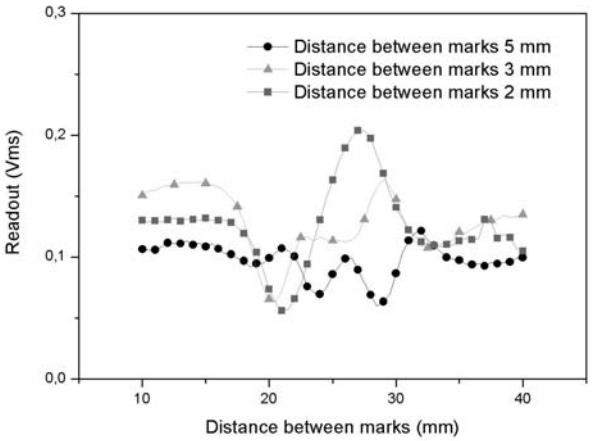

Fig. 8. The result of readout on laser scribed steel sheets. The applied laser density was 190 W/mm^2 (150 W)

3. Conclusions

Stable markers can be produced by the laser scribing within the power density range of 100-300 W (resulting good signal/ noise relation during the reading out). The distance between marks has of a crucial role from point of view of reading out. The exact reading out depends on the actual extension of the heat-affected zone around marks. Though the resulting markings are not always directly visible by light microscope, their thermal stability is sufficient up to 150 °C. Therefore one can conclude, that the FLUXSET type eddy current probe is suitable for detecting the laser-scribed markers on the surface of (0,1% C) Fe-C low carbon steel sheets even in the case of the signals produced by the lowest energy described. To reduce the length of barcodes should be important applying smaller laser diameter hereby decreasing the extension of heat affected zone.

****

This work has been supported by National Office for Research and Technology (NKTH).
Project number: AGE-00015/2003, TéTA-4/03.

****

4. References

[1] Gasparics A., Daroczi Cs.S., Vértesy G., Pavo J.: *Improvement of ECT probes based on Fluxset type magnetic field sensor*, in Electromagnetic Nondestructive Evaluation (II.), pp. 146-151, R.. Albanese et al. (Eds.), IOS Press, 1998.

[2] Takács J., Keszte R.. Markovits T., Posgai Gy., Molnár P., Béli J.: *Precision local laser heat treatments for information input*, 18th Internation Colloquium Dresden 20-22. 05. 2001 ISSN 1433-4135

[3] Vértesy G., Gasparics A., Szöllősy J.: *High sensitivity magnetic field sensor*, Sensors and actuators 85, pp.202-208, 2000

Zoltán KALINCSÁK PhD student
Department: Vehicles Manufacturing and Repairing
University: Budapest University of Technology and Economics
Address: H-1111 Bertalan L. 2., Budapest, Hungary
E-mail: kalincsak@kgtt.bme.hu
Dr. János Gábor TAKÁCS
Dr. Károly SÓLYOMVÁRI
Dr. Balázs GÖNDÖCS
Dept. of Vehicles Manufacturing and Repairing,
BUTE, H-1111 Bertalan L. 2., Budapest, Hungary
Dr. Géza Cs. NAGY
Faculty of Engineering, University of Pécs, Pécs
H-7624 Boszorkány u. 2. Hungary

Sylwia WERBIŃSKA

THE AVAILABILITY MODEL OF LOGISTIC SUPPORT SYSTEM WITH TIME REDUNDANCY

Any operational system, in order to successfully accomplish its intended mission, must rely on logistic support that will be available when required. According to this, unlike traditional approaches to availability development, the paper indicates on the problem of integration between two systems – operational and its supporting system into one 'system of systems'. Moreover, in many systems undesired event (system failure) occurs later than components failure, and only if repair is not completed within a defined period of time. The time dependency is a convenient approach for definition of interactions between the above systems. Thus, the paper considers the time dependent system of systems where the system total task must be executed during constrained time resource. For the developed model, there are derived general equations for the evaluation of system of systems availability function and steady-state availability ratio. The model solution is obtained based on analytical method. Furthermore, the mathematical expressions for the mean availability ratio are derived when the all probability density functions are to be exponential. The theoretical results are discussed with sensitivity analysis.

Keywords*: logistic support system, availability, time redundancy.*

1. Introduction

The proper organized and reliable logistic support affects the execution of operational tasks. When the logistic activity is narrowed down to the supply activity, we can say that the basic elements are focused on providing the necessary supplies and services on the proper time for the right money [23]. In the case of maintaining the operational processes of technical system, the supply stream consists of five elements presented in figure 1.

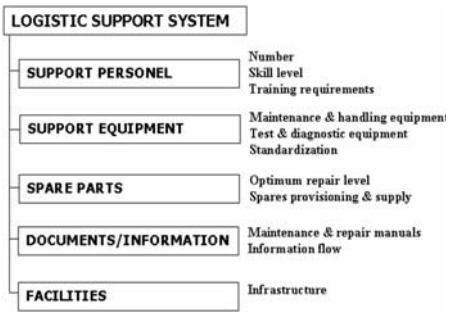

Fig. 1. Logistic support elements [2, 3, 4, 15]

On the other hand, every logistic support system, operating under an increasingly complex and diverse system environment, may fail what, in consequence, may lead to:

- disruption of supporting task realization,
- inability of system to undertake a new task.

As a result, there is a need to take into account the possible unreliability of logistic support elements, which may lead to decrease of performance of the system being supported. On the background of these considerations, the analysis of operational system reliability or availability cannot be done in isolation without taking into account the numerous links with its logistic support system. The plethora of studies dealing with the problem of designing the reliable and available support systems for repairable items confirms the necessity of this kind problem investigation.

At present, the studies which investigate the problem of logistic support system availability assessment may be divided into four main groups:

* *spare allocation models* – optimization models that consider the relationship between supply system performance and stock levels for individual items and use sophisticated techniques for the optimum allocation of inventory under funding constraints. Models of this type focus upon the procurement and depot repair of spare repairable items in a multi-echelon inventory systems.
* *design models* – focus on system design characteristics (equipment reliability, structure, redundancy, utilization) and their effects upon operational availability/reliability.
* *(r, s) models* – in which there is investigated the problem of providing necessary spare parts (s) and number/allocation of repair facilities (r). Most of these n-unit redundant system models base on the queuing theory, what means that the times to unit failure and unit repair have exponential probability distributions.
* *(rm, s) models* – except from the problem of necessary spare parts providing, there is also developed the impact of repairmen capability to recovery task performance on the system availability. As well as (r, s) models, this group of logistic support models mostly base on the queuing theory.

The table 1 serves to illustrate the examples of the above logistic support availability assessment models.

All the presented models investigate the problem of availability assessment for logistic support system and its supporting system separately. However, in order to achieve the availability assessment, there is a need both to integrate the logistic system fully with the operational system into one 'system of systems' model [23].

According to the definition, the system of systems context arises when a need or a set of needs are met with a mix of multiple systems, each of which are capable of independent operation but must interact with each other in order to provide a given capability. The loss of any part of the system will degrade the performance of the whole [5].

The literature on modeling system of systems is still scarce. The interactions between an operational system and its supporting system have not been clearly investigated. As a result, the major questions in this research area to be discussed are:

- how to describe the interactions between these two mentioned systems, and in fact develop the system of systems?
- what does it mean that system of systems is available?

2. System of systems with time dependency

In many systems undesired event occur later than components failure, if and only if the repair is not completed within a grace period. In other words, time redundant system has the ability to tolerate interruptions in their basic function for a specific period of time without having the negative impact on the system task performance.

Typically, the time redundant systems have a defined time resource, denoted by γ that is larger than the time needed to perform the system total task. However, unreliability of system element may cause time delays which in turn would cause the system total performance time to be unsatisfactory. As a result, considering the system task completion time as a random variable, the probability that mentioned time will be longer than the restricted time resource may be defined as the unreliability index [13, 23].

According to the present knowledge, the time redundancy is considered as the effective tool for e.g. reliability improvement. In the case of two or more independent systems integration problem, time dependency is a convenient approach used to integrate these systems. After having analyzed the literature on modeling systems with time dependency (see e.g. [19, 23]) it was possible to define the logistic support system for operational processes.

2.1. The model description

Consider a repairable system of systems under continuous monitoring, in which are integrated two independent systems: a single-unit operational system and its supporting system. Both systems have only two states: up state, when they are operable and can perform its specified functions, and down state, when they are inoperable.

Let's assume that the operational system experiences random failures in time, and each failure entails a random duration of repair time before this system is put back into service. After repair mentioned system is 'good-as-new'. Moreover, let's also assume that any information about these failures is reliable and immediately comes to the logistic support system.

On the other hand, the logistic support functions are narrowed down to one main task – providing the necessary spare parts to the operational system. As a result, the logistic support system is inoperable when there is no capability of supplying the operational processes with necessary spares.

On the background of these considerations, in the logistic support area there can be especially used the individual time redundancy to model the system of systems performance [23]. Thus, if there is defined the system of systems total task as the continuous performing of exploitation process, the only way to provide it is the cooperation between the operational and its supporting system. As a result, the system of systems reliability is defined as its ability to correctly complete the task during the corresponding time resource γ, which may be randomly distributed [23].

Taking into account the above considerations, the probability that the system of systems at the random point in time is in up/downstate depends on:

- random variables describing the life times of the systems,
- random variable defining the repair time of operational system,
- random variable describing the delivery time of ordered spare parts,
- chosen stock policy, used in the logistic support system,
- restricted time resource.

Tab. 1. The main models of logistic support systems for repairable items.

S. No.	Type	System description	Methodology	No. of o. s. elements	No. of r./rm.	Author(s)	Remarks
1	Spare allocation models	three-echelon repairable item inventory system	Queuing theory	J	-	Coughlin (1984)	-
2		two- and three-echelon repairable item inventory system	Queuing theory/ Markov processes	N		Gross, Gu & Soland (1993)	finding the steady-state probability distribution of the Markov process
3	Design models	aircraft spares provisioning decisions with respect to a user specified availability goals	Queuing theory			Cochran, Lewis (2002)	finite queuing spare models connected with component redundancy
4	(r, s) models	redundant repairable system with one operating unit	Simulation	1	1	Ke & Chu (2006)	investigation of three various types of lifetime distribution & two kinds of repairing time distribution
5		single unit system supported by a single spare	Analytical			Kumar & Sen (1995)	the use of the convolution of p.d.f. F of lifetime and d.f. G of repairing time
6		one-unit repairable system with s spares remained on cold standby			r	Sarkar & Li (2006)	lifetime distribution – arbitrary continuous CDF with density function f, repair times are exponentially distributed
7		m-out-of-n redundant & cold standby system	Analytical/ numerical	n		Gurov & Utkin (1995)	investigated different condition of repair
8		n-unit warm standby system with r repair facilities and PM	Queuing theory			Subramanian & Natarajan (1981)	PM rate is a constant
9		k-out-of-n redundant & hot standby system	Exact/ Approximate method		c parallel channels	Destombes, Heijden & Harten (2004)	p.d. functions are exponentially
10	(rm, s) models	machine repairable system with m-operating units & s warm standby units	Queuing theory/ numerical		1	Jain & Maheshwari (2004)	system with reneging
11		r-out-of-n standby system	Markov processes/ numerical		r = 1, rm = c ≥1	Barron, Frostig & Levikson (2006)	investigated cold and warm standby

Figure 2 illustrates the system of systems model, when the critical inventory level (CIL) is used as a stock policy.

According to the scheme, the operational system experiences random failure in time. Information is immediately sent to its logistic system. When there is available spare element in the remaining stock, the necessary one is sent to the operational system. In this situation, the time of supply task performance, denoted by τ is equal to zero. When there are no available spare parts, the time τ lasts from the moment of failure till the new delivery arrival. Finally the operational system is put back to service.

If there is restricted the system of systems total task completion time, defined as the time of operational system recovery process, the system of systems remains in upstate if this defined time will be shorter than time resource. Otherwise, the system of systems will fail and remain in downstate till the end of operational system maintenance process.

The chosen stock policy affects the possible periods of time without spare parts and the way the system of systems performs. The moment, when inventory level in logistic system achieves critical point is the impulse to place a new order. Before the new delivery arrival, the operational system can only use limited amount of spare elements taken from the remaining stock. Demand that is not immediately satisfied is backordered and filled when a new order arrives. After the delivery, new elements are used according to system demand until the stock level falls again to the critical point. The time between two orders placing defines a procurement cycle.

The main measure, which may define the presented system of systems failure, is the probability of its downtime caused by over crossing the defined time resource by the system total task performance.

2.2. System of systems downtime caused by over crossing the defined time resource

In a single cycle the system of systems may fail if:

- time of supply task performance lasts longer than the defined time resource (system of systems downtime includes the lead-time from the moment of over crossing the γ, and the time of operational system recovery),
- time of operational system recovery lasts longer than the defined time resource (system of systems downtime encompasses the remaining repair time from the moment of γ over crossing).

In order to evaluate the mathematical model of system of systems downtime, it is necessary to define the following assumptions:

- time to failure of operational system is described by known probability density function (p.d.f.) $F(t)$ with density $f(t)$,
- operational system recovery is defined as fault component replacing by a spare element taken from remaining stock in the logistic support system,
- repair time is described by known p.d.f. $G(t)$ with density $g(t)$,
- at the moment $t = 0$ spares level achieves the critical point and the new cycle begin,
- critical inventory level is equal to s elements in a stock,
- during the one procurement cycle operational system may use Q elements which is the ordered delivery quantity,
- lead-time (period between moments when a new order is placed and when it is delivered) is random variable with known p.d.f. $E(t)$ and density $\varepsilon(t)$,
- time resource γ is random variable described by known p.d.f. $\Phi(t)$ with density $\varphi(t)$.

To determine how long system of systems downtime caused by over crossing the defined time resource can last, it is necessary to evaluate the probability $n(t)$ that the last allowable operating element failure will occur in Δt period during one procurement cycle. It can be calculated as the $s+1$-fold convolution of function $f_1(t)$ [7]:

$$n(t) = f_1^{s+1}(t) \tag{1}$$

where: $f_1(t)$ = probability that operating element will fail and its replacement will be finished during the Δt period, derived as a convolution of functions $f(t)$ and $g(t)$:

$$f_1(t) = \int_0^t f(x)g(t-x)dx \tag{2}$$

where: $f(t)$ = probability of operational system failure, $g(t)$ = probability of its recovery.

Let's now assume, that random variable ξ_1 defines the period of time which elapses between two points in the procurement cycle:

- the moment when the whole process of operational system recovery over crosses the restricted time resource (the moment of system of systems failure),

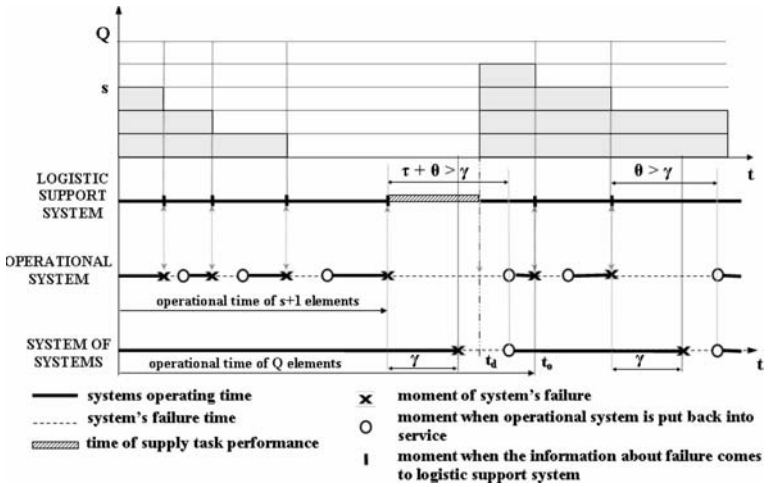

Fig. 2. Time dependent system of systems model with a single-unit operable system and CIL as a stock policy

- the moment when the operational system replacement process is completed (the supply task is completed and the repair process is also finished).

Consequently, ξ_1 defines the period of system of systems downtime. According to this, there can be obtained the mathematical function:

$$b_1(\xi_1) = \int_0^{\xi_1} b(x) \cdot g(\xi_1 - x)dx \tag{3}$$

where: $b_1(t)$ = probability function which defines the time of system of systems downtime, $b(t)$ = probability density function of system of systems downtime caused by over crossing the time resource due to lack of spare parts, defined by the following function:

$$b(\xi) = \int_0^{\infty} \varphi(t) \cdot \psi(t + \xi)dt \tag{4}$$

where: ξ = random variable which defines the period of system of systems downtime due to supply task performance time over crossing the time resource, $\varphi(t)$ = probability density function of time resource γ, $\psi(t)$ = probability density function which defines the period of supply task performance, obtained from the following formula:

$$\psi(\tau) = \int_0^{\infty} n(t) \cdot \varepsilon(t + \tau)dt \tag{5}$$

where: τ = random variable which defines the supply task performance time.

Function $\psi(t)$ defines the period of time between the operating unit failure and the new delivery physically execution.

According to the assumptions, when the operational system fails during the procurement cycle Q-1 times there will be allowable spare parts needed in the recovery process ($\tau = 0$) and only one time there can be such a situation that there is no available spare parts in the logistic system ($\tau > 0$). As a result, the possible system of systems downtime, due to replacement time over crossing the defined time resource, may be defined by:

$$w(\xi_1) = \int_0^{\infty} \varphi(t) g(t + \xi_1)dt \tag{6}$$

Consequently, the probability of any system of systems downtime during the procurement cycle may be defined as:

$$b_2(\xi_1) = \frac{1}{Q} b_1(\xi_1) + \frac{Q-1}{Q} w(\xi_1) \tag{7}$$

3. System of systems availability

Availability is the measure of the degree to which a system is capable of operating under stated conditions of use and maintenance, at an unknown (random) point in time [15]. If we make an assumption, that all elements which work in the system are characterized by identical probability distribution of lifetime and renewal time, the availability function can be defined by the following formula [7]:

$$A(t) = 1 - F(t) + \int_0^t [1 - F(t - x)]h(x)dx \tag{8}$$

where: $F(t)$ = cumulative of system lifetime probability distribution, $h(t)$ = process renewal density given by the following formula [7]:

$$h(t) = \sum_{i=1}^{n} f_1^i(t) \tag{9}$$

In order to obtain the availability function assessment for the analyzed system of systems with time dependency, it is necessary to consider three sub periods occurring during one procurement cycle. First sub period encompasses the time between the moment the stock reaches CIL and the moment the last allowable spare part is used. During this sub period availability depends on:

- time to failure of s allowable elements,
- time of operational system recovery.

The second sub period encompasses the time to failure of $s + 1$ element and its replacement time. In this sub period the system of systems may fail due to lack of spare parts or/and too long replacement time. The third sub period includes the time between the moments when the new delivery arrives till the instant of time when the stock achieves again the ordering point. Availability depends on:

- time to failure and recovery time of operational system,
- time of supply task performance.

As a result, the renewal density function h(t) changes during the procurement cycle. When the new cycle begins (inventory level reaches CIL):

$$h_1(t) = \sum_{i=1}^{s} f_r^i(t) \tag{10}$$

where: $fr(t)$ = the convolution of functions $m(t)$ and $w(t)$:

$$f_r(t) = \int_o^t m(t - x)w(x)dx \tag{11}$$

where: $w(t)$ = probability density function which defines the system of systems downtime due to replacement time over crossing the time resource, m(t) = probability that a system of systems will fail in the Δt period, given by the formula:

$$m(t) = \left[\int_0^t f(t - x)\varphi(x)dx\right] \cdot \int_t^{\infty} g(x)dx \tag{12}$$

When all allowable spare elements are used, system of systems may fail also because of supply task performance time over crossing the time resource. Thus, the sub renewal density is expressed by the formula:

$$h_2(t) = \int_o^t m(t - x)b_2(x)dx \tag{13}$$

As a result, all moments of consecutive failures may shift in time, and the sub renewal density may be defined as:

$$h_3(t) = \sum_{i=s+2}^{Q} \int_o^t f_r^i(t - x)\psi(x)dx \tag{14}$$

Consequently, the process renewal density is expressed as:

$$h(t) = h_1(t) + h_2(t) + h_3(t) \tag{15}$$

The mathematical model of system availability function is almost never used in practice. Instead of it, there can be evaluated the steady-state availability ratio.

3.1. System of systems availability ratio

The basic formula for steady-state availability ratio assessment is expressed as follows [7]:

$$A = \frac{T^O}{T^O + T^R} = 1 - \frac{T^R}{T^O + T^R} \tag{16}$$

where: T^O = expected system's time to failure, T^R = expected repair time.

For the presented system of systems with time dependency, the mean availability in one procurement cycle is expressed as:

$$A = 1 - \frac{T^{\xi_1}}{Q(T^O + T^R) + T^\tau} \tag{17}$$

where: T^{ξ_1} = expected system of systems downtime caused by the time of operational system recovery, T^O = expected time to failure of operational system, T^R = expected replacement time of operational system, T^τ = expected supply task performance time, Q = ordered delivery quantity which is accessible to be used during a single cycle.

The expected values, which define the mean duration of systems uptimes and downtimes in one procurement cycle, may be obtained from the following formulae:

- expected time to failure of operational system:

$$T^O = \int_0^\infty t \cdot f^Q(t)dt \tag{18}$$

where: $f^Q(t)$ = Q-fold convolution of function $f(t)$.

- expected time of operational system replacement:

$$T^R = \int_0^\infty t \cdot g^Q(t)dt \tag{19}$$

where: $g^Q(t)$ = Q-fold convolution of function g(t).

- expected time of supply task performance:

$$T^\tau = \int_0^\infty \tau \cdot \psi(\tau)d\tau \tag{20}$$

- expected system of systems downtime caused by system total task performance time over crossing the defined time resource:

$$T^\tau = \int_0^\infty \tau \cdot \psi(\tau)d\tau \tag{20}$$

4. System of systems steady-state availability ratio when all distributions are to be exponential

To evaluate the availability function $A(t)$ given by formulae (8)-(15), there have to be solved n-fold convolution of given functions (e.g. $f^n(t)$, $g^n(t)$, $f(t)*g(t)$). According to the literature, there have been made some suggestions to employ the Laplace transform technique (see, for example, [7]). However, a lot of problems arise in inverting the Laplace transform. Except in the case when the underlying distributions are exponential, this is a formidable task [12].

According to the above considerations, there have been made following simplified assumptions to evaluate system of systems mean availability ratio:

- time to failure of operational system and its replacement time are exponentially distributed with hazard rate λ and repair rate μ,
- lead-time is random and its probability distribution is exponential with parameter β,
- time resource is random and exponentially distributed with rate ν,
- system of systems is in steady state,
- the results from theoretical model are derived for quantity of s redundant elements kept as CIL, when s = 0, 1, 2, 3,
- relation: $\frac{\lambda}{\mu} \leq 1$.

The level of system of systems steady-state availability ratio depends upon the particular level of hazard rates λ, β, μ, ν and quantity of spare parts kept as CIL. Obtained chosen results of sensitivity analysis for theoretical model of mean availability ratio are presented in figures: 3-6.

The influence of mean operational system lifetime on the availability ratio is characterized by the level of hazard rate λ (figure 3). As might be expected, the greater the time between failures of this system, the less is required expensive maintenance, critical test equipment, unique training, as well as other logistic elements. Moreover, the availability ratio increases. It is also worth mentioning, that when the time between failures is longer, there is more possible, that new delivery will arrive before all available spare parts are used in the recovery process. As a result, when CIL level increases, the availability ratio also increases.

The next example (figure 4) serves to illustrate the influence of mean lead-time on availability ratio. When system of systems is in steady-state and there are no supply deliveries performed (β=0), availability ratio is equal to zero. On the other hand, when the time of delivery decreases (β increases), the probability that there will be no free spare parts when needed is lower. As a result, the probability that system of systems fails decreases what has the positive impact on the level of availability ratio.

As might be expected, there is also a strong connection between the level of mean time resource γ, characterized by ν, and the availability ratio. The greater the level of time resource for described total task performance, the greater system of systems ability to tolerate any interruptions during its normal processes realization. As a result, the availability ratio also increases due to shorter system of systems downtime periods.

Finally, there can be analyzed the interaction between mean operational system downtime (characterized by μ) and the level of availability ratio. When taking into considerations system of systems with $s > 0$, the longer the system is inoperable, the greater the probability that system of systems fails. In consequence, the

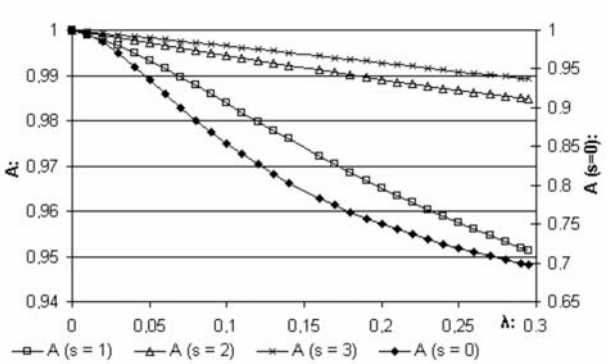

Fig. 3. Availability ratio for β = ν = 0.1 and μ = 0.3

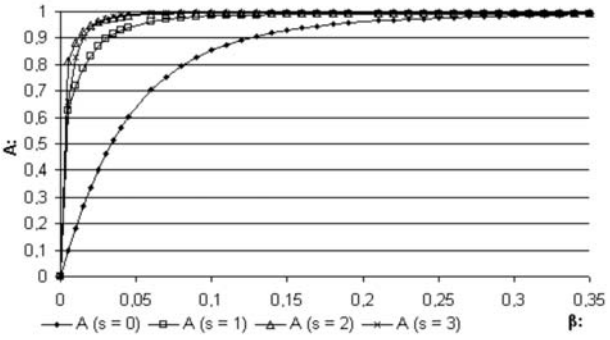

Fig. 4. Availability ratio for λ = ν = 0.1 and μ = 0.3

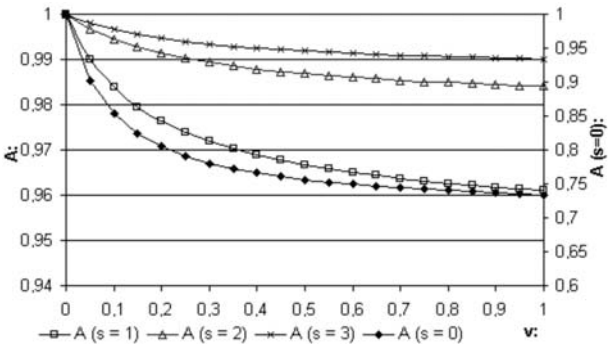

Fig. 5. Availability ratio for $\lambda = \beta = 0.1$ and $\mu = 0.3$

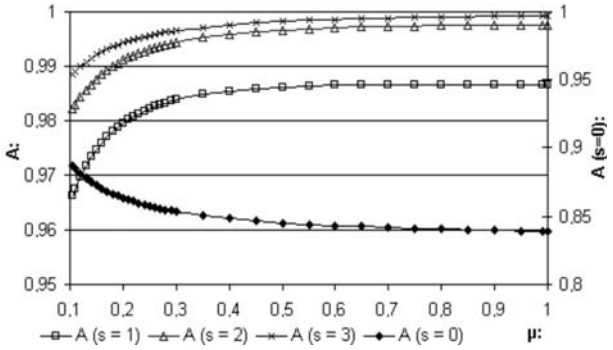

Fig. 6. Availability ratio for $\lambda = \beta = \nu = 0.1$

availability ratio decreases. However, for those specific assumptions made for system of systems model development, taking into account system with $s = 0$ the availability ratio decreases despite shorter downtime periods. This kind of system of systems behavior is connected with supply process organization. The new order is placed when operational system fails. In that situation the time of supply task performance has great influence on availability ratio due to affecting the total time of operational system recovery process, and the probability of system of systems failure.

All the presented examples shows, that despite the level of parameters λ, β, ν, μ, the more spare parts is kept in the logistic supply system, the greater the level of availability ratio can be obtained.

Thus, the analysis results confirm the theoretical view of the relations between the rates and the availability ratio. The obtained results from the sensitivity analysis will be different for: e.g. other repair frequency, various mean repair time, various periods of lead-time, or other time resource γ.

5. Conclusions

For summarizing the above considerations, it has to be underlined that:

- the analysis of operational system availability cannot be done in isolation without taking into account the problem of support processes performance and its reliability,
- the presented theoretical system of systems model provides the convenient framework for defining the optimal time resource period taking into account the economical constraints,
- the complexity of integration problem between operational system and its supporting system confirms the necessity of further development.

6. References

[1] Barron Y., Frostig E., Levikson B.: *Analysis of R out of N systems with several repairmen, exponential life times & phase type repair times: An algorithmic approach*. European Journal of Operational Research 169 (2006).

[2] Catuneanu, V. M., Moldovan, C., Popentin, Fl. & Gheorghin, M.: *Optimum system availability and spare allocation*. Microelectronic Reliability. Vol. 28 No. 3/1988.

[3] Cochran J. K., Lewis T. P.: *Computing small-fleet aircraft availabilities including redundancy and spares*. Computers & Operations Research 29 (2002).

[4] Coughlin, R. J.: *Optimization for spares in a maintenance scenario*. In proc. symp. Annual Reliability and Maintainability Symposium 1984.

[5] Crossley, W. A.: *System of systems: an introduction of Purdue University Schools of Engineering Signature Area*. http://esd.mit.edu/symposium/pdfs/papers/crossley.pdf (29.11.2006).

[6] de Smidt-Destombes K. S., Van der Heyden M. C., van Harten A.: *On the availability of a k-out-of-N system given limited spares and repair capacity under a condition based maintenance strategy*. Reliability Engineering and System Safety 83 (2004).

[7] Gniedenko, B. W., Bielajew, J. K. & Sulowiew, A. D.: *Mathematical methods of reliability theory*, (in Polish) Scientific & Technical Publishing House, Warszawa 1969.

[8] Gross, D., Gu B., Soland R. M.: *Iterative solution methods for obtaining the steady-state probability distributions of Markovian multi-echelon repairable item inventory systems*. Computers & Operations Research Vol. 20, No. 8 1993.

[9] Gurov S. V., Utkin L. V.: *The time-dependent availability of repairable m-out-of-n and cold standby systems by arbitrary distributions and repair facilities*. Microelectron. Reliability Vol. 35, No. 11 1995.

[10] Jain M., Rakhee, Maheshwari S.: *N-policy for a machine repair system with spares and reneging*. Applied Mathematical Modeling 28 (2004).

[11] Ke J-Ch., Chu Y-K.: *Comparative analysis of availability for a redundant repairable system*. Applied Mathematics & Computation 2006.

[12] Kopocinski B.: *A draft of renewal and reliability theory*, (in Polish) Scientific & Technical Publishing House, Warszawa 1973.

[13] Langer Y.: *System with time-redundancy; In proc. symp*. Annual Reliability and Maintainability Symposium 2001.

[14] Lisnianski A., Levitin G., Ben-Haim H.: *Structure optimization of multi-state system with time redundancy*; Reliability Engineering and System Safety 67 (2000).

[15] OPNAV Instruction 3000.12A.: *Operational availability of equipments and weapons systems*, Department of the Navy, Washington D.C. 2003.

[16] Sarkar, J. & Li, F.: *Limiting average availability of a system supported by several spares and several repair facilities*. Statistics and Probability Letters 76/2006.

[17] Sen P. K.: *Statistical analysis of some reliability models: Parametrics, semiparametrics and nonparametrics*. Journal of Statistical Planning & Inference 43 (1995).
[18] Subramanian R., Natarajan R.: *An n-unit standby redundant system with r repair facilities and preventive maintenance*; Microelectronic Reliability Vol. 22, No. 3, 1982.
[19] Vaurio J. K.: *Reliability characteristics of components and systems with tolerable repair times*; Reliability Engineering and System Safety 56 (1997).
[20] Wang K-H., Hsieh Y.: *Reliability of a repairable system with spares and a removable repairman*; Microelectronic. Reliability. Vol. 35 No. 2, 1995.
[21] Wang, K-H. & Sivazlian, B. D.: *Reliability of a system with warm standbys and repairmen*. Microelectronic. Reliability. Vol. 29 No. 5/1989.
[22] Wazynska-Fiok K., Jaźwiński J.: *The reliability of technical systems*, (in Polish) Scientific & Technical Publishing House, Warszawa 1990.
[23] Werbinska S.: *The reliability model of logistic support system with Time Dependency*. (in Polish) Logistics 3/2007.

Mgr inż. Sylwia WERBIŃSKA
Wroclaw University of Technology
Institute of Machines Design and Operation
Department of Logistics and Transportation Systems
Wybrzeze Wyspianskiego 27, 50-370 Wroclaw, Poland
E-mail: sylwia.werbinska@pwr.wroc.pl

Tomasz WĘGRZYN
Damian HADRYŚ
Michał MIROS

OPTIMIZATION OF OPERATIONAL PROPERTIES OF STEEL WELDED STRUCTURES

Safety and exploitation conditions of steel welded structure depend on many factors. The main role of that conditions is connected with materials, welding technology, state of stress and temperature. Because of that very important is good selection of steel and welding method for proper steel structure. For responsible steel structure are used low carbon and low alloy steel, very often with small amount of carbon and the amount of alloy elements such as Ni, Mn, Mo, Cr and V in low alloy steel and their welds. In the terms of the kind of steel it is used a proper welding method and adequate filler materials. In the present paper it was tested and optimized the chemical composition of metal weld deposit on the operational properties of steel welded structures.

Keywords*: alloy elements, welds, optimization, impact toughness.*

1. Introduction

Properties of Steel Welded Structures depend on many factors such as welding technology, filler materials, state of stress. The main role of that conditions is also connected with materials, chemical composition of steel and metal weld deposit. Chemical composition of metal weld deposit could be regarded as a very important factor influencing properties of metal weld deposit (MWD). Especially nickel, molybdenum, chromium, vanadium are regarded as the main factors effecting on mechanical properties and metalographical structure of low alloy welds. However there is different influence of those elements on mechanical properties of welds. The influence of the variable amounts of nickel, molybdenum, chromium, vanadium on impact properties of low alloy metal weld deposit was tested. The influence of manganese, nickel, molybdenum, chromium, vanadium contents in weld metal deposit on impact properties was well analysed in the last 15 years [1-8]. Chromium, vanadium, and especially nitrogen are regarded rather as the negative element on impact toughness properties of low alloy basic electrode steel welds in sub zero temperature, meanwhile nickel and molybdenum have the positive influence on impact properties. Authors of the main publications [3-6] present that the content of nitrogen in low alloy weld metal deposit should not be grater than 100 ppm, and that nickel content should not exceed 3%. It is observed that nickel (from 1% to 2%) in metal weld deposit gives good impact toughness properties of welds. The lowest amount of nitrogen in all weld metal gives the best impact results of metal weld deposit. It was suggested that nitrogen has similar role as carbon in the ferrite. The amount of nitrogen in low-carbon and low-alloy steel is limited, but in high alloy steel welds the amount of nitrogen could be sometimes even augmented to obtain optimal mechanical properties of welds. The highest amount of nitrogen (up to 0.04%) is in "Duplex" and "Super Duplex Steel". Toughness properties of low-carbon and low-alloy steel welds decrease in terms of the amount of nitrogen. However some authors [2, 3, 7] assume that some nitride inclusions such as TiN, BN, AlN could have a positive influence on the formation of acicular ferrite in welds. Because of that nitrogen might not be treated only as a negative element in steel and welds. Welding parameters, metalographical structure and chemical composition of metal weld deposit are regarded as the important factors influencing the impact toughness properties of deposits [7-8]. In the present paper it was tested and optimized the chemical composition of metal weld deposit on the operational properties of steel welded structures.

2. Experimental procedure

To assess the effect of nickel, molybdenum, chromium, vanadium on mechanical properties of deposited metals there were used basic electrodes prepared in experimental way. The electrode contained constant or variable proportions of the following components in powder form:

technical grade chalk	30%,
fluorite	20%,
rutile	4%,
quartzite	3%,
ferrosilicon (45%Si)	6%,
ferromanganese (80%Mn)	4%,
ferrotitanium (20%Ti)	2%,
iron powder	31%.

The principal diameter of the electrodes was 4 mm. The standard current was 180A, and the voltage was 22V. A typical weld metal deposited had following chemical composition:

0.08% C,
0.8% Mn,
0.37% Si,
0.018%P,
0.019% S.

The oxygen content was in range from 340 to 470 ppm, and the nitrogen content was in range from 70 up to 85 ppm The acicular ferrite content in weld metal deposit was above 50%. The oxygen content was in range from 340 to 470 ppm, and the nitrogen content was in range from 70 up to 85 ppm. The acicular ferrite content in weld metal deposit was always above 50%.

This principal composition was modified by separate additions:

ferromanganese (80%Mn)	up to 5 % (at the expense of iron powder),
ferrochromium powder	up to 2% (at the expense of iron powder),
ferrovanadium powder	up to 1.5% (at the expense of iron powder),
ferromolybdenum powder	up to 1.5% (at the expense of iron powder),

ferronickel powder up to 6.5%
(at the expense of iron powder).

A variation in the manganese, nickel, molybdenum, chromium, vanadium amount in the deposited metal was analysed from:

0.8 up to 2.4 Mn%,
1 up to 3 Ni%,
0.2 up to 0.6 Mo%,
0.2 up to 0.6 Cr%,
0.05 up to 0.15 V%.

3. Results and Discussion

After the welding process using basic coated electrodes there were gettable metal weld deposits with the variable amounts of tested elements (Mn, Cr, Mo, V, Ni) in it. After that the chemical analysis, micrograph tests, and Charpy notch impact toughness tests of the deposited metal were carried out. The Charpy tests were done mainly at +20°C and -40°C with 5 specimens having been tested from each weld metal. The impact toughness results are given in figures 1-5.

Analysing figure 1 it is possible to deduce that impact toughness of metal weld deposit is not strongly affected by the amount of manganese. Absorbed energy in terms of the amount of vanadium in metal weld deposit is shown in figure 2.

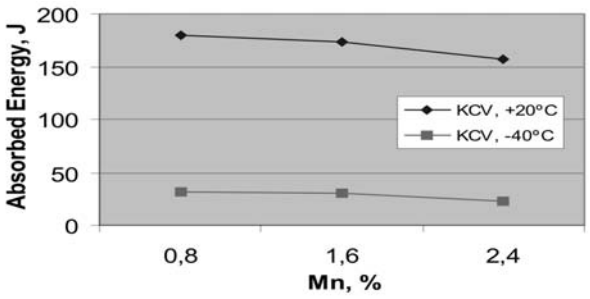

Fig. 1. Relations between the amount of Mn in MWD and the impact toughness of MWD

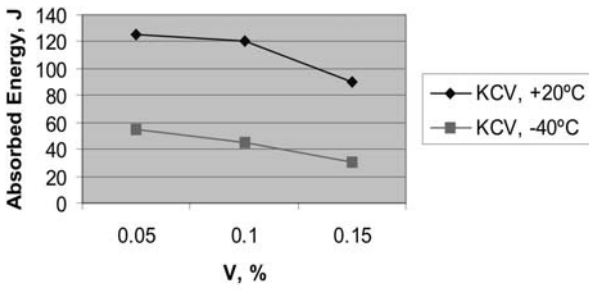

Fig. 2. Relations between the amount of V in MWD and the impact toughness of MWD

Analysing figure 2 it is possible to deduce that impact toughness of metal weld deposit is much more affected by the amount of vanadium than manganese. Absorbed energy in terms of the amount of chromium in metal weld deposit is shown in figure 3.

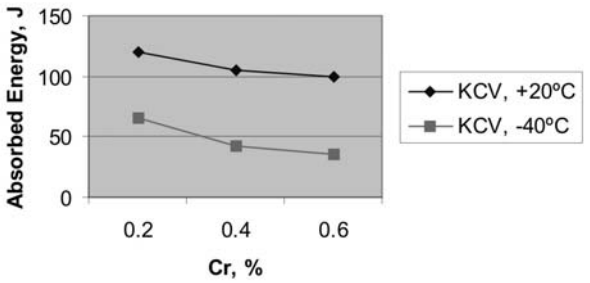

Fig. 3. Relations between the amount of Cr in MWD and the impact toughness of MWD

Analysing figure 3 it is possible to observe that impact toughness of metal weld deposit is also much more affected by the amount of chromium than manganese. Absorbed energy in terms of the amount of nickel in metal weld deposit is shown in figure 4.

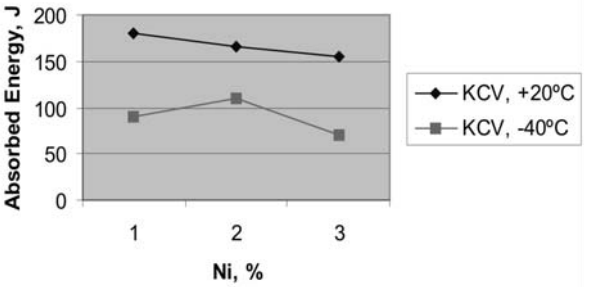

Fig. 4. Relations between the amount of Ni in MWD and the impact toughness of MWD

Analysing figure 4 it is possible to deduce that impact toughness of metal weld deposit is very positively affected by the amount of nickel. Absorbed energy in terms of the amount of molybdenum in metal weld deposit is shown in figure 5.

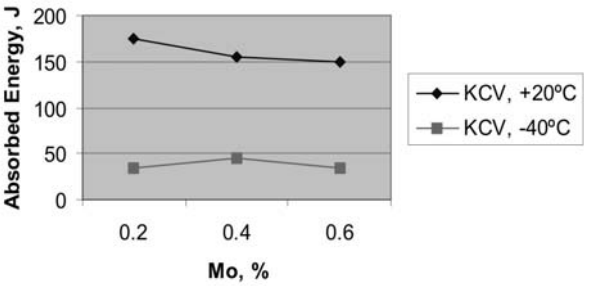

Fig. 5. Relations between the amount of Mo in MWD in MWD and the impact toughness of MWD

Analysing figure 5 it is possible to observe that impact toughness of metal weld deposit is also very positively affected by the amount of molybdenum. The microstructure and fracture surface of metal weld deposit having various amount of nickel and vanadium was also analysed. Acicular ferrite and MAC phases (self-tempered martensite, upper and lower bainite, rest austenite, carbides) were analysed and counted for each weld metal deposit. Amount of AC and MAC were on the similar level in deposits with Ni and Mo, also for deposits with V and Cr there were observed rather similar structure. Results of deposits with various structure are shown in figures 6, 7.

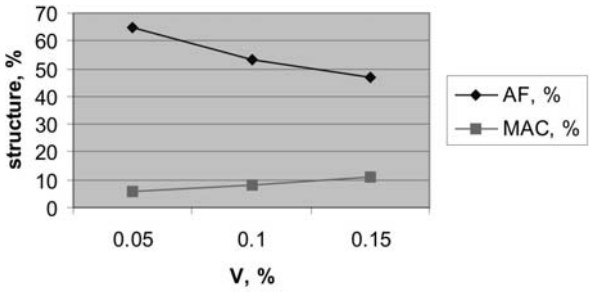

Fig. 6. Metalographical structure with V in MWD

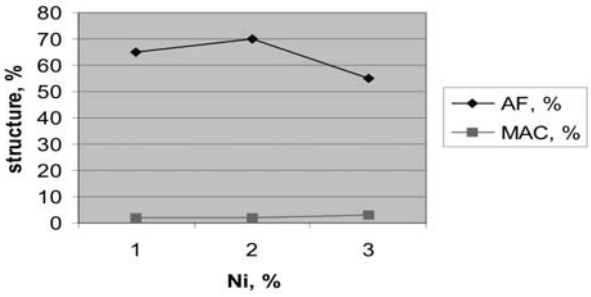

Fig. 7. Metalographical structure with Ni in MWD

It was easy to deduce that nickel and molybdenum have positive influence on the structure. That relation was firstly observed in impact toughness tests. Nickel and molybdenum could be treated as the positive elements influencing impact toughness and structure of MWD because of higher amount of acicular ferrite and lower amount of MAC. Chromium and vanadium could be treated as the negative elements influencing impact toughness and structure of MWD. Manganese could be treated as a neutral element influencing impact toughness of MWD. Additional fracture surface observation was done using a scanning electron microscope. The fracture of metal weld deposit having 1.1% Ni is presented in figure 7, and the fracture of metal weld deposit having 0.6% Cr is presented in figure 8.

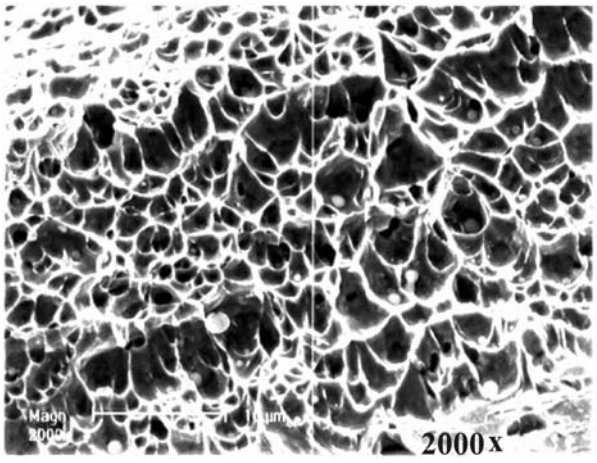

Fig. 8. Fracture surface of metal weld deposit

The surface is ductile, because of the beneficial influence of nickel on the deposit structure. After microscope observations it was determined that the amount of nickel (or molybdenum) has a great influence on the character of fracture surface. The surface was ductile also for MWD having Mo in it. The character of fracture surface changed from ductile to much breatle in terms of the increscent of the amount of vanadium (or chromium). The typical fracture of metal weld deposit having 0.6% Cr is presented in figure 9.

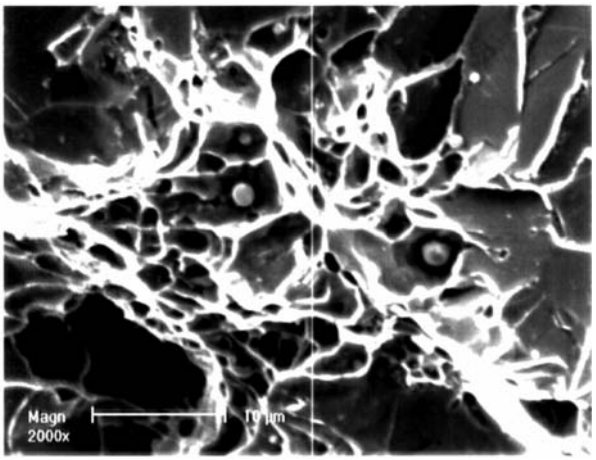

Fig. 9. Fracture surface of metal weld deposit

The surface is less ductile, because of the higher amount of chromium in deposit. The surface was breatle also for MWD having V in it. After microscope observations it was determined that the amount of chromium (or vanadium) has also a great influence on the character of fracture surface. The character of fracture surface changed from ductile to much breatle in terms of the increscent of the amount of chromium. In the present paper it was tested and optimized the chemical composition of metal weld deposit on the operational properties of steel welded structures. The influence of the variable amounts of nickel, molybdenum, chromium, vanadium on impact properties of low alloy metal weld deposit was tested. Chromium, vanadium, and especially nitrogen are regarded rather as the negative element on impact toughness properties of low alloy basic electrode steel welds in sub zero temperature, meanwhile nickel and molybdenum have the positive influence on impact properties. It was observed that nickel and molybdenum could be treated as the positive elements in low alloy metal weld deposits, meanwhile chromium and vanadium are negative elements influencing properties of MWD. The optimal chemical composition of steel low alloy MWD should be treated for deposits having 0.4 % Mo or 2% Ni.

4. Summary

Design engineers should base on actual welding technology. A close cooperation should be done with competent welding personnel during the design stage. Manufacture of welded structures ought to be supervised both by civil and welding engineers. Safety and exploitation conditions of steel welded structure depend on many factors. The cause of collapse, damages and deformation of steel structures is often connected with no proper choice of materials and their joining technology. The main role of that conditions are connected with welding technology. The damages of important constructions such as steel roof structures of workshops in Tychy (in 2006) and Zagreb (in 1993) are the best prove of that [9]. Summing up the paper it has been concluded, that especially important is a good selection of

steel and welding method for proper steel structure. For responsible steel structure are used low carbon and low alloy steel, very often with a small amount of carbon and amount of other alloy elements such as Ni, Mn, Mo, Cr and V in low alloy steel and their welds. Only some of that elements could be treated as positive elements influencing MWD properties. In the present paper it was tested and optimized the chemical composition of metal weld deposit on the operational properties of steel welded structures. It was found that only nickel and molybdenum are treated as the positive elements in low alloy metal weld deposits. It has been proved that optimization of operational properties of steel welded structures might be done in terms of the chemical composition of MWD.

5. Conclusions

1. Optimization of operational properties of steel welded structures might be done in terms of the chemical composition of MWD.
2. Nickel, molybdenum, chromium and vanadium could be treated as the elements strongly influencing impact toughness properties of low alloy MWD.
3. Nickel and molybdenum are positive elements in low alloy metal weld deposits.
4. Chromium and vanadium can not be treated as positive elements in low alloy metal weld deposits.
5. Manganese could be rather treated as a neutral element influencing impact toughness properties.

6. References

[1] Judson, P., Mc Keown, D.: *Advances in the control of weld metal toughness*, Offshore welded structures proceedings, London, V2., 1982.

[2] Lancaster, J.F.: *Physics of Welding*, Pergamon Press, 1986.

[3] Wegrzyn, T.: *Oxygen and nitrogen in low carbon basic electrode weld metal deposits*, IIW Doc.II-A-1181-92, 1992.

[4] Allum, C.J.: *Nitrogen absorption from welding arc*, IIW.Doc.II-1115-88, 1988.

[5] Wegrzyn,T.: *A relation between the impact strength and the contense of manganese, nickel, molybdenium and nitrogen in the deposited metal of low-alloy low-hydrogen electrodes*, Przeglad Spawalnictwa, Poland, Nş 11/12: 1-6, 1996.

[6] Paton, B.E,.Lakomsky, V.I.: *Interaction of molten metal with nitrogen from arc plasma*, IIW.Doc.II-A-871-92, 1992.

[7] Wegrzyn T.: *The influence of the main factors on the impact toughness properties of low carbon steel welds*, Proceedings of ISOPE'97, Honolulu, USA, 1997.

[8] Wegrzyn T.: *The classification of metal weld deposits in terms of the amount of nitrogen*, The Proceedings of ISOPE'2000, Seattle, USA, V4: 130-134, 2000.

[9] Turcic, F.: *The couse of collapse and rehabilitation of steel tanks roof structures" nitrogen*, The Proceedings of the XI International conference on metal structures, Seattle, ICMS-2006, Rzeszów 2006.

Dr hab. inż. Tomasz WĘGRZYN
Mgr inż. Damian HADRYŚ
Mgr inż. Michał MIROS

The Silesian University of Technology
Faculty of Transport
Department of Vehicle Service
Krasinskiego 8
40-019 Katowice, Poland

Juraj GRENČÍK
Václav LEGÁT

MAINTENANCE AUDIT AND BENCHMARKING - SEARCH FOR EVALUATION CRITERIA ON GLOBAL SCALE

Maintenance strategy and concept of management are very important for proper execution of maintenance of physical assets in different organizations. Authors present main objectives for maintenance and define maintenance strategy and concept. The key benefit of the paper is a methodology of strategy maintenance development. The methodology is based on input data definition and on proposed procedure of data processing. Proper developed maintenance strategy is a presumption of excellent maintenance effectiveness. The paper presents use of audit and benchmarking methods for development the maintenance strategies. Example of system of questions and their evaluation is presented. Some practical problems and experience from companies are discussed as well.

Keywords*: maintenance audit, benchmarking, maintenance performance indicators.*

1. Introduction

Maintenance strategy and concept influence the performance of physical assets especially in medium and long time horizon. This is reflected particularly in the effectiveness, productivity and economic efficiency of maintenance and in fulfillment of fundamental requirements asked from maintenance, such as:

a) Maintaining physical assets in up-state,
b) Prevention of failure occurrence and consecutive faults,
c) Flexible fixing the failures occurred,
d) Diminishing environmental effects of production equipment,
e) Ensuring operational safety,
f) Spending optimum costs on maintenance.

Aim of this paper is to outline the structure and methods for proposal of evaluation criteria on global scale.

2. Audit

Audit can be characterised as a systematic, independent and documented process of obtaining evidences from audit and its objective evaluation with the aim to determinate extent of the audit criteria fulfilment.

Audit criteria of maintenance management quality are mostly qualitative and composed of requirements for proper organization structure and management of all maintenance processes [1, 2, 4, 6, 8]. Gradually it is possible to create also quantitative criteria expressed by concrete values of measurable quantities, such as man-hours and maintenance operations duration, preventive maintenance ratio, external service ratio, all financial indicators of maintenance, etc. The basic tool for gaining these quantity based criteria is benchmarking – see below.

It is appropriate to split out the audit criteria into several areas of maintenance management [7]. The proposed example consists of ten areas:

1. Characteristics of business activities and production facilities in the company.
2. Strategies and systems of maintenance in the company.
3. Organisation and management of human resources in maintenance.
4. Administration and documentation of maintenance management.
5. Preventive maintenance.
6. Planning, scheduling and work orders in maintenance.
7. Implementation of maintenance processes.
8. Purchase, stock and supplies of spare parts and material management.
9. Measurements of effectiveness and efficiency of maintenance, its improvement and evaluation of customers' satisfaction.
10. Computer based support of maintenance management.

Note:
Generally, in each audit there is certain subjectivity and this is true especially in maintenance audit as there is no standard like ISO 9001:2000, ISO 190011 etc. However, the maintenance audits can be carried out, and conclusions and recommendations for creation of maintenance management strategies can be done.

3. Benchmarking

Creation of maintenance strategy requires knowledge of number of indicators to be used during proposal, implementation and verification of results gained during maintenance strategy improvement process.

Benchmarking is focused on comparison of a process and product against processes and products recognised as the best ones with purpose of discovering opportunities for quality improvement. It enables determination of objectives of tasks and priorities in preparing plans that will lead to competitive advantage in the market.

These general benchmarking principles are valid for any maintenance processes and can be used also in a maintenance management.

3.1 Evaluation criteria on global scale

From the above given characteristics of audit and benchmarking it is clear that both the maintenance audit and benchmarking need well prepared, and if possible, standardised quantitative and qualitative indicators of maintenance performance (KPI).

There are numerous different indicators for maintenance performance, e.g. 13 key indicators defined by EFNMS, or indicators defined in EN 15 341 standard "Maintenance Key Performance Indicators" [3], etc.

It was EFNMS ambition to carry-out a European-wide study on maintenance based on 13 indicators defined by working group Maintenance Benchmarking. But although the indicators were sufficiently publicised among the EFNMS member countries, the results were not adequate to effort and so far there is no European-wide database on the 13 selected indicators, besides the Nordic survey in 2000 [10] and successful workshops in some member countries. Strong impulse for creation of a large database is expected from above mentioned European standard.

Another possibility for facilitating collection of benchmarking indicators is their automatic generation from CMMS. There is a system developed by Infor based on usage of VDM (Value Driven Maintenance) indicators. Another one, developed for D7i package by Inseko, a.s. corp. [5] that generates indicators according to EFNMS benchmarking methodology, thus giving instant overview on actual position of maintenance in a company. The new indicators by European standard, or any other required, can be added to the system.

EN 15341

A new European standard entitled "Maintenance – Key Performance Indicators" was approved in the beginning of the year 2007 and besides other it should solve the problem with definitions and give higher importance to maintenance benchmarking as the indicators are now included in the European standard. Problem of understanding the indicators will transfer to the problem of their correct and effective usage (although understanding problems will probably never disappear). The new standard comprises 71 of them, which is rather high number and in a sense it contradicts to the original intention of EFNMS to select the least number of the most representative indicators. The new standard let the users decide which indicators will be utilised, but this on the other hand brings a problem of mutual comparison when companies will not use the same indicators. So this brings a new action area for the EFNMS benchmarking working group, which in the meantime adopted a new name of "European Maintenance benchmarking Committee", to prepare and disseminate a unified approach to utilisation of the standard based on the experience of leading (world class) companies.

The system of indicators is structured into three groups:

1. Economic indicators (time / money; money / money)
2. Technical indicators (time / time; number / time; time / number)
3. Organisation indicators (e.g. persons / persons; etc.)

The objective of indicators is to help management to support management in achieving maintenance excellence and utilize technical assets in a competitive manner. Most of the indicators apply to all industrial and supporting facilities.

These indicators should be used to:

a) measure the status;
b) compare (internal and external benchmarks);
c) diagnose (analysis of strengths and weaknesses);
d) identify objectives and define targets to be reached;
e) plan improvement actions;
f) continuously measure changes over time.

These indicators can be evaluated as a ratio between selected factors (numerator and denominator) measuring activities, resources or events, according to a given formula. Whenever a factor is defined as "internal" or "external", the derived indicator, should also be used only for "internal" or "external" influences.

To select relevant indicators, the first step is to define the objectives to be reached at each level of the enterprise. At the company level, the requirement is to identify how maintenance can be managed in order to improve global performance (profits, market shares, competitiveness etc). At the systems level and production lines, the maintenance objectives can address some particular performance factors, which have been identified through previous analysis, such as improvement of availability, improvement on cost-effective maintenance, retaining health, safety and environment preservation, improvement in cost-effective management of the value of the maintenance inventory, control of contracted services, etc. At the equipment level, machines or types of machines, better control of reliability costs; maintainability and maintenance supportability, etc may be desirable.

Figure 1 illustrates external and internal factors as well as the groups and levels of indicators.

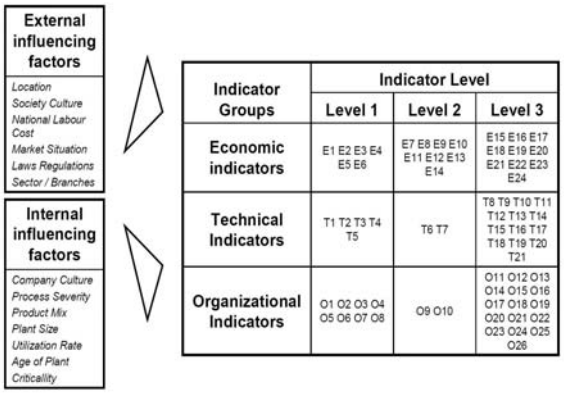

Fig. 1. Maintenance influencing factors and Maintenance Key Performance Indicators

When the objectives have been defined and the performance parameters to be measured have been identified, the next step is to find the indicators that allow measuring these parameters. The system can include capacity of maintaining the equipment, reliability of the equipment, efficiency of the maintenance activities, health, safety and the environment, etc. An indicator is relevant when its value or its evaluation is correlated with the evaluation of the performance parameter to be measured. A relevant indicator shall be one element of decision making.

It is necessary to precisely define:

- data to be collected to determine the values required for the indicator;
- measurement method (operating mode);
- tools required for the measurement (documents, counters, sensors, analyzers, computerized maintenance management system, etc.).

To make the possible evaluation and comparisons easier, it is necessary that the collected data are in conformity with the standardized definitions (e.g. EN 13306).

It is necessary to predetermine the frequency of the calculation and consider availability and time delay of the relevant data, changes over time and reactivity of the system to the actions undertaken.

Out of the scope of this standard remain definition of score, analysis and adopting required measures. The standard itself comprises a set of indicators, but their analysis will require additional projects.

SMRP (USA) metrics

Society for Maintenance and Reliability Professionals (SMRP) has defined and continually has been developing indicators (metrics as they call them) of the best practices to measure maintenance performance [11]. This process is ongoing and metrics can be found at www.smrp.org. The SMRP is active mostly in the USA and Canada, has over 1500 members of which 150 are executive company members.

Objective of the SMRP committee is to define best practices in maintenance and reliability and gradually create a set of the most frequently used metrics and definitions.

The SMRP best practices committee has selected 45 metrics (the number is not definite) that will be gradually defined in the following categories (see figure 2):

- Business and management.
- Manufacturing process reliability.
- Equipment reliability.
- People skills.
- Work management.

First comparisons

As the EFNMS indicators are now incorporated in the standard EN 15341 "Maintenance Key Performance Indicators" and SMRP is developing its system, these two activities lead during the Euromaintenance 2006 conference to meeting that initiated comparison activity aiming at a documentation of the similarities and the differences in the SMRP metrics and the EN 15341 standard.

The first indicators compared and identified as similar from EN 15341 and the SMRP metrics are:

SMRP Metrics		*EN 15341 "Maintenance Key Performance Indicators"*	
1.5 Annual Maintenance Cost per RAV	*Annual Maintenance Cost / Replacement Asset Value*	*E1*	*Total Maintenance Cost / Assets Replacement Value*
1.4 Stocked MRO	*Stocked MRO Inventory Value / Replacement Asset Value*	*E7*	*Average inventory value of maintenance materials / Asset Replacement Value*
5.13.1 Contractor Maintenance Cost	*Contractor Maintenance Cost / Total maintenance cost*	*E10*	*Total contractor cost / Total maintenance cost*
3.5.2 MTTR	*Total Repair Time / Number of Repair Events*	*T21*	*Total time to restore (MTTR) / Number of failures*
5.6.2 Proactive Work	*PM & PdM Related Work / Total Work*	*O18*	*Preventive maintenance man-hours / Total maintenance man-hours*
1.2 Stock Outs	*Inventory Requests not Fulfilled / Total Number of Inventory Requests (Inverted)*	*O26*	*Number of the spare parts supplied by the warehouse as requested / Total number of spare parts required by maintenance (inverted)*

To increase understanding and the application of the indicators, EFNMS and SMRP will organize workshop based on the indicators or metrics during Euromaintenance 2008 in Brussels.

With the increased globalisation and with companies acting globally, the need for a common understanding of the indicators to measure maintenance and availability performance is increasing, and there is no doubt that this activity in a short period of time will be a part in a global standard for maintenance indicators. This is highlighted by the fact that COPIMAN (Technical Committee on Maintenance of the Pan American Federation of Engineering Societies) is joining the comparison effort.

3.2. Discussion to existing indicators

From above given overview on current situation in the presented topic, one can see that there are various approaches to creation and classification of maintenance KPIs in the world. The first proposal of EFNMS (13 KPIs) has neither classification into groups nor hierarchy of indicators. The second system (EN 15 341 standard) extends the scope of KPIs up to 71 and defines three categories (economic, technical and organisation KPIs) and three hierarchy levels representing the breakdown structure of the assets in the company and enabling to measure performance indicators of the plant as the whole as well the production line and the piece of equipment. American (SMRP) approach is developing 45 (and more) metrics in 5 categories (business and management, manufacturing process reliability, equipment reliability, people skills, work management) and some kind of KPIs hierarchy can be recognised form the figure 2 (e.g. OEE is on higher level than downtime, etc.).

Although much has been done in the field of KPIs, we feel some weaknesses in the area of structuring and hierarchical composition of these KPIs. The structure by categories could be created e.g. in accordance with 10 audit areas of maintenance management. A set of KPIs would be defined in the area 9 (measurements of effectiveness and efficiency of maintenance, its improvement and evaluation of customers' satisfaction), while the individual KPIs would cover the remaining 9 areas of maintenance management audit. We can expect that for the area 4 (administration and documentation of maintenance management) and for the area 10 (computer based support of maintenance management) it would be very difficult to define measurable KPIs. On the other hand a proper structure of KPIs in accordance the areas of audit would increase its objectiveness and improve its usability. Unfortunately the presented 10 areas of maintenance management quality audit are not standardised and anyone may say why maintenance management quality audit could not have more or less areas with content than is presented in this paper.

Another possible structure of maintenance KPIs could be based on application of standardised quality management according to the ISO 9001:2000 that can be decomposed according to process model into four main areas: (1) maintenance management responsibility and performance, (2) maintenance resource management and performance, (3) maintenance realization and performance and (4) maintenance measurement, analysis and improvement. A set of maintenance KPIs would be defined in the fourth area and KPIs would be classified into the remaining three large categories.

Furthermore, from the brief analysis of maintenance performance indicators it can be recognised that complex (overall) indicators are missing, which could present maintenance performance possibly by one number. Currently indicator of overall equipment effectiveness (OEE) belongs to such indicators. The weak point of this indicator is that id does not comprise any data of economic character.

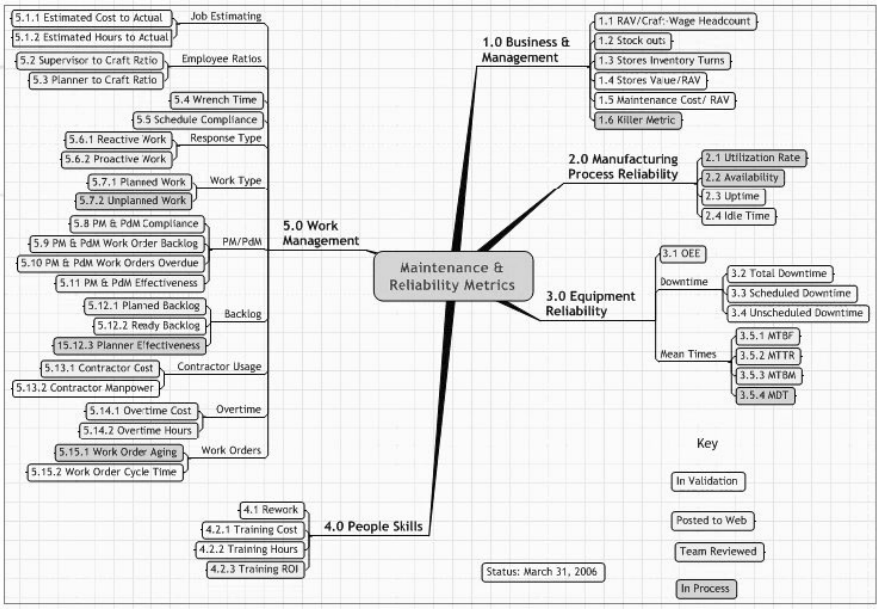

Fig. 2. Overview of SMRP maintenance best practices metrics

3.3. Proposal of overall indicators

Right in the beginning of these considerations it is necessary to say that definition of "absolute" overall indicator of total maintenance management quality and performance is very difficult and in fact almost impossible. However we will try to propose indicators that could at least partly fulfil requirements asked from overall indicator, which could characterise by one figure a maintenance management level that is its performance, effectiveness and efficiency.

The authors propose two overall indicators to further discussion:

a) the increment of profit caused by maintenance
b) indicator of maintenance management quality and performance

A. In practice it is necessary to leave the philosophical and strategic ideas and come up with practical solution. How can the efficiency of financial resources expended in maintenance be ensured in practice? The simplest solution is based on monitoring the shifts of the maintenance contribution to profits of the organisation caused by changes of total efficiency of the production equipment and changes of maintenance costs. The maintenance contributions are evaluated separately while all other factors remain constant. The increment of profit caused by maintenance can be formulated as follows:

$$\Delta PROFITm(\Delta T) = \Delta REVENUESm(\Delta T) - \Delta COSTSm(\Delta T) = REVENUESnom(\Delta T) * [TEE(T_2) - TEE(T_1)] - [COSTSm(T_2) - COSTSm(T_1)] \quad (1)$$

where: $\Delta PROFITm(\Delta T)$ – increment of maintenance contribution to the organisation's profits in time period of ΔT, $\Delta REVENUESm(\Delta T)$ – increment of maintenance contribution to organisation's revenues in period of ΔT, $\Delta COSTSm(\Delta T)$ – maintenance costs increment in period of ΔT, $REVENUESnom(\Delta T)$ – nominal revenues (revenues in case of 100% efficiency of production equipment) for period of ΔT, $TEE(T_2)$ – average level of total equipment efficiency in current period of ΔT, $TEE(T_1)$ – average level of total equipment efficiency in previous period of ΔT, $COSTSm(T_2)$ – costs of equipment maintenance in current period of ΔT, $COSTSm(T_1)$ – costs of equipment maintenance in previous period of ΔT, ΔT – examined calendar period (a month, quarter etc.)

By analysing the calculation (1) we can find out, that as the TEE in consecutive periods grows, so does the maintenance contribution to the organisation's profit in the period ΔT (positive increment of the maintenance contribution) and as the TEE in consecutive periods decreases, the maintenance contribution to the profit for the period ΔT decreases as well (the maintenance contribution increment is negative, i.e. drop in revenues). In the case of an increase of the maintenance costs (for period ΔT) in consecutive periods, the increment of maintenance costs $\Delta COSTSm(\Delta T)$ for period ΔT is positive. In the case of decreasing maintenance costs (for period ΔT) in consecutive periods, the increment of maintenance costs $\Delta COSTSm(\Delta T)$ for period ΔT is negative (this increases the maintenance contribution to profit).

It can be summarized, that the maintenance contribution to profit of an organisation will grow most rapidly, when the maintenance costs will decrease and the level of maintenance management will rise (the TEE will rise) – Table 1, variant 1. The increment of the maintenance contribution to the organisation's profit can be positive also in the case of an increasing level of the total efficiency of equipment and the maintenance costs remain unchanged or will grow more slowly than the maintenance contribution to the profit – Table 1, variants 2 and 3. Entirely bad economical situation (loss) occurs, when the total equipment efficiency stays constant (at a lower level) or decreases, while the maintenance costs grow – Table 1, variants 4 and 5.

The indicator of maintenance contribution to an organisation's profits makes it possible to monitor the dynamics of the financial impact of maintenance management and maintenance financing to entire organisation's profit. The positive increment of this indicator for certain period of time definitely represents the positive, desirable trend in maintenance management and its negative increment indicates negative, undesirable trend in

Tab. 1. Illustration of typical variants of maintenance contribution to organisation's profit – calculated according to (1)

Variant	1	2	3	4	5
REVENUESnom(ΔT)	1 000 000,-	1 000 000,-	1 000 000,-	1 000 000,-	1 000 000,-
TEE(T_2)	0,8	0,7	0,9	0,45	0,90
TEE(T_1)	0,5	0,6	0,9	0,45	0,95
COSTSm(T_2)	60 000,-	50 000,-	40 000,-	60 000,-	55 000,-
COSTSm(T_1)	100 000,-	50 000,-	60 000,-	50 000,-	50 000,-
ΔPROFITm(ΔT)	340 000,-	100 000,-	20 000	- 10 000	- 55 000,-

maintenance management. However, some temporary negative fluctuations of this indicator should not be seen by definition as unfavourable because the calculation of the revenues increments does not include effects out of the growth of production equipment efficiency (for example, it does not include the factors Safety, environmental profile, reducing the stock, customer acquisition and lock-in etc.). The negative increments can be, of course, also expected in case where there are variations in the factors considered constants (e.g. substantial expansion of production, reduction of production, changes in production programme etc.). In this case it is necessary to consider those factors. When high levels of maintenance management have been reached (other factors stay constant), the increments of maintenance contribution should be kept at zero, because the total efficiency of production equipment and the level of maintenance management reached its peak and remains there, and the maintenance costs remain unchanged at this optimal level (inflation is not considered). From above stated, it is obvious that the most substantial increments of this indicator can be expected during maintenance management improvements (positive increments) and during the drop in quality of the maintenance management (negative values). Verification of this indicator in practice will show its possible application.

B. Basic inputs for the second propose overall indicator of maintenance management quality and performance could be composed of the following items:

a) total internal and external maintenance costs *Cm* of all physical and intangible assets in organisation per certain period of time, e.g. month, quarter, year etc. (wages, salaries and overtimes for managerial, supervision, support staff and direct staff; payroll added costs for the above mentioned persons (taxes, insurance, legislative contributions); spares and material consumables charged to maintenance (including freight costs); tools and equipment (not capitalized or rented); contractors, rented facilities; consultancy services; administration costs for maintenance; education and training; costs for maintenance activities carried out by production people; costs for transportation, hotels, etc.; documentation; CMMS (computerized maintenance management software) and planning systems; energy and utilities; depreciation of maintenance capitalized equipments and workshops, warehouse for spare-parts. Not included: costs for product changeover or transaction time (e.g. exchange of dies); depreciation of strategic spare parts; downtime costs.

b) overall equipment effectiveness *(OEE)* related to certain period of time, e.g. month, quarter, year etc.; this coefficient is composed of indicator of availability *A* covering required operation time, corrective maintenance), indicator of performance efficiency *P* covering lowered performance caused by worsened technical state due to maintenance and indicator of quality *Q* expressing ratio of nonconforming products due to maintenance. OEE is calculated by the following formula:

$$OEE = A * P * Q \qquad OEE, A, P, Q \in \langle 0;1 \rangle \tag{1}$$

More detailed methodology for OEE calculation can be found e.g. in [9].

c) ideal revenues of organisation *Rid* for coefficient of overall equipment effectiveness OEE = 1 (ideal state when production would run without any loses caused by maintenance and total ideal production for paying customers) related to certain period of time, e.g. month, quarter, year etc.

d) real revenues of organisation *Rreal* corresponding to real overall equipment effectiveness related to certain period of time, e.g. month, quarter, year etc.

e) costs for environmental damage and injuries *Cedi* affected by maintenance and related to certain period of time, e.g. month, quarter, year etc.

Based on these input data it is possible to create formula that expresses overall indicator of maintenance management quality and performance *Iqp:*

$$Iqp = 1 - \frac{Cm + Cedi + (1 - OEE)Rid}{Rreal} \tag{2}$$

The presented quality and performance of maintenance management (2) can reach theoretically ideal value 1, and that is in case when total maintenance costs Cm and costs for environmental damage and injuries Ced will be zero and OEE will equal 1. In reality value of this indicator will always be less than 1; however, it is clear that nearing to value one (or 100%) is positive and desired trend.

Advantage of this indicator is in its property to attain and represent more effects and factors of maintenance management (e.g. influence of ratio of internal and external maintenance, preventive and corrective maintenance, influence of worsening of technical state on equipment performance, effects of nonconforming products, influence of maintenance on environmental damage and injuries, influence of training level of maintenance personnel, maintenance tools, etc.)

Disadvantage lays in difficulty to obtain of some data, in inflation financial processes, effects of currency rates, in market and other constraints of maximum utilisation of production capacities; in short term interval it can be, in speculative or another way, influenced by temporary reduction of expenditures on maintenance, etc.

4. Conclusion

Authors of the paper have characterised the existing state in the area of maintenance performance indicators used in maintenance benchmarking and emphasised also possible links with audits of maintenance management and various possibilities for creation of structure of these indicators.

Based on the analysis two overall indicators were proposed for further discussion. These indicators link maintenance performance measurement with its economy - that is basically relation of production equipment availability with costs on its maintenance.

But what is even more important, the significance of indicators lays in their progress during period of time which enables to recognise changes after a new strategy was adopted in maintenance management.

5. References

[1] Campbell, J. D.: *UPTIME Strategies for Excellence in Maintenance Management,* Productivity Press Portland, Kreton, 1995, ISBN 1-56327-053-6ň

[2] ČSN EN ISO 19011:2003: Directions for auditing of quality of system management and/or system of environmental management

[3] EN 15341: Maintenance – Key Performance Indicators

[4] Grencik, J., Legat, V.: *Audit and benchmarking – tools to develop maintenance strategy,* In: Conference proceedings Euromaintenance 2006, May, 2006 Basel.

[5] Grencik, J., Lazar, M., Hrubsa, A.: *Benchmarking of maintenance by EFNMS in the maintenance information system environment*, conference proceedings Central European Forum on Maintenance 2005, SSU, 2005, Vysoke Tatry, pp.192-198, ISBN 80-8070-392-2

[6] ISO/TS 16949, 2002: Catalogue of questions to audit of quality management based on processed orientated approach towards to audit. Catalogue of questions to audit according to ISO/TS 16949. ČSJ Praha 2002. ISBN 80-02-01518-5

[7] Legat, V., Jurca, V., Hladik, T.: *Money Centred Maintenance*. In: Conference proceedings Euromaintenance 2004, AEM, 11-14 May, 2004 Barcelona, pp. 239-250

[8] Müller, M.: *Quick check of maintenance management*. Conference proceedings National Forum on Maintenance 2004, SSU, 2004, Vysoke Tatry, pp. 19-30, ISBN 80-8070-248-9

[9] Nakajima, S.: *TPM Development Program. Implementing Total Productivity Maintenance*. Cambridge, Massachusetts, Productivity Press 1989.

[10] Svantesson, T.: *Nordic Benchmarking Analysis and EFNMS Key Figures*. In: Conference proceedings Euromaintenance 2002, KPY, 3 - 5 June, 2002, Helsinki, pp. 129 -142

[11] www.smrp.org

Doc. Ing. Juraj GRENČÍK, Ph. D.
Department of Transport and Handling Machines
University of Žilina, Mechanical Engineering Faculty
Address: Univerzitná 1, 010 26 Žilina, Slovakia
E-mail: juraj.grencik@fstroj.utc.sk

Prof. Ing. Václav LEGÁT, Dr Sc.
Department for Quality and Dependability of Machines
Czech University of Life Sciences, Faculty of Engineering
Address: Kamýcká 129, 165 21 Praha 6 – Suchdol, Czech Republic
E-mail: legat@tf.czu.cz

Andrzej RUSIN
Adam WOJACZEK

SELECTION OF MAINTENANCE RANGE FOR POWER MACHINES AND EQUIPMENT IN CONSIDERATION OF RISK

The operational safety of power units depends upon many factors, including the methods of their operation, their working conditions, age, regularity and range of maintenance. The scope of the paper is the analysis of maintenance options for power machines and equipment. The assumed criterion for the selection of the range of repair works is the level of technical risk posed by a given facility below the accepted allowable level. Detailed discussion is focused on the water and steam system of the boiler. The influence of the maintenance on the probability of failure of certain components is described on the grounds of Kijima's model. For the assumed maintenance periods minimal sets of equipment were determined, the repair of which should secure the operation of the water-steam system for a successive interval with the risk level lower than the allowable one.

Keywords*: power equipment, operation, maintenance, risk.*

1. Introduction

The operational safety of power units depends upon many factors, the most important of which are: design and technology of their components, working conditions and methods of their operation, age, quality and regularity of the conducted maintenances. A good measure of their operational safety is the level of technical risk posed by the facilities. The possibility of influencing the level of risk, i.e. risk management, arises at each phase of their operation as well as during overhauls and standstills. The control of the processes and phenomena occurring in the course of the operation of particular machines and equipment is commonly provided by acting on the process parameters with the use of various monitoring and control systems: for example, thermal limitations blocks (BOT) [1, 2]. Such blocks are prepared for boilers and turbines, enabling the tracking of the level of stresses in all components and, depending on the recorded values, controlling the parameters of steam so as not too exceed the allowable values of the stresses.

Diagnostic tests play an important role in the assessment of the probability of damage of certain components and the ensuing risk posed by such damage. The results of the tests may be used to reduce the level of uncertainty in the estimation of the technical condition of the component and verification of theoretical analyses [3]. A proper selection of the tests, in terms both of their range and regularity should secure the technical risk on the allowable level.

Another method of risk management are applicable maintenance procedures, not only as far as current small repairs are concerned, but also general overhauls. In the planning of the range and period of the maintenance the level of the risk posed by particular components should always be considered, leading to the reduction of the risk involved in the successive operational intervals. The planning of maintenance range shall be discussed in more detail in consideration of such risk, with the main focus on the water and steam system of the boiler.

2. The risk management procedures

A general scheme of the procedures of managing the technical risk involved in the operation of power machines and equipment is shown in Fig. 1. At the first stage of the procedures, the analyzed system is separated and divided into subsystems and elements [4]. Such division is made in consideration of the structural and functional connections between particular elements. The second stage, i.e. the assessment of risk, requires the definition of the hazard scenarios, that is, of all potential events that may result in the damage of the elements and subsystems of the analyzed system. For these scenarios , or, in other words, undesirable events, the probability of their occurrence and its changes in time should be estimated. The next step in the risk assessment procedure is the estimation of the consequences involved in the failure of particular elements, which may have financial implications, environmental impacts, or potential casualties. The estimated probability of failures and their implications make it possible to calculate the technical risk posed by a certain element, and, subsequently, the risk posed by the whole system. The comparison of the calculated risk with the levels allowable under definite operational conditions leads to the conclusion about the safety of the system. If the current risk level is regarded as too high, the elements that contribute the most to such risk should be identified and various options of reducing the risk level considered. Among potential methods of risk management the option of operational control should be taken into account [5], or, optimization of the diagnostic procedures, or proper selection of the range and regularity of maintenance and repair works.

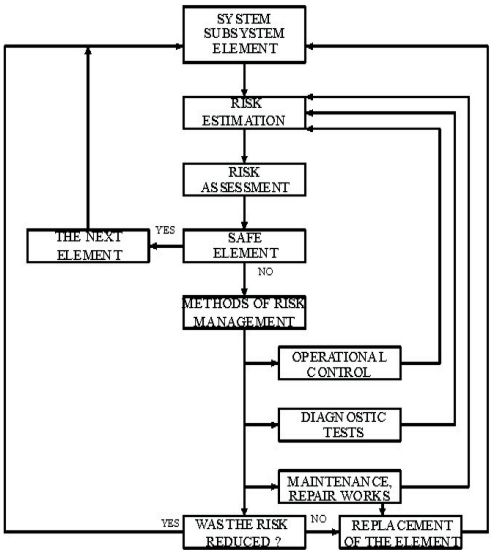

Fig. 1. General procedures of risk assessment and risk management

3. Assessment of the technical risk posed by the water-steam system of the boiler

The subject of detailed analysis is the water-steam system of a steam boiler. Basing on the operational data of several power units of the same type, collected in the course of many years of their operation, the elements and events that cause most frequent damages of the system have been identified. Accordingly, the following fault tree describing the damages of the water-steam system was derived (Fig. 2).

The following primary events were assumed:

- damage of the economizer – event A,
- damage of the boiler drum –event B,
- damage of the waterwall - event C,
- damage of the first section of steam superheater (IPPP)- event D,
- damage of the second section of steam superheater (IIPPP)- event E,
- damage of the fifth section of steam superheater (VPPP)- event F,
- damage of the second section of steam reheater (IIPPW)- event G.

The elements enumerated above are characterized by the biggest rate of failure. The damages of the remaining elements, including, among others, other section of steam superheaters, reheaters, supply pipes of superheaters and coolers were marked as event H in the above diagram.

It was concluded, on the grounds of the data on real failures of these elements, that the most common reasons of the damage of the water system are leakages caused by:

- defects of the welds,
- material faults,
- assembly errors,
- ash and water erosion,
- low-oxygen corrosion,

as well as by the boiler drum overflow and leakages in measuring instruments. As far as the steam system is concerned, the leakages caused by the same reasons dominate. Other causes include: creep, overheating, fatigue, cracking, improper compensation of the strain, mechanical damages. Thanks to the data on the failure rate, the time of the operation and failure periods of particular elements were established, giving grounds for the identification of the type and parameters of the distribution of the time between failures. On the basis of Kołmogorov's tests, in all analyzed cases, the Weibull's distribution was assumed in the following form of the cumulative distribution function CDF:

$$F(t) = 1 - exp\,[-(t^{\beta})/\alpha] \quad (1)$$

where: α- scale parameter, β- shape parameter.

The graph of the cumulative distribution function in time for particular elements is shown in Fig. 3. The graph of the failure rate function is presented in Fig. 4.

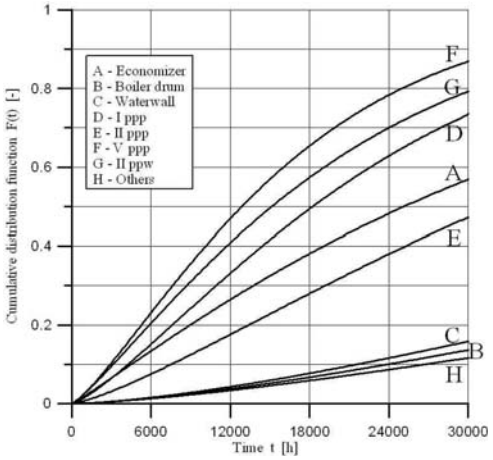

Fig. 3. Cumulative distribution function of the water-steam system

Thanks to the availability of the data on the costs incurred upon the failures of particular facilities, the technical risk involved in their operation was assessed. The risk was calculated from the following equation:

$$R = P \cdot C \quad (2)$$

where P is the probability of failure of a given element calculated from equation (1); whereas C is the average cost of the failure, including both the costs of the ensuing repair works and the losses made by the standstill of the unit due to the failure. The costs were presented in a relative percentage scale in comparison with the average costs of the standstill of the unit caused by typical failures, without the costs of the repair.

The value of the probability of failure of particular facilities and the costs incurred due to their failures are indicated on the risk diagram in Fig. 5. The levels of the risk posed by particular elements after 6000h of their operation were demonstrated in Fig. 6. The changes in the value of the risk in time are shown in Fig. 7.

Among the analyzed elements of the water-steam system, the highest level of risk is posed by the second section of reheater and the fifth section of steam superheater. The lowest risk is involved in the operation of the boiler drum.

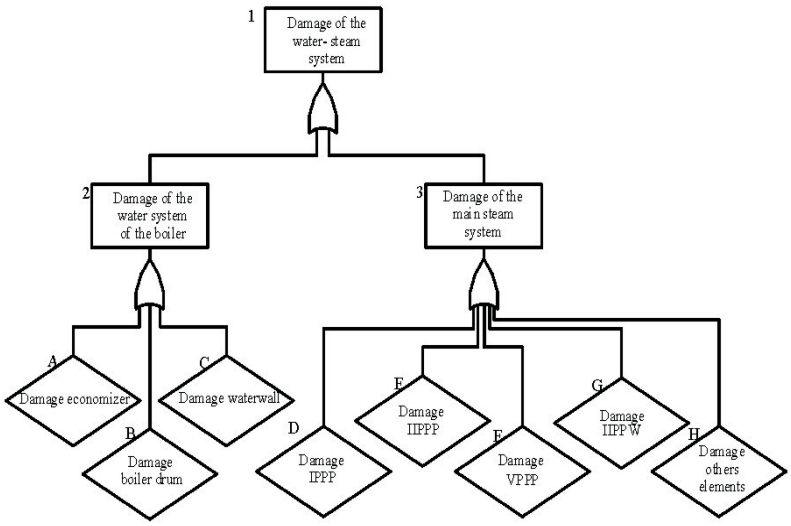

Fig. 2. Fault tree of the water-steam system of the boiler

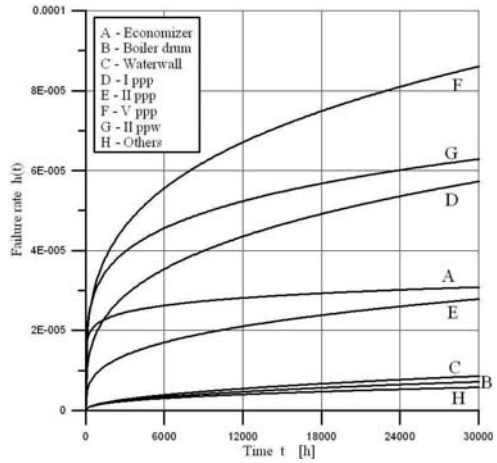

Fig. 4. Failure rate function for the elements of the water-steam system

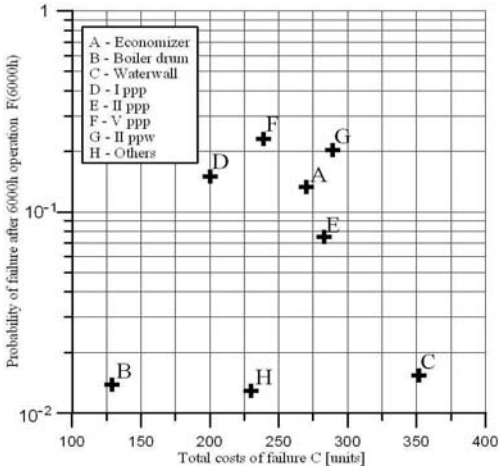

Fig. 5. Risk diagram

4. Selection of the range of repair works of the water-steam system in the boiler

The research task of the rationalization of the range of maintenance was formulated in the following way: to select the ranges of maintenance for the water-steam system conducted at specified time intervals, so that the risk involved in the operation of the system does not exceed the accepted allowable level.

Such formulation stems from a specific nature of the operation and repairs of power units, entailing variable demand for thermal energy during the calendar year and the resulting necessity of conducting the required repairs at the time when the demand is the lowest. Accordingly, the period of the maintenance is more or less planned for the same time each year. It was assumed in the analysis that the maintenances are conducted at regular intervals, after every 6000 hours of the operation of the facility in question. The second assumption was the allowable risk level for the water-steam system amounting to 400 units. Such level may result from the risk analysis made for the entire power unit, or, from the financial standing and the size of a given power plant.

The assessment of the entire risk posed by all elements of the water-steam system at the first stage of the repair period reveals that it is almost two times lower than the allowable level, which might indicate the absence of the necessity of conducting the

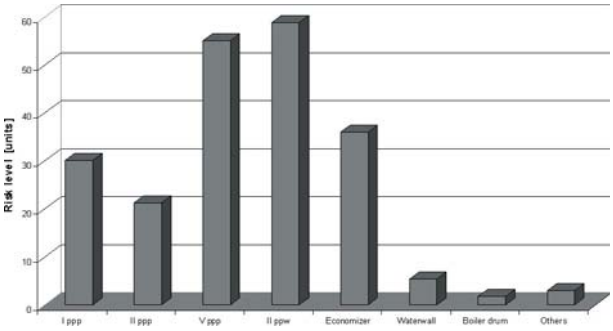

Fig. 6. Risk of particular elements after 6000 h of their operation

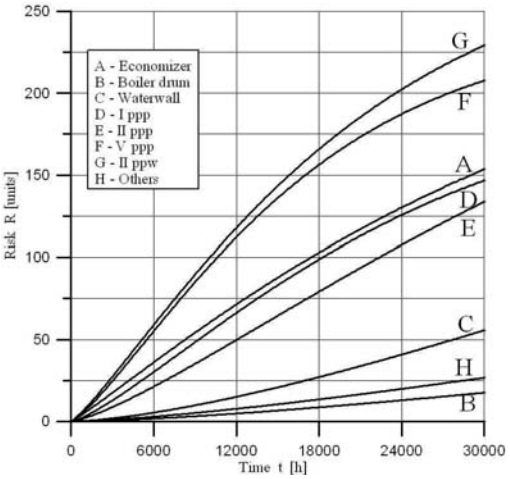

Fig. 7. Risks posed by the elements of the water-steam system in the course of operation

repair works. However, if the system was operated without any maintenances for the successive period, the risk would exceed the allowable level at the end of the time interval. As it was assumed that the repairs must be conducted at specific times of the year, it is required that the initial works should be administered after the first 6000h of the operation of the system. Accordingly, the selection of the range of the repairs, i.e. the elements that should be repaired, was made in accordance with the criteria of the greatest probability of damage and the minimal number of the elements in question. It was decided that the first stage of the repair works should cover: the economizer, waterwalls and the fifth section of steam superheater (VPPP). The next stage, after 12000 operational hours, should cover: the first and second section of steam superheater (IPPP, IIPPP) and the second section of reheater (IIPPW). The third stage of the repair works should cover the economizer, waterwalls and V PPP. At the fourth stage of the repair works, the range of the second stage repairs should be repeated. The course of the risk is described by curve B in Fig. 8.

The options and combinations described above do not exclude the range of all possibilities, yet, they fulfill the accepted assumptions. The level of risk may also be reduced if the second section of steam superheater is repaired at the first stage. Accordingly, in the second stage the second and fifth section of steam superheater should be repaired, and in the third one- economizer, the first section of steam superheater and the second section of reheater , as well as the waterwalls; subsequently, the next stage should cover the repairs range from the second stage. The graph of the risk for such course of the procedures is illustrated by curve

C in Fig. 8. Additionally, lines A in Fig. 8 indicate a rise in the risk level when no repair works are administered.

It was assumed in the above analysis that the repairs should restore the technical condition close to the initial one, corresponding to the so called Kijima's model of the first type with the life reduction ration "*a*" equal to zero [7, 8, 9]. According to the model, the failure rate after each successive operation period *T* and the administered maintenance is defined as:

$$h_{i+1}(t) = h_i(t + a_i T_i) \tag{3}$$

where: $t \in (0, T_i)$, $0 \le a_i \le 1$

The graphs of the failure rate function *h(t)* for particular elements are shown in Fig. 9.

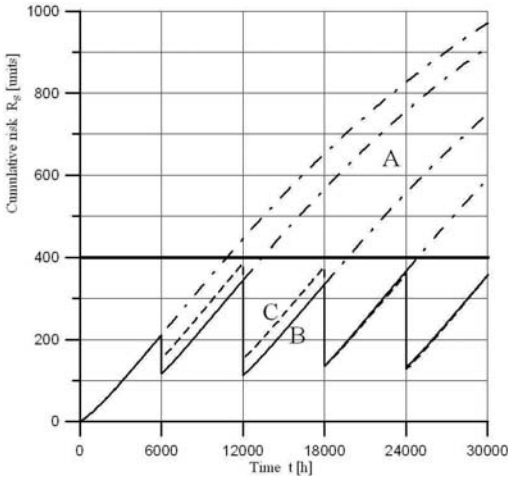

Fig. 8. Technical risk posed by the water-steam system in consideration of maintenances

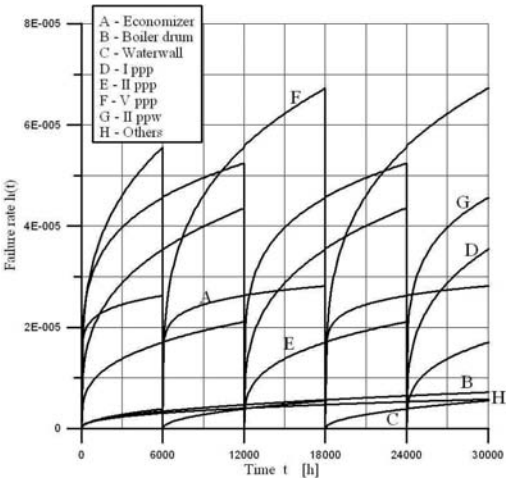

Fig. 9. Failure rate function in consideration of maintenances

5. Conclusion

The discussed method of selecting the range of maintenance for power machines and equipment takes into account a specific nature of repair procedures followed in power engineering. The repairs are conducted in distinct time frames, and the selection of their range is a very pertinent issue. On the example of the water-steam system of the boiler that constitutes one of the subsystems that are very prone to failure, the options of selecting the range of maintenance at particular stages are discussed. The assumed selection criterion is the principle of keeping, throughout the analyzed operation period, the level of technical risk below the limit values. Different options of the sets of facilities subjected to repair works and fulfilling the assumed criteria are presented. The decisive criterion of the optimal solution is the minimization of the costs of the maintenance.

6. References

[1] Rusin A., Banaszkiewicz M., Lipka M., Łukowicz H., Radulski W.: *Continuous control and optimization of thermal stresses in the process of turbine start-up*. Congress of Thermal Stresses. Wienna, s. 425-428, 2005.
[2] Rusin A.: *Koncepcja układu śledzenia ryzyka eksploatacyjnego turbin*, Archiwum Energetyki, tom XXXVI, s. 211-219, 2006.
[3] Rusin A.: *Ocena prawdopodobieństwa uszkodzenia wirników turbin z pęknięciami na podstawie badań diagnostycznych*, Zagadnienia Eksploatacji Maszyn z 1, 149, s. 141-155, 2007.
[4] Stewart M., Melchers R.: *Probabilistic risk assessment of engineering systems*. Chapman and Hall, London, 1997.
[5] Rusin A., Lipka M.: *Operational risk reduction of turbines by optimization of its start-ups*. Advanced in Safety and Reliability, ESREL 2005, vol. 2, s. 1721-1727, 2005.
[6] Rusin A.: *Assessment of operational risk of steam turbine valves*. Int. J. of Pressure Vessels and Piping, vol. 81, nr 4, s. 373-379, 2004.
[7] Pham H., Wang H.: *Imperfect maintenance*, European Journal of Operational Research 94, s. 425-438, 1996.
[8] Kahle W.: *Optimal maintenance policies in incomplete repair models*, Reliability Engineering and System Safety 92 , s. 563-565, 2007.
[9] Zhou X., Xi L., Lee J.: *Reliability-centered predictive maintenance scheduling for a continuously monitored system subject to degradation*, Reliability Engineering and System Safety 92 , s. 530-534, 2007.

Dr hab. inż. Andrzej RUSIN, prof. P.Śl.
Mgr inż. Adam WOJACZEK
Instytut Maszyn i Urządzeń Energetycznych , Politechnika Śląska
ul. Konarskiego 18, 44-100 Gliwice, Poland
E-mail: andrzej.rusin@polsl.pl

Gerard KOSMAN
Henryk ŁUKOWICZ
Krzysztof NAWRAT
Wojciech KOSMAN

ASSESSMENT OF THE EFFECTS OF THE OPERATION OF POWER UNITS ON SLIDING-PRESSURE

In the article the results of an analysis of the performance of a unit operated with incomplete sliding-pressure and with full sliding-pressure adjusted each time to a specific load are shown. The article also presents the gain obtained from the use of full sliding-pressure resulting from the reduction of thermodynamic loss in the system and the reduction of the unit's own needs. The measurements of the condensation-heating turbo set operated with incomplete sliding-pressure was used in the analysis. The method of choosing the reference steam pressure before the turbine was worked out to ensure minimal loss.

Keywords: *steam turbines, adjustment, sliding-pressure.*

1. Introduction

The control of power units designed to operate with sliding-pressure should for partial loads keep up the pressure after the boiler at slightly higher values (to make up for the loss in the piping, the control valve fully open) than the pressure before the first stage of the turbine (made for this type of control without regulation stage). The pressure after the boiler for partial loads results from the equation of the turbine flow capacity and the hydraulic loss in the piping. For operational reasons, i.e. to provide a possibility of quick changes of the unit power, a combination of sliding-pressure control with throttle control is used to retain higher pressure after the boiler than before the flow system of the turbine. Such unit operation results in a reduction of the cycle efficiency due to increased loss of the throttling at the control valve. Additional loss results from increased operation of the feed pump.

The analysis used an algorithm of calculations for the heating system of a unit formulated on the grounds of the equations of performance of the elements determined for this system, the equations of the turbine flow capacity and efficiency characteristics of the turbine, and the characteristics of heat exchangers. In order to determine these characteristics operational measurements of the unit were used.

To analyse the loss resulting from the unit operation with incomplete sliding-pressure an algorithm and a computer programme for balance calculations of the heating system were worked out to make it possible to determine the working medium parameters at individual cycle points for any value of the electric and heating load, and for different from the nominal values of: live steam pressure and temperature, the temperature of reheated steam, the temperature of feed water, the pressure in the condenser.

2. Turbine sliding-pressure control

Up till now basically two methods of control have been used to change the power of the turbine: throttle control and group (filling) control. In the former steam flows through one or two valves which open simultaneously. In the latter there are several valves which open successively. In both cases steam pressure in the boiler is steady and kept so with the pressure control.

In block systems sliding-pressure control also can be used by means of reducing appropriately the pressure after the boiler without the throttle valve intervention. The difference between a unit operating in the steady-pressure and sliding-pressure systems results from the scheme shown in Fig. 1 [1].

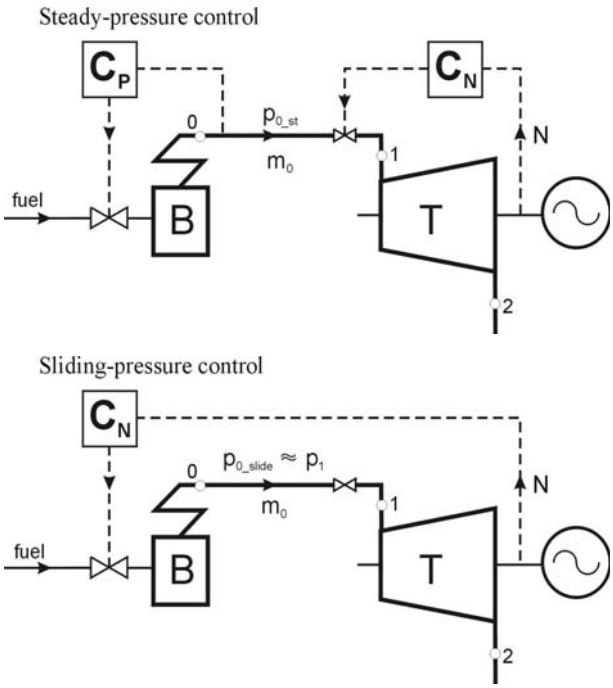

Fig. 1. The principle of operation of steady-pressure and sliding-pressure control of the boiler-turbine unit

In steady-pressure control the steam unit has two controls: the power of the turbine is adjusted with control C_N, which has an effect on the turbine valves and changes the steam jet according to demand. Control C_P maintains steady pressure after the boiler p_{o_st} (before the turbine valves) adjusting the steam jet generated in the boiler to the current turbine demand for steam. Control C_P acts on the steam jet delivered to the boiler.

The steam pressure before the blade system of turbine p_1 changes according to the principle of flow capacity. In sliding-pressure control the unit has only one control – power control C_N, with no pressure control. In consequence, the steam pressure after the boiler p_{0_slide} is the same as the pressure before the blade

system (except for the loss caused by the hampering in the piping). Power control C_N measures the power of the turbine and acts directly on the stream of fuel adjusting the amount of steam to demand. The turbine consumes as much steam as is currently being produced by the boiler.

The pressure of the steam in the boiler varies in proportion with the steam efficiency of the boiler. At the same time the temperature control maintains a steady temperature of live steam.

Fig. 2 shows the variation of the parameters before the turbine with throttle and sliding-pressue controls.

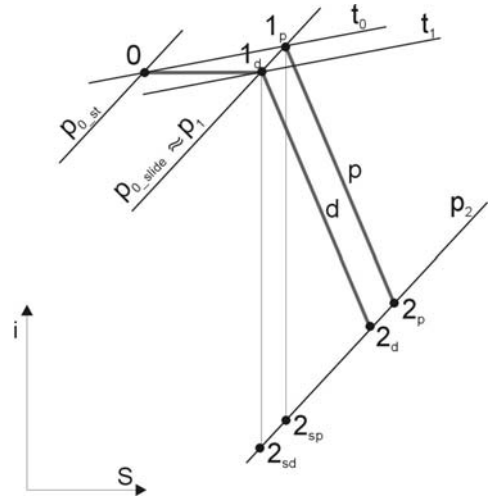

Fig. 2. Expansion in the turbine with sliding-pressure (p) and throttle (d) control

As the pressure of live steam diminishes, the efficiency of the cycle comes down as well. However, the efficiency fall is smaller than with throttle control because there is no loss of pressure in the turbine valves (p_{o_st}-p_1), and, resulting from it, the decrease of the steam temperature before the first stage of the turbine (T_0-T_1). Also, with throttle control the feed pump forces the condensate for the full nominal pressure of the boiler whereas with sliding-pressure control, in the conditions of partial load, the pressure in the boiler – and the force pressure of the pump – is lower, the power needed to drive the feed pump is lower (Fig. 3).

The main advantage of the sliding-pressure control in comparison with the throttle control is the labour saving of the feed pump under partial loads. The saving rises in proportion to the nominal pressure of live steam.

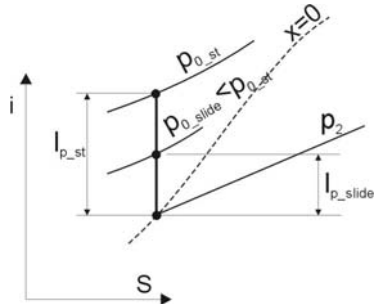

Fig. 3 Operation of the feed pump under partial load with steady-pressure (l_{p_st}) and sliding-pressure (l_{p_slide}) control

3. Scope of research and calculations

The aim of the research is to assess the effects of the change of the turbine control from incomplete sliding-pressure control to full sliding-pressure control. For the analysis a condensation-heating unit of the electric power of 145MW was assumed. The measurement scheme of the turbine is shown in Fig. 4. For the calculations of the turbine heating system the data from guarantee measurements were used. The measurements were within the full range of the turbine power (55-155MW) [2].

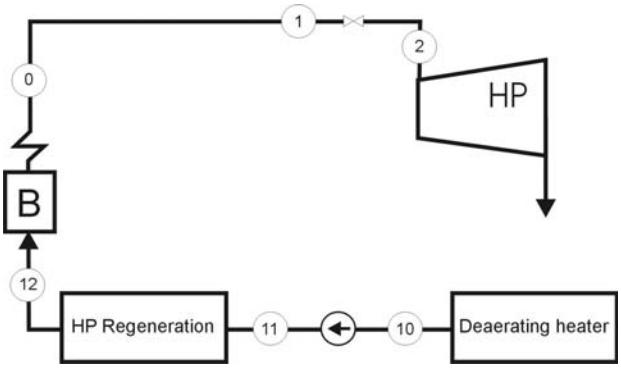

Fig. 4. Simplified scheme of the turbine heating system

4. Determination of nominal sliding-pressure

The condensation-heating turbine operates usually, under partial loads, with partly closed control valves of the HP part. This leads to the throttling of the steam jet and losses involved with it. These losses can be divided into thermodynamic and those caused by the excess power of the feed water pumps. The losses can be avoided by switching to sliding-pressure operation only. In this case the turbine control valves should be fully open. The pressure adjustment is then made with the boiler. The value of this particular pressure results from the current load of the turbo set. A method to determine it is shown below [3].

The equation of flow capacity for the HP part determines the pressure at the steam admission into the flow system (1) – i.e. before the first stage of the turbine.

$$\frac{m_2}{m_{02}} = \sqrt{\frac{T_{02}}{T_2}}\sqrt{\frac{p_2^2 - p_{10}^2}{p_{02}^2 - p_{010}^2}} \Rightarrow p_2 = f\left(m_2, p_{10}, T_2\right) \qquad (1)$$

where: m_2 – steam jet passing through the HP part of the turbine, m_{02} – steam jet passing through the HP part of the turbine for reference conditions, T_2 – temperature before the HP part of the turbine, T_{02} – temperature before the HP part of the turbine for reference conditions, p_2, p_{10} – pressure before and after the HP part of the engine (p_{10} determined by measurement), p_{02}, p_{010} – pressure before and after the HP part of the engine for reference conditions.

1. Allowing for the loss of pressure in the piping from the boiler and losses in the isolation and control valves, the pressure after the boiler is:

$$\zeta_{kot-2} = \frac{p_0 - p_2}{p_0} \qquad (2)$$

where: p_0 – pressure after the boiler, p_2 – pressure before the turbine

For the analysis the value of the loss (2) determined by the measurement of the turbine for full power (control valves fully open) was assumed. It amounts to:

$$\zeta_{kot\_2} = 0.037$$

2. The loss of pressure in the boiler (3) is determined by the measurements of the unit.

$$\zeta_{kot} = \frac{p_{wz} - p_0}{p_{wz}} \quad (3)$$

where: p_{wz} – pressure of feed water before the boiler (Point 65 in the heating scheme)

The characteristics of the resistance in the boiler in the function of the steam jet are shown in Fig. 5, and a straight line was approximated with the following equation (4):

$$\zeta_{kot} = 0.000808645 * m_0 + 0.00902612 \quad (4)$$

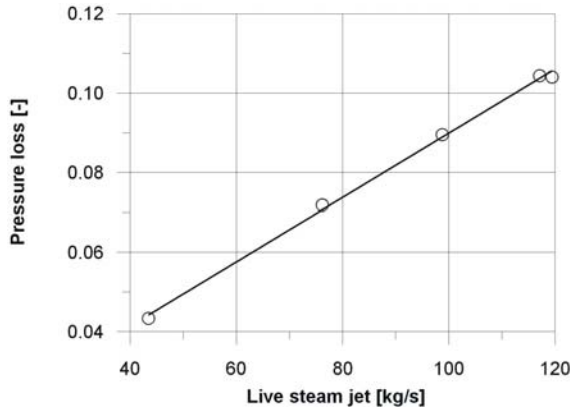

Fig. 5. Relative pressure loss in the boiler in the function of live steam jet

3. Determination of the feed water pump pressure on the grounds of the losses derived from formula (5):

$$\zeta_{pom\_kot} = \frac{p_{pom} - p_{wz}}{p_{pom}} \quad (5)$$

where: p_{pom} – pressure at feed water forcing

The average value of the loss determined by the measurements for various loads amounts to:

$$\zeta_{pom\_kot} = 0.047$$

5. Thermodynamic losses in cycle

The pressure of live steam after the boiler for various conditions of the turbine load was maintained in accordance with curve (o) shown in Fig. 6. In order to adjust the steam pressure before the first stage of the HP part of the turbine, the steam jet had to be throttled in the control valves. The decrease of the pressure of live steam in the valves is described as the difference between the pressure before the valves (o) and the pressure before the turbine (x). The difference between the two is shown as the marked area between the course of the pressures in question. The loss is illustrated as the curve in the bottom part of the chart (Fig.7). The lower the power of the turbine, the bigger the throttle waste, which involves significant losses connected with the change of the thermodynamic parameters of the steam jet.

The throttling of the heating medium together with the decrease of the pressure cause a fall in its temperature. This change is shown in the chart as the area which makes up the difference between the course of the steam temperature before the valves and before the turbine. The difference is also shown as the curve in the bottom part of the chart (Fig. 7). The lower the power of the turbine, the bigger the loss caused by the decrease of the parameters of steam conducted to the turbine. In such cases the temperature of live steam differs considerably from nominal temperature (cf Fig. 7).

Adjusting steam pressure before the turbine to individual load conditions through the throttling process generates thermodynamic losses in the system. The analysis which was carried out makes it possible to present the losses in the shape of the function shown in Fig. 8. Operation under maximum load does not generate thermodynamic losses in the system, but the lower the load, the bigger the loss. For minimal loads of the turbine in question it amounts to 50 kJ/kWh. This constitutes about 0.55% of the heat consumption per unit of the turbo set (Fig. 9).

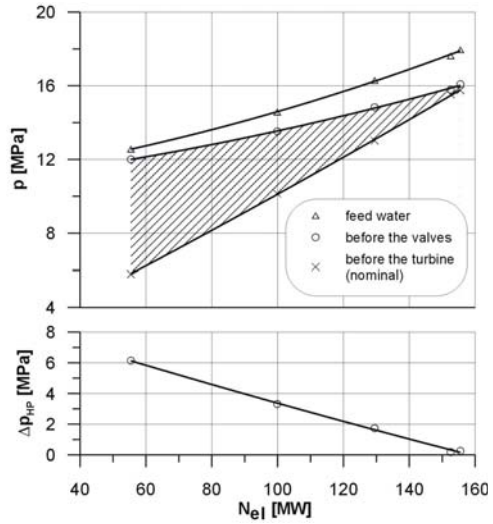

Fig.6. Pressure loss in the valves

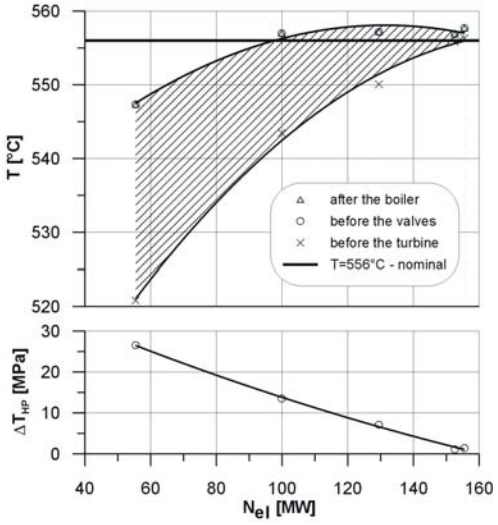

Fig. 7. Temperature loss in the valves

6. Assessment of the effects of the change in the type of control

The second stage of the analysis comprised the determination of the effect of the change in the type of control, from incomplete sliding-pressure to full sliding-pressure, on the power of the feed pump. The power of the pumps for the current operation conditions of the unit was shown in Fig. 10 as a curve marked in the chart as (Δ). After assuming full sliding-pressure (curve "x" in Fig. 6), the power needed to drive the pumps for partial loads of the unit will diminish. The value of this power for particular turbine loads is shown in Fig. 10 as curve (□). The difference between the power of the pump for current operation conditions and the power for full sliding-pressure is illustrated as the area marked in Fig. 10. The loss resulting from excessive power of the feed water pump for altered load conditions is shown in the bottom part of the chart.

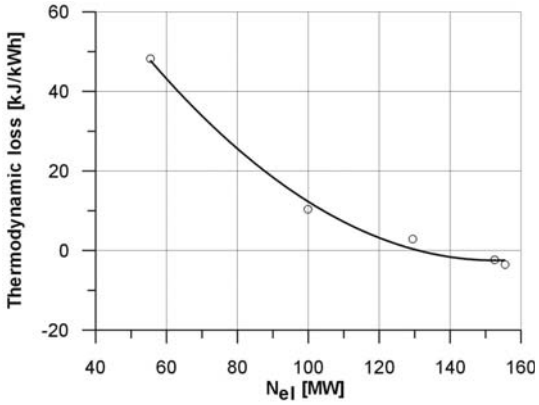

Fig. 8. Thermodynamic loss resulting from failure to keep the parameters of live steam

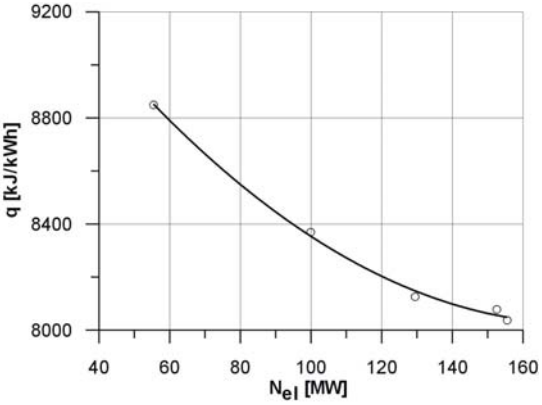

Fig. 9. Heat consumption per unit

7. Assessment of the reduction of own needs of the power plant after the change of the type of control

The assessment of the unit's own needs reduction which results from the decrease in the feed water pump labour was carried out for measurement data from a period of a two-week running of the turbo set. The data collection was done at one-minute intervals for the whole sampling period. In this way, the course of the turbine power shown in Fig. 11 was achieved. According to the course, the turbine operated usually in two scopes of power: the first comprised maximum powers (approx. 11800 min of operation – unit load in peak hours); the second – minimal powers (approx. 4000 min of operation – unit load during the night off-peak hours). The percentage of the turbine operation in individual scopes of power is shown in Fig. 12.

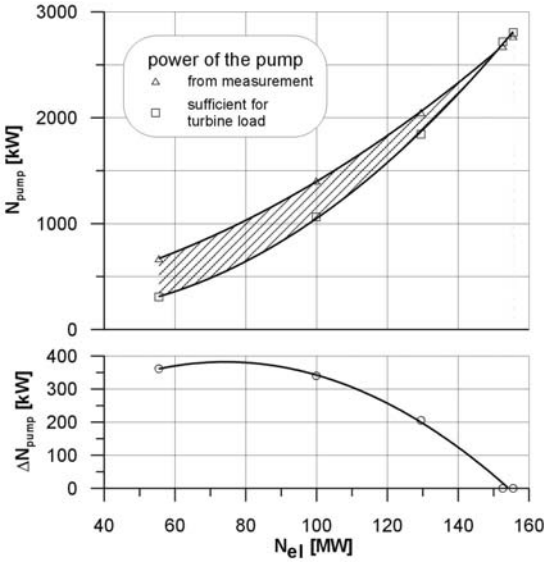

Fig. 10 Power change of the feed water pump

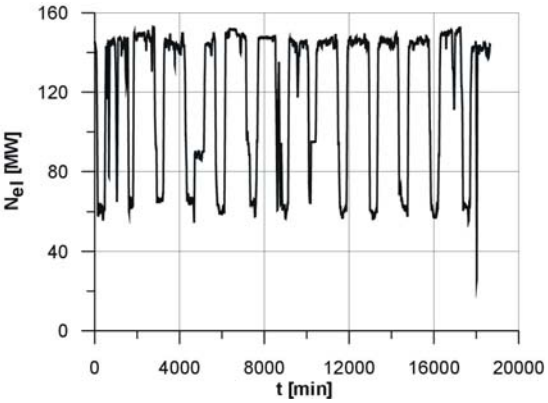

Fig. 11 Course of the turbine power

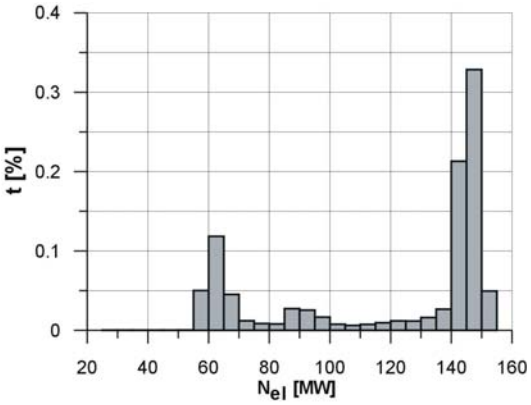

Fig. 12 Time of operation in particular scopes of power

For the first kind of operation (maximum power) the turbine does not generate any losses connected with type of control. However, with partial load the losses, as has been shown above, reach significant values (Fig. 8).

In the lower range of the turbo set load, with the operation of the turbine with full sliding-pressure, the estimated fall in the power of the feed water pumps is about 360 kWh. For the considered time of operation of t = 3985 min the gain amounts to about 24000 kWh. Assuming that the turbine operates like this for a whole year (allowing for maintenance works) the gain totals about 529000 kWh.

The longer the time when the turbine operates with loads smaller than nominal, the bigger the effect.

8. Conclusion

The operation of units running with sliding-pressure for partial loads is more advantageous in comparison with other types of control. This results from the fact that in such conditions the unit does not generate thermodynamic losses being a consequence of steam throttling in control valves, which in turn causes a fall in the temperature of steam before the first stage of the turbine. Also, the own needs of the power plant are smaller as the feed water pressure is lower.

In the case of turbine operation with incomplete sliding-pressure, where steam pressure before the turbine is partially adjusted to loads, a substantial gain can be achieved due to a change of the type of control in the shape of a decrease in the heat consumption per unit and a reduction of the own needs of a power unit.

9. References

[1] Perycz S.: *Gas and Steam Turbines*, Wydawnictwo PAN Wrocław 1992 (in Polish).
[2] Energopomiar.: *A Report on Thermal Guarantee Measurements*. Record Nş: 249/ZC/2005 (in Polish).
[3] Kosman G., Łukowicz H., Kosman W.: *An Analysis of Unit Losses Determined by Direct Balance Calculations*. 10th International Conference of Boiler Technology 2006, Prace IMiUE Politechniki Śląskiej, 2006 (in Polish).

Prof. dr hab. inż. Gerard KOSMAN
Dr hab. inż. Henryk ŁUKOWICZ
Dr inż. Krzysztof NAWRAT
Dr inż. Wojciech KOSMAN
Institute of Power Engineering and Turbomachinery
The Silesian University of Technology
ul. Konarskiego nr 18, 44-100 Gliwice, Poland
E-mail: krzysztof.nawrat@polsl.pl

Leszek PIASECZNY
Krzysztof ROGOWSKI

MODELLING THE MECHANICAL PROPERTIES OF SCREW PROPELLERS FOR SELECTION OF THE TECHNOLOGY OF THEIR REPAIRS

During repairing screw propellers by welding and plastic deformation it is indispensable to know their material features and strength properties relative to the propeller part subject to repair. The authors have conducted statistical and empirical research aimed at determining those features depending on the propeller's chemical composition and blade thickness. These dependencies are presented in the form of mathematical models useful both cognitively and utilitarian-wise.

Keywords: *screw propellers, mechanical properties, technology of repairs.*

1. introduction

Damages of screw propellers (fractures, fissure of blades) may occur during the vessels operation. These damages may result from the unfavourable overlapping of the ship's vibrations, screw propeller and propulsion engine. Moreover, some fissures, bends and nicks of the blade rubbing edges might also occur and it frequently happens when the screw propeller strikes against floating beams or ice floes. When the screw propeller works close to the area's bottom, it is worn by the erosion of sand raised from the bottom. Screw propellers are also worn by fatigue corrosion and cavitational erosion. Depending on the kind and extent of damage, location on the propeller and the possibilities of welding or hot straightening, screw propellers are repaired or replaced.

The up-to-date screw propellers are made of highly resistant multicomponent copper alloys, among which there can be distinguished manganese brass (Cu1-category alloys), aluminium brass (Cu2-category alloys), aluminium-nickel bronze (Cu3-category alloys) and manganese-aluminium bronze (Cu4-category alloys).

At present, in each category several kinds of copper alloys screw propellers are produced, and in the case of Cu3 category, even dozens of them, appearing under various trade names. Such a large number of copper alloys produced is the cause why before the screw propeller is repaired the exact chemical composition of the propeller material is not known (frequently the chemical composition of propeller material is protected by patent and constitutes an industrial secret), neither the mechanical properties of the screw propeller are known, in particular the blades with variable thickness of the cylindrical section on the propeller radius; whereas such information is indispensable for selecting suitable parameters and proper repair technology for the screw propeller.

Whereas the chemical composition of the propeller material can be roughly determined without destroying the screw propeller, it is more difficult to determine the mechanical properties of the propeller in places repaired. Taking samples from the propeller blade for determining mechanical properties is out of the question.

The mechanical properties of screw propellers given in technical documentation (certificate) are determined by testing separately cast ingots of 25 mm diameter. The results of this examination are only approximate, and are not the real mechanical properties of the blades of the screw propeller cast, and these can be determined only by taking samples from the screw propeller blade corresponding places.

2. Conditions for the efficient screw propellers repair

The knowledge of real mechanical properties, in particular the plastic properties of propeller blades in the area of repair by hot straightening or welding, permits to select suitable repair parameters (copper alloys of categories Cu1, Cu2, Cu3 and Cu4 have different heating temperatures for the repair of screw propeller blade by hot straightening, as well as welding – Tables 1), facilitates performing the repair, permits the decrease of welding deformation and stress and to avoid possible fissures in the weld and in the HAZ of the welded joint.

Tab. 1. Recommended welding materials and temperatures of thermal treatment at welding and straightening screw propeller blades made of cooper alloys [3]

Alloy category	*Welding materials*	*Minimal preheating temperature [°C]*	*Maximal temperature between runs[°C]*	*Temperature of relief annealing [°C]*	*Temperature of hot straightening [°C]*
Cu1	*Aluminium bronze [1] Manganese bronze*	*150*	*300*	*350-500*	*350-500*
Cu2	*Aluminium bronze Nickel-manganese bronze*	*150*	*300*	*350-550*	*350-550*
Cu3	*Aluminium bronze Nickel-aluminium bronze [2] Manganese-aluminium bronze*	*50*	*250*	*450-500*	*450-500*
Cu4	*Manganese-aluminium bronze*	*100*	*300*	*450-600*	*450-600*

Remarks:
1) Nickel-aluminium and manganese-aluminium bronze can be applied.
2) Relief annealing is not required if nickel-aluminium bronze is applied as welding material.

3. The dependence of the screw propeller mechanical properties in the place of its repair on the blade's thickness

Fragmentary research conducted in the laboratories of screw propeller manufacturers, e.g. the firm LIPS in Holland (a known producer of screw propellers), showed that the properties of screw propeller alloys spread over the propeller blade radius.

This stimulated an attempt to collect measurement data of copper alloys for screw propellers (Table 2) and subjecting them to statistical analysis which showed that the nature of dependences in mechanical properties and increased thickness of the screw propeller cast is best described by regression equation, $WZ\_WM = a+b \cdot lg(W)$ where W – propeller blade thickness in repair place [mm].

The graphic distribution of measurement points in the coordinate system (relative value of mechanical properties– blade thickness, Fig.1) and the lines obtained by way of multiple regression analysis describe fairly well the location of mean result values and suggest that when preparing statistically the measurement data in a common coordinate system – thickness, regression curves can be described by the following equations:

$$WZ(R_m, R_{0,2}, A_5, HB, D_z) = a + b\,lg(W)$$

where: WZ – relative value of mechanical properties; a- absolute term; W – propeller blade thickness (in repair place) [mm], b – coefficient; D_z – grain diameter.

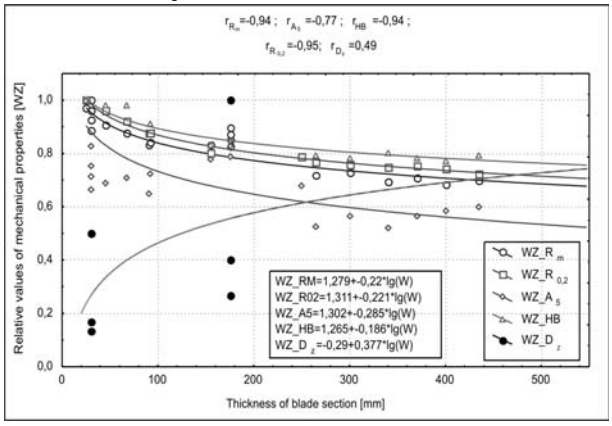

Fig. 1. Dependence of cast properties on the thickness of screw propeller section $WZ\_R_m=R_m/679$; $WZ\_R_{0.2}=R_{0.2}/262$; $WZ\_A_5=A_5/22.3$; $WZ\_HB=HB/163$; $WZ\_D_z=D_z/0.30$ [4]

Regression curves designated in a common coordinate system show that the changes in the properties of screw propeller cast occur mainly with increased blade thickness in the range from 25 mm to 175 mm and are close to the course of increase in grain diameter D_z; with further screw propeller blade increase, on the other hand, the changes are not very large. This permits the recognition that the deterioration of mechanical properties along with increased thickness of screw propeller blade is due to accompanying grain diameter increase of the copper alloy from which the propeller was cast.

4. The dependence of the screw propeller mechanical properties in the place of its repair on the blade's chemical composition

In order to obtain regression equations, data about mechanical properties and chemical composition of copper alloys from various research centres were collected and compared according to categories. The data concerned screw propellers made by various manufacturers, in various conditions of casting. The casts within the framework of the category had different designations, different chemical compositions and different mechanical properties. The contents of main alloy components in particular categories of copper alloys for screw propellers are presented in Table 2. They are generally in agreement with content differences of components in alloys given by classification societies.

Results of the following model parameters have been obtained (Table 3). In spite of certain deviations in the contents of the main alloy components (Table 2), essential regression equations have been obtained for most cases. Correlation coefficients and the results of Fisher test for checking the essentiality of regression calculated for dependent variables R_m and A_5 have been presented in Table 4.

The fact that R_m correlates stronger (Table 4) with the chemical composition than A_5 results from the measurement technique. The determination of value A_5 depends on the accuracy of comparing both parts of the culled sample.

As shown by Table 4, only regression equations for alloys of category Cu4 with the addition of zinc proved to be non-essential for the value R_m, and possibly incidental for the value A_5. This was probably decided by the overly large discrepancy of zinc content in those alloys ranging from 3.0% to 8.2%, whereas in alloys of other categories the content of particular components is kept within narrower bounds.

Tab. 2. The contents of main alloy components in particular categories of copper alloys for screw propellers

COPPER ALLOYS OF CATEGORY Cu1						
The contents of main alloy components [%]						
Cu	Zn	Al	Mn	Ni	Fe	Sn
58±4.0	37.5±2.5	1.75±1.25	2.25±1.75	0.5±0.5	1.5±1.0	0.75±0.75
COPPER ALLOYS OF CATEGORY Cu2						
The contents of main alloy components [%]						
Cu	Zn	Al	Mn	Ni	Fe	Sn
59±9.0	35.5±2.5	3.03±2.55	2.5±1.5	4.25±3.75	2.75±2.25	0.77±0.72
COPPER ALLOYS OF CATEGORY Cu3						
The contents of main alloy components [%]						
Cu	Zn	Al	Mn	Ni	Fe	Sn
81.80±4.8	0.62±0.37	9.0±2.0	3.25±2.75	2.92±2.67	4.0±2.0	0.2±0.15
COPPER ALLOYS OF CATEGORY Cu4						
The contents of main alloy components [%]						
Cu	Zn	Al	Mn	Ni	Fe	Sn
73.0±10.5	4.35±3.85	7.5±1.5	13.5±6.5	2.0±1.0	4.5±2.5	0.55±0.45

Tab. 3. Regression equations of the model

No.	Copper alloy	Regression equations for particular categories of copper alloys for screw propellers with model parameters
1.	Cu 1	$R_m = -6.931 \cdot c_{Zn} + 61\,241 \cdot c_{Al} - 18\,926 \cdot c_{Mn} - 32\,660 \cdot c_{Ni} - 101\,284 \cdot c_{Fe} - 90\,363 \cdot c_{Sn} + 907\,069$ $A_5 = -0.067 \cdot c_{Zn} + 3.093 \cdot c_{Al} - 3.636 \cdot c_{Mn} - 1.170 \cdot c_{Ni} - 2.043 \cdot c_{Fe} - 5.375 \cdot c_{Sn} + 34.312$
2.	Cu 2	$R_m = 4.595 \cdot c_{Zn} + 43.680 \cdot c_{Al} + 2.154 \cdot c_{Mn} - 10.632 \cdot c_{Ni} - 21.809 \cdot c_{Fe} - 103.980 \cdot c_{Sn} + 442.035$ $A_5 = 0.090 \cdot c_{Zn} - 1.265 \cdot c_{Al} + 0.298 \cdot c_{Mn} + 0.983 \cdot c_{Ni} + 1.521 \cdot c_{Fe} + 12.339 \cdot c_{Sn} + 8.233$
3.	Cu 3 (without Zn and Sn)	$R_m = -63.538 \cdot c_{Al} + 17.021 \cdot c_{Mn} + 12.697 \cdot c_{Ni} + 42.621 \cdot c_{Fe} + 978.803$ $A_5 = -7.277 \cdot c_{Al} + 2.704 \cdot c_{Mn} - 0.977 \cdot c_{Ni} + 4.010 \cdot c_{Fe} + 71.940$
4.	Cu 4 (without Zn and Sn)	$R_m = -63.538 \cdot c_{Al} + 17.021 \cdot c_{Mn} + 12.697 \cdot c_{Ni} + 42.621 \cdot c_{Fe} + 978.803$ $A_5 = -7.277 \cdot c_{Al} + 2.704 \cdot c_{Mn} - 0.977 \cdot c_{Ni} + 4.010 \cdot c_{Fe} + 71.940$
5.	Cu 4 (with Zn but without Sn)	$R_m = -1.612 \cdot c_{Zn} - 2.804 \cdot c_{Al} + 1.383 \cdot c_{Mn} + 14.214 \cdot c_{Ni} - 8.111 \cdot c_{Fe} + 704.306$ $A_5 = -0.037 \cdot c_{Zn} - 1.296 \cdot c_{Al} - 0.444 \cdot c_{Mn} + 1.639 \cdot c_{Ni} + 0.608 \cdot c_{Fe} + 31.704$

Tab. 4. Assessment of regression equations

Copper alloy	Dependent variables	Correlation coefficient	Value of Fisher test	Assessment of regression
Cu1	R_m A_5	0.937 0.909	5.989 3.982	essential essential
Cu2	R_m A_5	0.966 0.906	16.247 5.376	essential essential
Cu3 (without Zn and Sn)	R_m A_5	0.836 0.631	12.179 3.483	essential essential
Cu4 (without Zn and Sn)	R_m A_5	0.870 0.933	7.780 16.903	essential essential
Cu4 (with Zn but without Sn)	R_m A_5	0.806 0.997	0.370 32.597	non-essential incidental

It can be stated on the basis of results obtained that the matching of the model is satisfactory and that the prognostic value of the model high and statistically.

5. Conclusions

In result of statistical calculations conducted, the following conclusions can be drawn:

1. Regression equations of mechanical properties and chemical composition of marine screw propeller casts made of Cu1, Cu2, Cu3 and Cu4 alloys may be essential and permit the modelling the mechanical properties of the propeller with an accuracy sufficient for repair technology.
2. There has been formulated a new, original shape of regression equations of mechanical properties and chemical composition values of screw propeller casts made of copper alloys of categories Cu1, Cu2, Cu3 and Cu4. There are no such equations in the world's literature.
3. Vessel repair technologies have been given a method of modelling the mechanical properties of screw propeller in the blade section being repaired, which will facilitate the preparation of an effective technology (without shrinkage cracks) of repairing the screw propeller by welding or hot straightening of blades.

6. References

[1] Scarabello J. M..: *Contribution a l'etude du systeme trenaire Cu-Al-Mn*. Détermination de la coupe Cu- Mn-Al_6 limitée au domaine riche en cuivre. Revue de metallurgie 1982. Vol. 79. No 12. pp. 695 – 708

[2] Marine News: *New propeller blades in double – quick time*, 2005. N°2. pp. 36÷37.

[3] PRS. Przepisy. Publikacja nr 7/P. Naprawy śrub napędowych ze stopów miedzi. Gdańsk 2002.

[4] Piaseczny L., Rogowski K.: *Zmiana właściwości mechanicznych na promieniu (0.25 – 1)R odlewu okrętowej śruby napędowej*. Zeszyty Naukowe Akademii Marynarki Wojennej, Rok XLIV Nr 3 (154)2003.

[5] Wenschot P.: *The Properties of Ni-Al bronze sand cast ship propellers in relation to section thickness*. Naval Engineers Journal, September 1986. pp. 58 - 69.

[6] Ruddeck P., Koch W.: *Cumanal - ein neuer Werkstoff fur hochbeanspruchte Schiffspropeller*. Seewirtschaft 1972. H. 3. ss. 196 - 199. H. 4. ss. 269 - 272.

Prof. dr hab. inż. Leszek PIASECZNY
Dr inż. Krzysztof ROGOWSKI

Polish Naval University
Institute of Construction and Maintenance of Ships
Smidowicza Str. No 69 , 81-103 Gdynia, Poland
e-mail:l.piaseczny@amw.gdynia.pl

Zbigniew SKROBACKI

SELECTED METHODS FOR THE ESTIMATION OF THE LOGISTIC FUNCTION PARAMETERS

The logistic function can be employed as a model of record for a number of processes occurring in the management of technical objects and in logistics. The methods used for function parameter estimation include the analytical methods by Hotelling and Tinter and the numerical procedure of optimization in Excel with the Theil index as the optimization criterion. A numerical example is presented to illustrate the estimation accuracy of the methods discussed.

Keywords: *estimation, logistic function, Hotelling's method, Tintner's metod, Theil's index, optimization in Excel.*

1. Introduction

In the management of technical objects, there are a number phenomena with a trend of the function in which the rate of increase accelerates in the initial range of the independent variable until it reaches a maximum at the turning point and then tails off and the function tends asymptotically to a certain dependent variable. The trend model with an increasing and then decreasing rate of changes can be written as many exponential functions called S-functions because of their shape [4]. Examples of the exponential functions are given in Table 1. The considerations will focus on one of the functions, i.e. a logistic function, and the estimation of its parameters. As there are many interesting applications of the logistic function, whether in forecasts [3, 4] or economic models based on empirical data, one may hope to find more applications, for instance, in logistics and management of technical objects.

2. Logistic function

The logistic function, also known as logistic curve [3, 4], is described by Eq. (4) given in Table 1. The basic mathematical properties of the function can be established by determining its first (7) and second (8) derivatives. The function is increasing for $x \geq 0$ and has a horizontal asymptote with equation $y = a$ and a turning point with coordinates $x_p = (1/c)lnb$ and $y_p = a/2$.

$$y' = \frac{abc\exp(-cx)}{(1+b\exp(-cx))^2} > 0 \tag{7}$$

$$y'' = abc^2\exp(-cx)\frac{b\exp(-cx)-1}{(1+b\exp(-cx))^3} \tag{8}$$

The logistic function is convex for $0 \leq x < (1/c)\ lnb$ and concave for $x > (1/c)\ lnb$. Figure 1 shows examples of logistic functions for four series of data assuming that parameters a and b are constant and they are: $a = 100$ and $b = 4$. Parameter c is different for different series: for series 1 $c = 0.0462$, for series 2 $c = 0.2773$, for series 3 $c = 0.0924$, and for series 4 $c = 0.0231$.

The logistic function is nonlinear with respect to variable x. With respect to parameters a, b, and c, it is not linear either, so their values may be difficult to determine. Gąsiorowski and Kuszewski [4] suggest that a special case of the logistic function (so called Pearl's function), when $c = 1$, should be analyzed. The function is defined by the formula:

$$y_x = \frac{a}{1+b\exp(-x)} \tag{9}$$

where: $a > 0$, $b > 1$.

Tab. 1. Selected exponential and related functions corresponding to S-shaped trends (source: Ref. [3])

	function TYPE	*function form*	*COMMENTS*
1	exponential	$y = exp[a + (b/x)]$ (1) $x \geq 0,\ b < 0$	turning point at $(-b/2,\ e^{a-2})$ $\lim_{x\to\infty} y = e^a$
2	exponential	$y = exp[a + (b/\sqrt{x})]$ (2) $x \geq 0,\ b < 0$	turning point at $(-b^2/9,\ e^{a-3})$ $\lim_{x\to\infty} y = e^a$
3	exponential	$y = exp[a + (b/x^2)]$ (3) $x \geq 0,\ b < 0$	turning point at $\left(\sqrt{-\frac{2}{3}}b, e^{a-3/2}\right)$ $\lim_{x\to\infty} y = e^a$
4	logistic	$y = \frac{a}{1+b\exp(-cx)}$ (4) $a > 0,\ c > 0,\ b > 1$	turning point at $[(\ln b)/c,\ a/2]$ $\lim_{x\to\infty} y = a$
5	generalized logistic	$y = d + \frac{a-d}{1+b\exp(-ct)}$ (5) $c > 0,\ b > 1,\ 0 \leq d < a$	turning point at $[(\ln b)/c,\ d+(a/2)]$ $\lim_{x\to\infty} y = d+a$
6	Gompertz's	$y = ab^{c^x}$ (6) $a > 0,\ 0 < b < 1,\ 0 < c < 1$	turning point at $[\ln(-\ln b)/\ln c,\ a/e]$ $\lim_{x\to\infty} y = a$

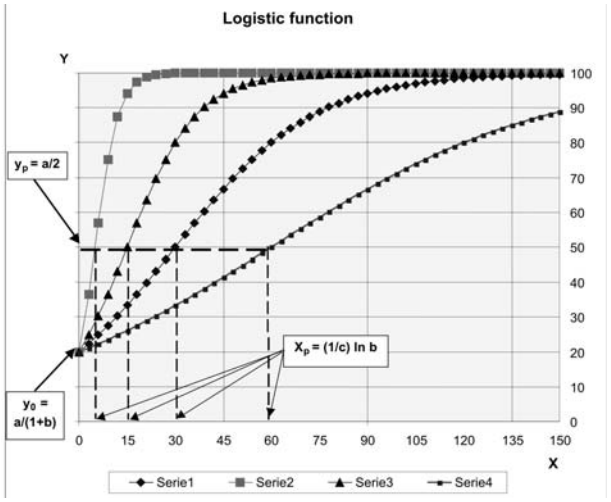

Fig. 1. Logistic functions with different parameter c

Two parameters of Pearl's function can be determined using the following substitutions:

$$\hat{y}_x = \frac{1}{y_x} \qquad \square = \frac{1}{a} \qquad \hat{b} = \frac{b}{a} \qquad \hat{x} = exp(-x)$$

which will result in the linear relationship:

$$\hat{y}_x = \hat{a} + \hat{b}\hat{x} \tag{10}$$

Basing on the transformed empirical data, i.e. the reciprocal of the original data, it is possible to estimate the parameters of function (10) with the least squares method and then calculate the parameters of Pearl's function (9).

Estimating parameters of a logistic function requires applying a more complex methodology. In Ref. [3] Stanisz provides an interesting discussion of three analytical methods of estimation of the logistic function parameters:

a) Hotelling's method,
b) Tintner's method,
c) Bonus's method.

The author states that only the first method has been popular with Polish scientists. Tintner's and Bonus's methods are generally less known. Stanisz analyzes the three methods thoroughly and proves that Tintner's method is the most accurate. He includes a complete derivation of formulas so that each method of estimation can be understood and applied properly. In this paper, the first two methods, i.e. Hotelling's and Tintner's, are discussed.

3. Estimation of the logistic function parameters with Hotelling's method

The idea of this method is to transform the logistic function into a linear one, with the new parameters being simple functions of parameters *a, b* and *c*. Thus, it is essential to transform the formula into the derivative of logistic function (7):

$$\frac{y'}{y} = c - \frac{c}{a}y \tag{11}$$

where: y, y' – the logistic function and its first derivative, respectively, *a, c* – parameters of the logistic function.

Hotelling writes the left side of Eq. (11) as a differential quotient assuming that the increment of the argument is equal to 1. It is also assumed that increments of the left side of the equation have values close to those of quotient y'/y for the consecutive $x = 1, ..., n-1$, where n is the number of data of the time series. Equation (11) is written as:

$$\frac{y_{x+1} - y_x}{y_x} = c - \frac{c}{a}y_x \ \text{(x=1, ..., n-1)} \tag{12}$$

Basing on the empirical data in the form of the time series $(1, y_1), ..., (n, y_1)$, one can calculate the relative increments

$$u_x = \frac{y_{x+1} - y_x}{y_x} \ \text{(x=1, ..., n-1)} \tag{13}$$

and create a new time series $(1, u_1), ..., (n, u_{n-1})$. Differential equation (12) can be written in the linear form

$$u_x = c - \frac{c}{a}y_x \ \text{(x=1, ..., n-1)} \tag{14}$$

Now applying the least squares method to the above equation and the new series $(y_1, u_1), ..., (y_{n-1}, u_{n-1})$, one obtains the estimates of parameters *a* and *c*. Parameter b can be determined from the formula:

$$\hat{b} = \frac{1}{n}\sum_{x=1}^{n}\left(\frac{a}{y_x} - 1\right)\cdot e^{c\cdot x} \tag{15}$$

The following twenty-element time series: $(x, y_x) = \{(1, 3), (2, 3.5), (3, 5.5), (4, 6), (5, 9.5), (6, 12.7), (7, 15), (8, 16), (9, 20), (10, 24), (11, 26.5), (12, 28), (13, 29.5), (14, 36), (15, 37), (16, 38), (17, 40), (18, 44), (19, 46), (20, 47)\}$ was used in the calculations as the empirical data to obtain the differential equation in the linear form (14) (see its graphical representation in Fig. 2).

Using the parameters of the linear function (14), it was possible to calculate the parameters of the logistic function: $a = 44.02$; $b = 19.54$; $c = 0.35$.

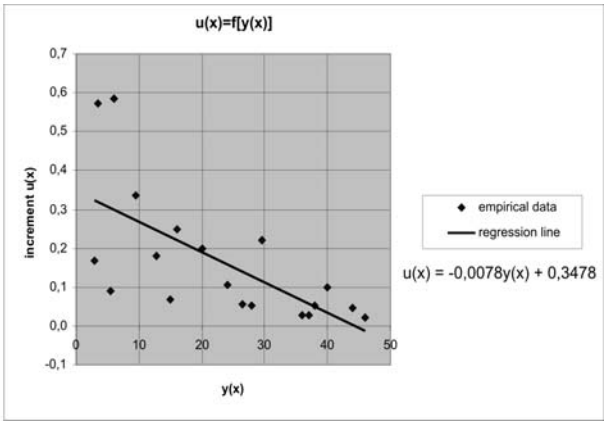

Fig. 2. Relationship (14) for the assumed empirical data

4. Estimation of the logistic function parameters with Tintner's method

The first operation is the transformation of the empirical data of the series $(1, y_1), ..., (n, y_n)$ into a new series given by the formula: $(z_x, z_{x+1}) = (1/y_x, 1/y_{x+1})$, $(x=1, ..., n-1)$,

where:

$$z_x = \frac{1}{y_x} = \frac{1 + b\,exp(-cx)}{a} \tag{16}$$

$$z_{x+1} = \frac{1}{y_{x+1}} = \frac{1 + b\,exp(-c(x+1))}{a} \tag{17}$$

Then, the equations are transformed into a differential equation:

$$z_{x+1} = (exp(-c))z_x + \frac{1 - exp(-c)}{a} \tag{18}$$

which can be represented as a linear equation with respect to the new parameters:

$$z_{x+1} = \delta z_x + \Gamma \tag{19}$$

where:

$$\delta = exp(-c) \qquad \Gamma = \frac{1 - exp(-c)}{a}$$

The least squares method was used for the differential equation (19) and the data of the new series (z_x, z_{x+1}). It was possible to establish, first, the estimates of the parameters of the differential equation, and then the estimates of parameters *a, b* and *c* of the logistic function. The estimates of the parameters can be determined from the following formulas:

- for parameter *a* $$\alpha = \frac{1 - d}{g} \tag{20}$$

- for parameter *c* $$\gamma = -ln\,d \tag{21}$$

- for parameter *b* $$\beta = \frac{1}{n}\sum_{x=1}^{n}\left(\frac{a}{y_x} - 1\right) \cdot exp(\gamma x) \tag{22}$$

where:

$$g = \frac{U_0}{U} \qquad d = \frac{U_1}{U} \qquad U = (n-1)\sum_{x=1}^{n-1} z_x^2 - \left(\sum_{x=1}^{n-1} z_x\right)^2$$

$$U_0 = \sum_{x=1}^{n-1} z_{x+1} \sum_{x=1}^{n-1} z_x^2 - \sum_{x=1}^{n-1} z_x \sum_{x=1}^{n-1} z_x z_{x+1}$$

$$U_1 = (n-1)\sum_{x=1}^{n-1} z_x z_{x+1} - \sum_{x=1}^{n-1} z_{x+1} \sum_{x=1}^{n-1} z_x$$

The parameters of the logistic function were calculated basing on the same empirical data as those in Section 3. Tintner's method was applied and the parameters of the logistic function estimated from the values of the linear function parameters were: $a = 50.83$; $b = 23.71$; $c = 0.28$. The graphical representation of relationship (19) is the diagram in Fig. 3.

5. Numerical estimation of the logistic function parameters

State-of-the-art mathematical computer programs can generate a nonlinear function optimally fitted to the given data. Also, the popular spreadsheet Microsoft Excel can be used to fit the function to the data within the line trend determination procedure. First, open an XY-type point diagram. Then, by clicking with the right button of the mouse several data series, select from the menu "add a trend line". The program offers six types of the trend function: *linear, moving average, logarithmic, polynomial, power and exponential*. To fit another model, for instance, the logistic function, which is of interest to us, one needs to use an additional program - *Solver* - compatible with Excel. The program selected from the pull-down menu of Excel is employed to optimize the calculations.

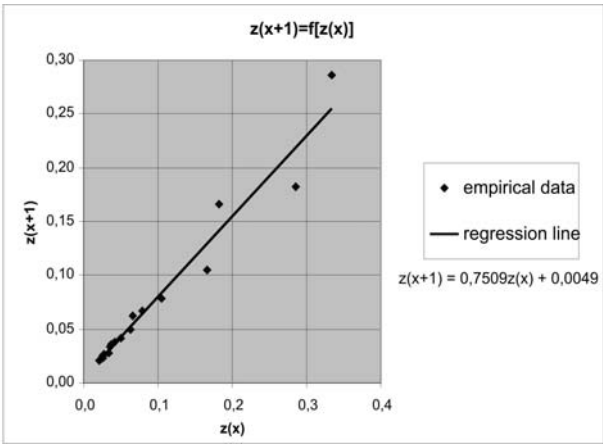

Fig. 3. Relationship (19) for the same empirical data as those in Hotelling's method

The information about the program included in the spreadsheet help guide is not sufficient. Similarly, a very brief description is given in Ref. [1]. Bourg writes that Solver uses the generalized reduced gradient algorithm developed by Leon Lasdon and Allan Waren for optimizing nonlinear problems. The algorithm will be employed to approximate the time series data (x, y_x). It is assumed that in the example the approximation function $\hat{y}_x$ will be the logistic function. The determination of parameters of the function $\hat{y}_x$ will be reduced to an optimization problem, in which the value of the measure selected to fit the function $\hat{y}_t$ to the empirical data is minimized. The optimization involves the following operations [1]:

a) in *Solver*, specify the optimization criterion or the target function; enter the address of the target cell containing the formula that will be modified by the program until it reaches a maximum, minimum or another desired value;
b) specify the constraints that define the relationships between the variables; in the program only one-side constraints, e.g. $h_i(x_i) \geq k_i$, can be specified in the "Constraint conditions" window;
c) specify the boundary conditions that provide information about the ranges in which the required variables can be found in the optimal solution; in the program the boundary conditions are also specified in the "Constraint conditions" window;
d) define the variables; in the program we enter the addresses of the cells being changed.

Analyzing Bourg's comments [1], one will notice that the target cell may contain numerous references to other cells with subsequent formulas. The cells with the formulas may have further references, etc. Thus, there seem to be a great many possibilities of expansion of the target function. In the example, it was assumed that the optimization criterion is the minimization of the Theil index, which is described by Eq. (23). In the original record (see Ref. [2]) the Theil index is employed to assess a forecast error. For the purpose of the example, the formula for the Theil index will be converted into the following form:

$$I^2 = \frac{\sum_{x=1}^{n}(y_x - \hat{y}_x)^2}{\sum_{x=1}^{n} y_x^2} \tag{23}$$

where: y_x – empirical values of the time series, $\hat{y}_x$ – values of the logistic function.

The index is assumed to be equal to zero, if the fitting of the logistic curve to the empirical data is accurate. In the optimization problem, the Theil index is the target function because it is a sum of three components, each with a different estimate of fitting.

$$I^2 = I_1^2 + I_2^2 + I_3^2 \tag{24}$$

In forecasts, the first component I_1^2 determines the size of errors relating to the forecast biasability. The errors result from the fact that the average value of the forecasting variable has not been defined. In the example, the component should be used as a measure of loadability of approximation. It can be determined according to the formula:

$$I_1^2 = \frac{\left(\bar{y} - \bar{\hat{y}}\right)^2}{\frac{1}{n}\sum_{x=1}^{n} y_x^2} \tag{25}$$

where: $\bar{y}$ - arithmetical mean of the empirical values of the time series, $\bar{\hat{y}}$ - arithmetical mean of the values of the logistic function.

In forecasts, the second component I_2^2 determines the size of errors relating to the insufficient flexibility of forecast. The errors result from the fact that the fluctuations of the forecasting variable have not been defined. In the example, the component should be used as a measure of insufficient flexibility of approximation. It can be determined according to the formula:

$$I_2^2 = \frac{\left(s_r - s_p\right)^2}{\frac{1}{n}\sum_{x=1}^{n} y_x^2} \tag{26}$$

where: s_r , s_p – standard deviation of the empirical values of y_x, and standard deviation of the values of the logistic function $\hat{y}_x$, respectively.

In forecasts, the third component I_3^2 determines the size of errors relating to the insufficient consistency of forecasts with the actual direction of changes in the forecasting variable. In the example, the component should be used as a measure of consistency of approximation. It can be determined according to the formula:

$$I_3^2 = \frac{2 s_r s_p (1 - r)}{\frac{1}{n}\sum_{x=1}^{n} y_x^2} \tag{27}$$

where: r – coefficient of the linear correlation between y_x and $\hat{y}_x$.

6. Example of the estimation of the logistic function parameters in the Solver program

It is assumed that the twenty-element set (x=1, 2, ..., 20) of values forming a time series of quantity Y with values identical with those in the examples presented in Sections 3 and 4, where (x, y_x)={(1, 3), (2, 3.5), (3, 5.5), (4, 6), (5, 9.5), (6, 12.7), (7, 15), (8, 16), (9, 20), (10, 24), (11, 26.5), (12, 28), (13, 29.5), (14, 36), (15, 37), (16, 38), (17, 40), (18, 44), (19, 46), (20, 47)} is known. Another assumption is that the model of changes in variable Y in the function of time is the logistic function given by Eq. (4). The problem requires determining the values of three parameters of the logistic function for which the Theil index (23) reaches a minimum. The calculations were made in the Solver program by performing the following operations:

a) the values of y_x (hereafter called empirical set) were represented in a graphical form; then, the parameter values were calculated for a = 50 and b = 9, which results from the assumption that the initially determined logistic function intersects the OY axis at point $(y_0 , x_0) = (5 , 0)$ (see Fig. 1), and c = 0.219722, which results from the assumption that the abscissa of the turning point of the logistic function, x_0, is equal to 10 (see Fig. 1);
b) the estimated parameters a, b and c were used to determine the values of the logistic function and calculate the Theil index;
c) the components of the Theil index were employed as measures of:
   - I_1^2 – biasability of approximation,
   - I_2^2 – flexibility of approximation,
   - I_3^2 – consistency of approximation.
d) the optimization criterion was the minimization of the Theil index; the values of $\hat{y}_x$ in the formula of the Theil index (23) were calculated after substituting the estimated parameters a, b and c,
e) the constraints and boundary conditions were established: a> = 0.001; b >= 1.001; c >= 0.001 to satisfy the assumptions in formula (4); it was also assumed that the parameters to be changed are quantities a, b and c.

The optimization results obtained with the Solver program are presented in Table 2 and Fig. 4. After the optimization, the logistic curve is better fitted to the empirical data, the evidence of which is a favorable change in the Theil index. Lower values of the first and second components of the Theil index are attributable to smaller differences between the averages of the empirical data and those of the logistic function. The logistic function takes into account the

Table 2. Comparison of the model parameters before and after optimization and applying Hotelling's and Tintner's methods

Name	Value before the optimization (for the estimated a, b, c)	Value after the optimization	Hotelling's method	Tintner's method
Parameter a	50.0	51.1	44.0	50.8
Parameter b	9.0	15.3	19.5	23.7
Parameter c	0.22	0.25	0.35	0.28
Theil index	$7.8*10^{-3}$	$1.8*10^{-3}$	$12.3*10^{-3}$	$3.9*10^{-3}$
1st component of the Theil index	$3.3*10^{-3}$	$0.0*10^{-3}$	$3.5*10^{-3}$	$0.1*10^{-3}$
2nd component of the Theil index	$3.2*10^{-3}$	$0.1*10^{-3}$	$0.0*10^{-3}$	$1.2*10^{-3}$
3rd component of the Theil index	$1.4*10^{-3}$	$1.7*10^{-3}$	$9.1*10^{-3}$	$2.7*10^{-3}$

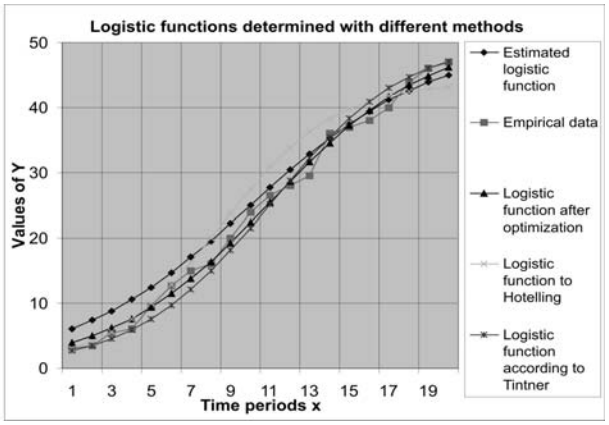

Fig. 4. Result of the estimation of the parameters of the logistic function determined with different methods for the given empirical data

fluctuations of the empirical data. Unfortunately, there is hardly any change in the third component after optimization and its high share in the value of the Theil index shows poor consistency of curve fitting. It may seem necessary to look for another function to record the changeability of a given phenomenon. The results show that the best fitting was obtained for Tintner's method.

7. Conclusions

- The paper presents a set of functions for modeling certain phenomena and processes, which may be of use to record trends with an initial increase and then a decrease in the rate of changes. The logistic function was selected for detailed analysis.
- To popularize the complex analytical methods of estimation of nonlinear curves, which include the logistic function, it was necessary to explain in a simple way the mathematical concept of Hotelling's and Tintner's methods. It was also essential to discuss the practical application of the numerical method of nonlinear optimization of the generalized gradient available in the Solver-Excel program.
- The above-mentioned methods were employed to assess three parameters of the logistic function assuming that the example set of empirical data is in the form of a time series.
- It is suggested that the Theil index can be used as a measure of estimation accuracy for the methods discussed above. The index components can be employed to assess the approximation.
- An example shows that the most accurate is the numerical method. A slightly less accurate is Tintner's method, where the Theil index is twice as big and the values of each component are higher. It should be noticed that Hotelling's method is the least accurate method. The Theil index in this case is 0.012, which testifies to good fitting of the logistic curve to the assumed empirical data.
- The result of the method comparison cannot be generalized, as it is based on the solution of one problem only. The considerations require further investigations based on more advanced mathematical methods.

8. References

[1] Bourg D.: *Excel w nauce i technice. Receptury*. Wyd. Helion S. A. 2006. Tłumaczenie z: Excel Scientific and Engineering Cookbook 1st edition ©2006 O'Reilly Media, Inc.
[2] Cieślak M. (pod red.) i inni: *Prognozowanie gospodarcze. Metody i zastosowania*. Wyd. Naukowe PWN, Warszawa 1997.
[3] Stanisz T.: *Funkcje jednej zmiennej w badaniach ekonomicznych*. Państwowe Wydawnictwo Naukowe, Warszawa 1986.
[4] Szapiro T. (pod red.) i inni: *Decyzje menedżerskie z Excelem*. Polskie Wydawnictwo Ekonomiczne, Warszawa 2000.

Dr inż. Zbigniew SKROBACKI
Kielce University of Technology
Faculty of Mechatronics and Machine Building
Al. 1000-lecia Państwa Polskiego 7
25-314 Kielce, Poland
e-mail: zbigs@tu.kielce.pl

Bogdan ANTOSZEWSKI

A NON-CONVENTIONAL METHOD FOR THE IMPROVEMENT OF THE FUNCTIONAL PROPERTIES OF SLIDING PAIRS

One of the ways to improve the functional properties of sliding friction pairs is to apply heterogeneous rubbing surfaces. Although this approach is still under investigation, heterogeneous surfaces are commonly employed in friction pairs under extreme lubrication conditions. The paper is concerned with the modeling of the friction process of flat textured sliding surfaces. The results can be used for the design of sliding friction pairs operating under extremely high loads.

Keywords*: sliding friction pairs, heterogeneous surfaces, geometrical texture.*

1.Introduction

Numerous studies have been undertaken to establish the effect of various physical, chemical and mechanical phenomena on the friction and wear processes. Advanced experimental methods make it possible to determine precisely the real loads that machine parts will be exposed to and select the right material for a friction pair to eliminate its damage or failure. Since the most frequent cause of the product malfunction is wear due to friction, a lot of attention is paid to the development of methods of friction reduction.

The number of materials that can be used for this purpose and technologies to harden these materials is limited. Designers carefully select the geometrical features of friction pair elements to reduce to a minimum the negative effects of friction. The selection is made both at the micro and macro levels, which is possible thanks to rapid advances in technology.

As was observed long ago, in certain cases of lubrication, pores or other specially generated (honed) cavities help trapping lubricant films and reducing the probability of the occurrence of loads leading to seizure of a friction pair. The paper discusses a nonconventional method of friction reduction in a sliding pair that involves applying heterogeneous surfaces. In conventional methods friction is reduced by using special techniques, lubricants, materials and self-lubricating films.

2. Heterogeneous surfaces

Surfaces are called heterogeneous when they possess regularly distributed areas characterized by different geometrical, physical-mechanical and physical-chemical properties. The areas constituting surface heterogeneities are generated by applying a technology different from that used to produce the rest of the surface. Thus, surface heterogeneities can include:

- cavities around the surface of the sliding rings, e.g. grooves, channels, form cavities produced by milling, erosion, etching, laser treatment, etc.,
- areas with different physical-chemical and mechanical properties, e.g. surfaces locally differing in hardness and mechanical strength due to surface hardening (laser, electron or thermal-chemical treatment),
- areas with different surface microgeometry, e.g. areas obtained by point erosion (laser treatment) or ones with shaped surface microgeometry, e.g. specially designed orientation of microirregularities or surface load capacity (laser treatment and electrospark deposition).

The regular cavities around the sliding surface produced with different techniques are reported to be of benefit to the friction process. The increased amount and better circulation of lubricant, which is trapped in the cavities, result in a lower temperature and more favourable distribution of pressure in the clearance, which improves the load capacity of the sliding pair [1, 2, 3].

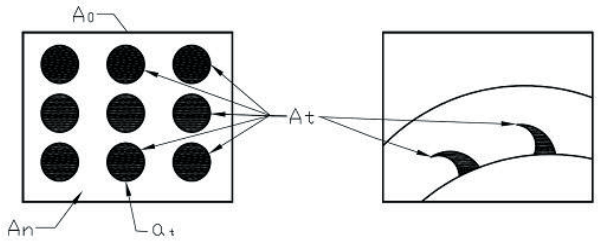

Fig. 1. Examples of heterogeneous surfaces: A_t – total area of heterogeneity (cavities, hardened areas), a_t – area of a single heterogeneity, A_n – flat surface, A_o- nominal surface

It should be noticed that the system of regular heterogeneities constitutes the geometrical surface texture, which may cover the whole area of the sliding friction pair or only selected areas regularly distributed around this surface. Figure 1 shows examples of heterogeneous surfaces.

2.1. Analysis of the geometry of contact and load

The analysis of the geometry of surfaces whose depth of heterogeneity is comparable to that of the height of roughness involves determining standard roughness parameters and the load curve. However, in a number of cases, the depth of surface heterogeneity is considerably higher than the height of surface roughness. It may turn out that the geometry of cavities is of importance in the formation of real contact. Surface heterogeneity should be considered in three aspects:

- cavities at the friction interface constitute the lubricant traps,
- cavities reduce the contact area and increase the load; in this way, they affect the value of the coefficient of friction,
- cavities at the friction interface have influence on the distribution of pressure in the clearance, which may cause changes in the load capacity of the sliding pair.

The changes in the load profile may be due to load and wear. Figure 2 analyzes changes in the load capacity for a profile form with spherical cavities. The strain due to load or wear causes a decrease in the depth of cavities by the value h, so the cavity radius decreases to the value R_h:

$$R_h = A_1B_1 = \sqrt{R^2 - (R - h_0 + h} = \sqrt{(h_0 - h)(2R - h_0 + h)} \quad (1)$$

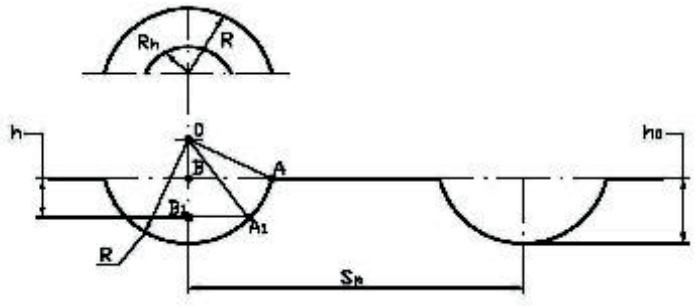

Fig. 2. Schematic diagram of the geometrical surface structure with spherical cavities

For 2R>>h $$R_h = A_1B_2 = \left(R - h_0\right)^{\frac{1}{2}}\left(h_0 - h\right)^{\frac{1}{2}} \quad (2)$$

The load capacity α (ratio of the surface without cavities to the nominal surface) will change into the value α_h:

$$\alpha = \frac{A_n}{A_0} \qquad \alpha_h = \frac{A_h}{A_0} \quad (3)$$

where : $A_n = A_0 - k\pi R^2 \qquad A_h = A_0 - k\pi R_h^2$

Applying force F, we obtain the following relationship for the load against the surface:

$$\sigma_h = \frac{F}{A_h}$$

After substituting relationships (2) and (3), we get:

$$\sigma_h = \left(\frac{1}{A_0 - k\pi\left(R - h_0\right)\left(h_0 - h\right)}\right)\sigma_0 \quad (4)$$

2.2. Analysis of friction resistances

Assuming the regularity of the cavities around the rubbing surfaces, we can develop a model of friction which takes into account both the area of flat surfaces and the area with cavities, here called the area of wavy surfaces. In the model, the flat surfaces are ideally flat, and the porous ones have roughness with equivalent parameters [4, 5].

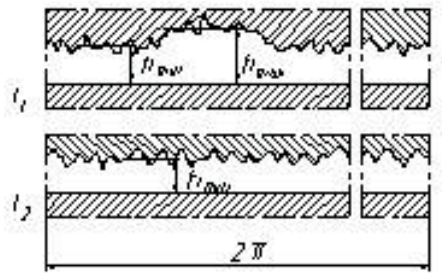

Fig. 3. Model of the clearance: fragment of surface with the cavitation area (upper part) and a fragment of surface without cavities (lower part)

In the general case, the total load force of a flat sliding pair with regular cavities around the opposing surfaces is expressed by the relationship:

$$W = W_m + W_h \quad (5)$$

where : W_m - mechanical component of the load force, W_h- hydraulic component of the load force.

The mechanical component of the load force resulting from the contact of the peaks of the microirregularities after taking into consideration the cavities [6] has the following form:

$$W_m = \alpha \cdot A \cdot P(H > h) \cdot p_g \quad (6)$$

where : A – area of microirregularities taking part in the transmission of loads, p_g - shearing strength of the softer material, $P(H>h)$ – probability of the occurrence of the assumed clearance height.

Because of the surface heterogeneity, the load force of the fluid film has two components:

$$W_h = W_{h1} + W_{h2} \quad (7)$$

where : W_{h1} – load force of the fluid film in the areas with no cavities, W_{h2} – load force of the fluid film in the cavitation areas.

For areas without cavities, the relationship is:

$$W_{h1} = \frac{\mu \cdot U}{h^2}\alpha \cdot A \cdot L \cdot f(L, \Delta r) \quad (8)$$

where: $f(L,\Delta r)$ – function determining the probability of occurrence of the fluid film [7], μ - viscosity of the fluid in the clearance, U – sliding speed, $L,\Delta r$ – length and width of the friction area.

For the cavitation areas, we adapt the relationship given by Lubeck [8]:

$$W_{h2} = (1-\alpha)A\left[\frac{k \cdot \mu \cdot \omega}{8\pi} \cdot \frac{(\Delta r)^2}{(h_{min})^2} \cdot f_1\left(\frac{h_a}{h_{min}}\right) + \frac{p_0}{4}\right] \quad (9)$$

where, additionally:

$$f_1\left(\frac{h_a}{h_{min}}\right) = 1 - \frac{1}{\left(1 + 2\frac{h_a}{h_{min}}\right)^2}$$

h_a - waviness amplitude, h_{min} – minimum clearance height, ω - rotational speed, p_0 - fluid pressure in the clearance.

Finally, taking into account the above, we obtain the relationship for the load force of the flat sliding pair:

$$W = W_m + \frac{\mu \cdot U}{h^2}\alpha \cdot A \cdot L \cdot f(L, \Delta r) + \\ +(1-\alpha)A\left[\frac{k \cdot \mu \cdot \omega}{8\pi} \cdot \frac{(\Delta r)^2}{(h_{min})^2} \cdot f_1\left(\frac{h_a}{h_{min}}\right) + \frac{p_0}{4}\right] \quad (10)$$

For simplicity, we shall consider a real case of a flat sliding pair, i.e. a pair of rings of a face seal, which is shown in Fig. 4.

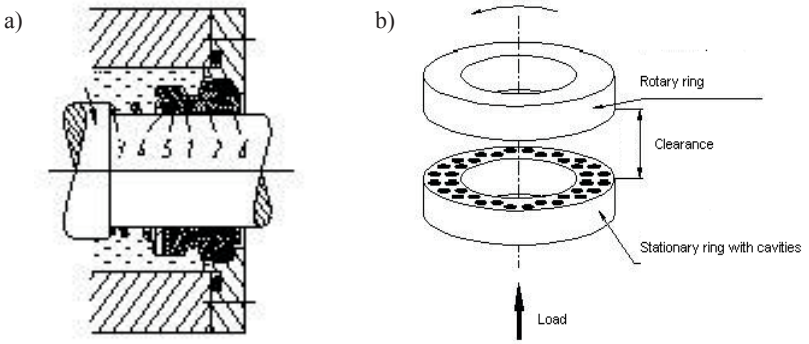

Fig. 4. a) Schematic diagram of the face seal: 1- axially shifted sliding ring, 2- anti-ring, 3- spring, 4- clamping ring, 5,6 – secondary seals, b) model sliding pair with textured surface

Case 1

Let us consider the case when $h_{min} > h_c$, where h_c is the clearance height for which the peaks of the microirregularities are in contact. The clearance height is big enough so there is no contact of the microirregularities.

Since $W_m = 0$, relationship (10) can be written as:

$$W = \frac{\mu \cdot U}{h^2}\alpha \cdot A \cdot L \cdot f(L,\Delta r) + \\ +(1-\alpha)A\left[\frac{k \cdot \mu \cdot \omega}{8\pi} \cdot \frac{(\Delta r)^2}{(h_{min})^2} \cdot f_1(\frac{h_a}{h_{min}}) + \frac{p_0}{4}\right] \quad (11)$$

In the general case, the friction force between the rubbing surfaces will be a sum of two components:

$$F = F_h + F_m \quad (12)$$

where: F_h – friction force of the fluid film, F_m – friction force of the peaks of the microirregularities in contact.
Thus, when $h_{min} > h_c$, $F_m = 0$.

The friction force of the viscous fluid, F_h, can be described by a known relationship:

$$F_h = A\frac{\mu \cdot U}{h} \quad (13)$$

Let us consider the case of complete fluid film with a variable thickness. If we base the considerations on the works by Stanghan-Batch and Ina [6] and Lebeck [8], we can calculate the coefficient of friction as follows:

$$f = \frac{\pi \cdot G \cdot r_m}{f_2 \cdot h_{min}} \quad (14)$$

where:

$$f_2 = \sqrt{1 + 2\left(\frac{h_a}{h_{min}}\right)} \quad (15)$$

In relationship (14), h_{min} is an unknown quantity, so it needs to be determined from other conditions. As the axial forces are in equilibrium, the load force in the clearance of the flat sliding pair of a face seal is counterbalanced by the external axial forces acting on the axially flexible element of the sliding pair. Thus, the condition of the equilibrium of the axial forces:

$$W = A \cdot p_0(b + \frac{p_s}{p_0}) = A \cdot p_0 \cdot b' \quad (16)$$

where: p_s – spring tension, b – coefficient of load, b' – corrected coefficient of load:

$$b' = b + \frac{p_s}{p_0} \quad (17)$$

Comparing relationship (11) with (16) and including the size of the friction area, we can calculate the clearance height:

$$h_{min} = \sqrt{\frac{\mu \cdot U \cdot \alpha \cdot L \cdot f(L,\Delta r) + (1-\alpha)\frac{k \cdot \mu \cdot U}{8\pi \cdot r_m}\Delta r^2 f_1(\frac{h_a}{h_{min}}}{p_0 \cdot b' - (1-\alpha)\frac{p_0}{4}}} \quad (18)$$

Using the definition of parameter G, we calculate the minimum clearance height:

$$h_{min} = C_1\sqrt{G} \quad (19)$$

where:

$$C_1 = \sqrt{\frac{\frac{1-\alpha}{4}k \cdot (\Delta r)^2 f_1(\frac{h_a}{h_{min}}) + 4\alpha\pi^2 r_m^2 f(L,\Delta r)}{1 - \frac{1-\alpha}{4b'}}} \quad (20)$$

$$G = \frac{\mu \cdot U \cdot \Delta r}{W} \quad (21)$$

Substituting the calculated clearance height to relationship (14) and performing certain transformations, we obtain the value of the coefficient of friction:

$$f = \frac{\pi \cdot r_m \cdot \sqrt{G}}{f_2 \cdot C_1} \quad (22)$$

Case 2

We consider a situation when there is a direct contact of the peaks of the microirregularities, i.e. when $h_{min} = h_c$. The clearance height is known, as it results from the height of the microirregularities. Like in Refs. [9, 10], it is assumed that the distribution of the peaks of the microirregularities is the Gaussian distribution and the height the of microirregularities in contact, h_c, is 3σ, with σ being a standard deviation defined by the following relationship:

$$\sigma = \sqrt{\sigma_1^2 + \sigma_2^2} \quad (23)$$

where: σ_1, σ_2 - standard deviations of random variables representing the profiles of both surfaces.

Like in the previous case, the load force of the seal resulting from the fluid film is calculated according to formulas (8) and (9). The value of the friction force of the fluid film is given by relationship (13), while the friction force of the microirregularities in contact is defined by the following relationship:

$$F_m = f_b \cdot W_m \tag{24}$$

where f_b - coefficient of boundary friction.

Calculating W_m from relationship (10), we get:

$$W_m = W - \frac{\mu \cdot U}{h^2}\alpha \cdot A \cdot L \cdot f(L,B) - \\ -(1-\alpha)A \left[\frac{n \cdot \mu \cdot \omega}{8\pi} \cdot \frac{(\Delta r)^2}{(h_{min})^2} \cdot f_1(\frac{h_a}{h_{min}}) + \frac{p_0}{4}\right] \tag{25}$$

Using relationships (5), (11) and (25) and performing certain transformations, we obtain the following relationship for the coefficient of friction:

$$f = f_b\left[1 - G \cdot f(L,\Delta r) \cdot \alpha \cdot \frac{4 \cdot \pi^2 \cdot r_m^{\,2}}{h_{min}^{\,2}} - (\frac{1-\alpha}{4}) \right. \\ \left. (G \cdot k \cdot f_1(\frac{h_a}{h_{min}})\frac{(\Delta r)^2}{(h_{min})^2} + \frac{1}{b'})\right] + \frac{2\pi \cdot r_m \cdot G}{f_2 \cdot h_{min}} \tag{26}$$

The model of friction assumes that the opposing surfaces are in contact or that there is no contact between them. The model can be used for the analysis of friction of seals with rings characterized by different geometries of surface heterogeneities.

2.3. Examples of the model analysis

The model was analyzed in a numerical example using the MATHCAD 7.0 program for the following data:

μ – 700 10^{-6} Pa s – dynamic viscosity of the medium,
μ h_c – 10^{-6} m – clearance height in the area of the flat surface,
h_a – 10^{-6} m – clearance height in the cavitation area,
k – 3, 6,.... 12 – number of cavities per surface unit,
α – 0.2...0.8 – share of the flat surface,
r_m = 0.0205 m – average ring radius,
Δr = 0.005 m – ring width.

The relationship between the coefficient of friction and parameter G was analyzed for different shares of the flat surface α and different number of surface structures k in the friction area. It was necessary to define the influence of these parameters on the coefficient of friction for the following cases $h > h_c$ and $h = h_c$

Figures 5 and 6 show typical relationships between the coefficient of friction and parameter G both for the regime of mixed friction and that of fluid friction. As can be seen in Fig. 5, in the mixed friction regime, the coefficient of friction decreases when there is a rise in parameter G. In the regime of fluid friction, an inverse relationship is observed (Fig. 6). This general relationship between the coefficient of friction and parameter G is not at all dependent on the number of cavities k or the share of flat surface α. The influence of parameters k and α is not analyzed in this paper.

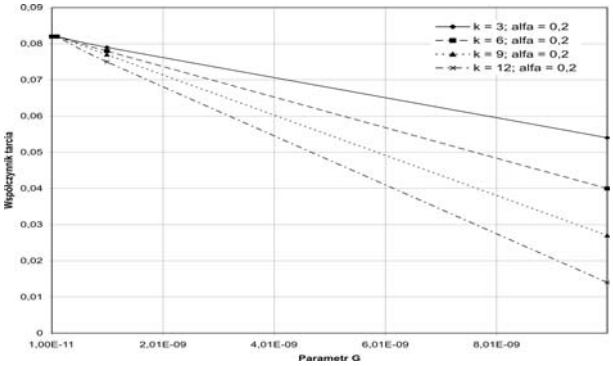

Fig. 5. Coefficient of friction between the face seal rings vs. parameter G in the regime of mixed friction for surfaces with a different number of cavities k and a constant share of flat surface α

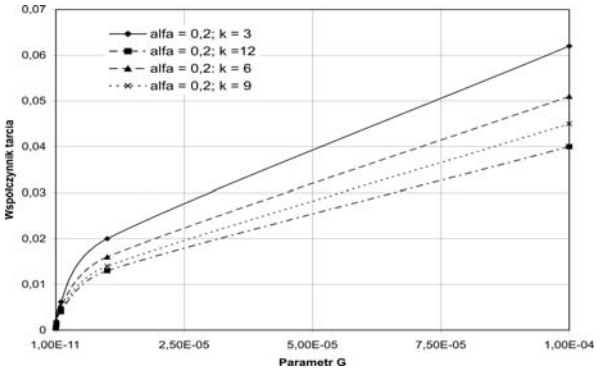

Fig. 6. Coefficient of friction between the face seal rings vs parameter G in the regime of fluid friction for surfaces with a different number of cavities

The proposed model of friction makes it possible to determine the values of the coefficient of friction and parameter G for which there is a transition from mixed friction to fluid friction. Figure 7 shows the values of the coefficient of friction recorded for both regimes. The transition point is in the range of parameters $G = 10^{-7} \div 10^{-8}$. The exact position of the transition point is shown in Fig. 8. The hypothetical values of the coefficient of friction f and parameter G at the transition point were established by comparing the mathematical model for mixed friction with that of fluid friction.

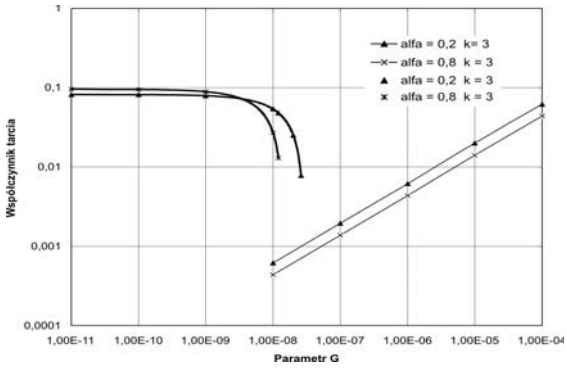

Fig. 7. Coefficient of friction between the face seal rings vs parameter G (logarithmic scale)

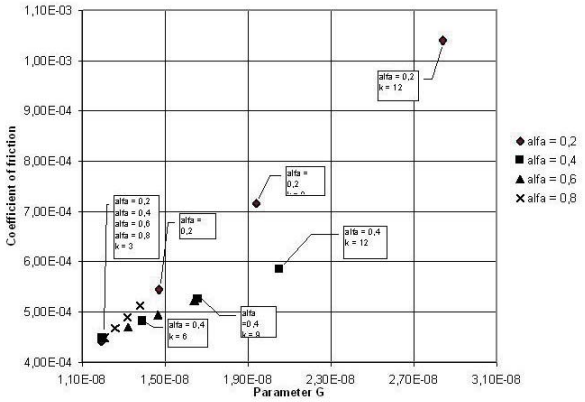

Fig. 8. Positions of the points of transition from mixed to fluid friction for the mating face seal rings

3.Conclusions

Analyzing the above diagrams, one can draw the following conclusions about face seal rings whose surfaces are partly flat α and partly with cavities *k*:

- the greater the number of cavities k on the surface of a face seal ring, the lower the coefficient of friction both in the regime of fluid friction and that of mixed friction,
- the greater the area of the flat surface *α*, i.e. the greater the share of the flat surface in the total area of friction in the regime of mixed friction, the greater the coefficient of friction; the relationship is true for all the considered number of cavities (Fig. 6.15),
- for fluid friction, an increase in the share of the flat surface α causes a decrease in the coefficient of friction, the exception being the case when $k = 12$ for which the coefficient of friction rises slightly with an increase in *α*,
- a rise in the value of parameter *G* causes that the type of friction between the seal rings changes from mixed into fluid; the developed model makes it possible to assess the parameters of the transition point depending on the number of cavities and the share of the flat surface.

4. References

[1] Izhak Etsion.: *State of the Art in Laser Surface Texturing* – Transaction of the ASME January 2005 Vol. 127.
[2] X.Q. Yu, S.He, R.L.Cai.: *Frictional characteristics of mechanical seals with a laser textured seal face* - Journal of Materials Processing Technology 129(2002) 463-466.
[3] Antoszewski B.: *Własności laserowo i plazmowo modyfikowanych ślizgowych węzłów tarcia na przykładzie uszczelnień czołowych* Zeszyty Naukowe Politechniki Świętokrzyskiej, Nr 17/1999.
[4] Christensen H.: *A Theory of Mixed Lubrication*. Proceedings of the Institution of Mechanical Engineers Vol. 186, 41/72, 421–430.
[5] Lebeck A.O.: *An evaluation of the average flow model for surface roughness effects in lubrication*. ASME Journal of Lubrication Technology, 1980, 102, 360–367.
[6] Stanghan-Batch B. Iny E.H.: *A Hydrodynamic Theory of Radial Face Mechanical Seals*. Journal of Mechanical Engineering Science 1973, Vol. 15 No. 1.
[7] Halling J.: *Principles of Tribology*. Macmillan Press Ltd, London and Brasingstoke 1975.
[8] Lebeck A.O.: *A Study of Contacting Mechanical Face Seal Performance Data Using Mixed Friction Models*. 12th International Conference on Fluid Sealing, Brighton UK 10–12 May 1989, Paper F2, 271–289.
[9] Lebeck A.O.: *Parallel Sliding Load Support in the Mixed Friction Regime* – Part 1 – The Experimental Data. Journal of Tribology, Vol. 109, January 1987, 189–195.
[10] Lebeck A.O.: *Parallel Sliding Load Support in the Mixed Friction Regime* – Part 2 – The Evaluation of the Mechanisms. Journal of Tribology, Vol. 109, January 1987 196–205.

Dr hab. inż. Bogdan ANTOSZEWSKI
Chair of Terotechnology
Kielce University of Technology
Al. 1000-lecia PP 7 25-314 Kielce, Poland
E-mail: ktrba@tu.kielce.pl

Krzysztof OLEJNIK

THE USE OF THE ADDITIONAL LIGHTING OF THE SEMI TRAILERS FOR THEIR SAFETY EXPLOATATION

The report has pointed out the need to provide the truck driver with a semi trailer, the ability to see the contour of the semi trailer and road illumination in the insufficient lighting conditions. The need for equipping the vehicle with additional contour light and lamps illuminating the section of the road overrun by the semi trailer wheels has been assessed. This is particularly important during manoeuvring with such truck – semi trailer unit at night to ensure safety, as the semi trailer has a different tracking circle than the towing truck. Current regulations are too (categorical) restrictive and limiting possibility of introducing additional lights. The proposal for technically solving this problem as well as amending the regulations, has been presented. The existing technical requirements included in current regulations on lighting do not take into account the need to ensure the visibility of these areas for the truck driver with a semi trailer.

Keywords*: lighting, semi trailer, visibility, safety.*

1. Introduction

The analysis of the reasons of collisions and accidents indicates the limited visibility as the essential cause of their occurrence. The tests were made and the drivers driving the trucks with trailers and semitrailers at night were interviewed. It appears from them that on the roads and in the manoeuvring areas which are not lit up by the street lamps, the drivers have the invisible areas on the right and left sides of the vehicle along all its entire length. The reason is the lack of the lighting of the above mentioned areas. If the area is not illuminated by the street lamps, in the darkness they are also not illuminated by the lamps of the own vehicle. Besides these vehicles have unilluminated side edges and they are not visible for their drivers. The driver is unable to observe the shifting of his own vehicle and its position against the other objects, so to avoid the collision or accident.

In Poland at night there are also unilluminated pedestrians on the roads, cyclists, horse carriages etc.

While passing the unilluminated objects, the driver is unable to define the position of the side of the driven truck in relation to the unilluminated objects.

The similar situation takes place when manoeuvres are carried out in none lit up place and there are unilluminated objects either side of the vehicle.

2. The estimation of the situation and changes proposed

The driver of the vehicle or group of vehicles should have the possibility to observe the surroundings of the vehicle together with the elements of the contour of this vehicle – see Figure 1 [1, 2]. The drawing presented below shows these areas around the vehicle.

The driver should have the ability to observe them during driving, both during a day and at night. It should be possible under the street lighting and without it.

The possible directions of relocation of the vehicle were studied: forwards, backwards and sideways. During the day light, the vehicle driver does not receive the direct or indirect visual information transfer from the part of the area surrounding the vehicle, although they are very important for collision free movement. This is a result of obscuring visibility by the none transparent elements of the vehicle cab and vehicle body.

The area not visible around the vehicle at night becomes considerably bigger. The front headlights light the road ahead. The reverse lamps light the road during driving backwards. If there are no street lamps, the rest of the vehicle surrounding (if it does not emit the light itself) is dark. The obstacles that find themselves in these areas are not visible to the driver.

Besides, the vehicle without the trailer while movement around the curve has insignificantly widened corridor of the movement. But the vehicle with the semitrailer moves in the other (wider) corridor than the vehicle without the semitrailer – Figure 2.

During driving round the curves, the wheels of the semitrailer move along quite another track than the wheels of the truck tractor – Figure 3. In this situation at night (without the street lighting) the driver has the unilluminated area, which the wheels of semitrailer run on. Although the driver can look at the mirrors, he cannot see the side of his vehicle; where and what the wheels of the semitrailer run over [3]. The tractor and semitrailer are not equipped with the lamps which could light up the area which their wheels run over during driving round the curve.

Minimum two typical cases of this situation can be isolated.

1. The driving of the group of the vehicles for example: on the crossing and turning right or left.
2. Avoiding pedestrians or cyclists who move on the road at night and are not illuminated. Additionally at night in the darkness the driver cannot see the side of the semitrailer.

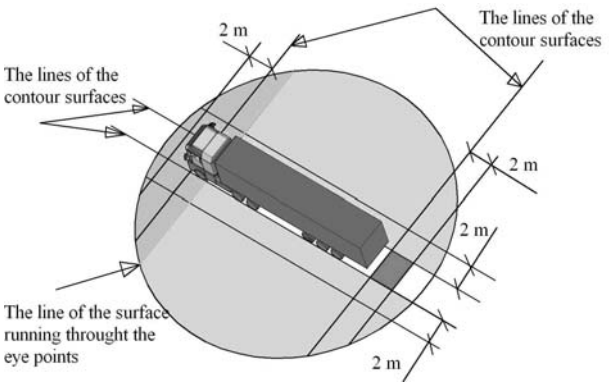

Fig. 1. Extensibility and spacing of the areas around the vehicle which should be seen by the driver

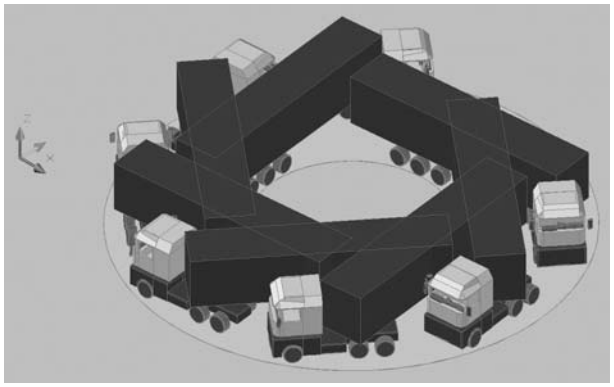

Fig. 2. The tracks of the tractor wheels' movement and those of the semitrailer running around the curve

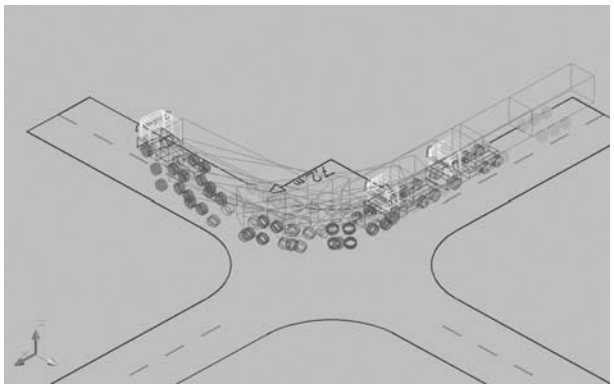

Fig. 3. The movement tracks of the vehicle with semitrailer during turning at the crossing

In the first case, the driver „feeling his way" drives the tractor on around such a curve as to avoid wheels overrunning the kerb or other obstacles. In the second case the situation is similar, but on the narrow road the vehicle coming from the opposite side forces the driver of the group of the vehicles, to return earlier on to his traffic lane. This can cause the collision of his semitrailer with the pedestrian or cyclist who is in the unilluminated area.

The driver is not able to observe the relative position of his vehicle against pedestrian or cyclist.

In such a situation, the unilluminated area, in which the collision took place, does not give the driver any information about the accident.

He drives away from the place of the accident, unaware that he should give help.

To avoid such a situation, the experiment to select and add the additional lighting of the semitrailer was conducted:

- this additional lighting should show the driver where the contour of the vehicle is – the additional white contour lights,
- the headlamps mounted on the sides of the semitrailer to light the road which the wheels of the semitrailer run on, when the group of the vehicles is moving round the curve.

The fulfilment of these assumptions contradicts the rules of Regulation 48 ECE UN, which are currently in force, regarding this matter, in Europe. The authors of these rules did not take into account the need of more lighting of these areas to enable the driver to watch the road there and see what his vehicle runs over on it.

Fig. 4. The view of semitrailer and the placement of the additional lights

In the experiment conducted, the additional white contour lights were used. They were placed at the end of semitrailer, at upper and lower parts. Additionally, the white light was mounted, directed downwards at the road. One lamp being placed on either side of the semitrailer around wheel arches, Figure 4.

Functionally, the additional lamps illuminating the road around the wheels of the semitrailer are connected with the position lights. They are switched on when the position lights are also on. Similarly, the additional contour lights are connected. Photo Figure 5 shows the effect of the additional semitrailer side lighting, on the right hand side, around the wheels.

Additionally, the view of this situation in the darkness is shown, when photos were illuminated by the flash light. When the same area is not lit up by the additional lamp of the vehicle, the driver is not able to observe it in the darkness, during the manoeuvre and to avoid, for example, a pedestrian.

In the light of the gained experiences, actual state of the knowledge, technical progress and the development of the devices for indirect visibility and lighting, it is possible to assist the driver of the group of the vehicles to receive the information from the hitherto invisible areas. In the future, it may be necessary to extend some requirements, concerning the vehicles equipment with regards above mentioned issue.

Fig. 5. The photo of the man on the road side, shown in the additional lights of the semitrailer and the view of the same area in the lighting of the flash light

3. Conclusion and recommendations

The aim of these considerations was to obtain the answers to the questions:

- is the need to introduce the additional lighting, justifiable?
- what should it be like
- should this lighting be nonobligatory or obligatory,
- should it be constantly on or only when it is necessary,
- is it necessary to attempt to change the regulations in this field.

The additional lighting in the above mentioned situations is necessary.

To remedy the above mentioned flaw, it is necessary to act for the benefit of the safety system improvement and introduce the additional lighting of the vehicle. It will enable the increase of the areas around the vehicle, which driver should have possibility to observe.

The research programme is being prepared to evaluate this solution in the normal road conditions and to obtain answers to the questions asked.

Problems indicated, allow to understand the scale of the projects with the objective of road traffic safety system improvement. Significant part of these projects may provide measurable effects – decrease of dangers to the population and of serious accidents indicators.

4. References

[1] Olejnik K.: *Operating problems of buses and trucks – safe reversing*. Journal of 17th European Maintenance Congress, 11th – 13th of May 2004 Barcelona – Spain, 343–348.

[2] Olejnik K.: *Critical analysis of the current traffic regulations concerning visibility from the position of a vehicle driver.* Quarterly Motor Transport 2/2003 distributed by Motor Transport Institute, Warsaw, Poland, 69–80.

[3] Regulation no. 46 ECE UN. Uniform provisions concerning the approval of devices for indirect vision and of motor vehicles with regard to the installation of these devices.

[4] Regulation no. 48 ECE UN. Uniform provisions concerning the approval of vehicles with regard to the installation of lighting and light-signalling devices.

Dr inż. Krzysztof OLEJNIK

Instytut Transportu Samochodowego
ul. Jagiellońska 80
03-301 Warszawa, Poland
tel. (+48 22) 811-32-31 w. 303
e-mail: krzysztof.olejnik@its.waw.pl

Zdzisław CHŁOPEK

ECOLOGICAL ASPECTS OF USING BIOETHANOL FUEL TO POWER COMBUSTION ENGINES

Out of many ways of lowering harmful effects of motorism on the environment, more and more attention is being paid to popularising the use of biofuels. Using bioethanol enables combustion engines to run on fuels containing high content of biocomponent. They are E95 fuels for the self ignition engines, E85 and in the foreseeable future, E100 for the spark ignition engines. Engines running on ethanol fuel are especially adapted for that, with spark ignition engines being multi–fuel ones able to run on a mixture of ethanol fuel with petrol in any proportion. The use of bioethanol fuels makes it possible to lower the emission of harmful pollutants, such as, nitrogen oxides , or – in case of self ignition engines – particulate matter, and also global reduction of carbon dioxide emission. Paper presents results of pollutants emission studies, from the engines powered by bioethanol fuel.

Keywords*: bioethanol, combustion engines, pollutants emission.*

1. Introduction

From amongst most important criteria of evaluating quality of the combustion engines, particular significance is being attached at present to the ecological characteristics. At first, there have been limitations imposed on combustion engines' harmful pollutants emission. [3, 4]. International legislation has highlighted methods of evaluating harmfulness of substances emitted by combustion engines, to human health and environment. These methods encompass [3, 4]:

- subject range of substances, whose emission is limited, as well as those of restricted impact (exhaust smokiness),
- test methods together with equipment requirements,
- physical values system, characterising harmfulness to health and environment of the substances emitted.

Combustion engines progress is unequivocally connected with limiting emissions harmful to health and environment. Out of many methods, (with which great hopes on decreasing negative impact of the motorism on the environment, are linked), the use of bio fuels is being mentioned [1, 2, 4 – 17, 20, 21]. The use of bio fuels is seen as enabling the decrease of environmental threats on the local and global scales as well as improving fuel balance, together with other consequences of such actions, covering economic and social spheres as well as energy safety of each individual country.

Following ecological threats caused by combustion engines are singled out: local and global [3 – 9].

The greatest local threats caused by motorism are: particulate matter and nitrogen oxides, especially in the great city agglomerations, where the degree of harmfulness is even grater, because it affects larger human population remaining for long periods in the endangered area [3 – 9]. The main emission sources of these substances are first of all self ignition engines. In the case of the spark ignition engines, a significant progress has taken place as far as limiting emission of substances harmful to health and environment is concerned. The development of effective methods of catalytic exhaust purification has contributed to that [3, 4, 6 – 9].

From amongst global threats, caused by combustion engines, one can distinguish first of all greenhouse gasses emission, contributing to the climate warming up [3 – 9]. This is first of all carbon dioxide, and its emission being a direct consequence of using fossil fuels containing carbon.

Using bio fuels enables lowering emission of pollutants harmful to health and global emission of carbon dioxide, connected with carbon circulation in the nature, in the closed cycle of about one year period [4]. Engines running on bio fuels are characterised by lower emission of solid particles (particulates) [5, 9 – 17, 20, 21]. In the case of nitrogen oxides emission, the situation is more complicated. Running self ignition engines on diesel oil with added vegetable oil esters, usually causes slight increase of nitrogen oxides emission [11, 12], while in case of bioethanol additives, particularly with their high content, the emission of nitrogen oxides actually significantly comes down [1, 2, 5, 10, 13 – 21]. Positive effect of limiting greenhouse gasses emission on a global scale is dependent on the use of bio fuels with bio component content [4].

With ecological threats caused by motorism present, particularly great hopes are linked with beneficial results for the environment of the use of bioethanol [1 – 3, 5 – 10, 13 – 18, 20, 21]. This comes from not only from positive experiences of using engines powered that way, but also from the possibility of producing bioethanol in our climatic region and socio–economic realities.

Ethanol is used in the standard combustion engines as a low percentage additive to petrol and diesel oil. The use of bio fuels with high content of bioethanol requires engines specially adapted to that [1, 2, 5, 10, 13 – 18, 20, 21]. In case of spark ignition engines, they are multi–fuel engines, which can run on mixture of petrol and bioethanol, with 0% to about 85% bioethanol content (E85 fuel) [1, 2, 15, 21]. And in the foreseeable future of a few years, even E100, that is almost 100% bioethanol [1, 2, 15, 21]. The only self ignition engine, that can run on high content bioethanol fuels is DSI9E 01 produced by Scania [2, 4, 9, 15, 17, 19, 20]. It is powered by E95 fuel of bioethanol content exceeding 90% [2, 5, 10, 15, 18 – 21].

2. Ecological characteristics of self ignition combustion engines powered by E95 bioethanol fuel

First self ignition engine on high bioethanol content fuel, was designed by Scania corporation in the eighties, last century. It is Scania DSI9E 01 engine, which was a modification of Scania DSC9 11 engine powered by diesel oil [5, 10, 18, 20]. The most important alterations introduced [18]:

- increasing compression ratio from 18 to 24,
- changes in the induction system such as: changes in the fuel metering control, increasing effectiveness of the fuel pump, increasing diameter of the injector or changing gaskets and filters due to their design and materials,

– changes of the intercooler parameters.

Scania DSI9E 01 engine is a six cylinder in–line unit, of 8,7 dm^3 capacity. It develops nominal 169 kW at (1800 ÷ 2000) RPM. DSI9E 01 engine is used to power urban bus Scania Omnicity [18].

E95 fuel contains, according to the specification SEKAB [19] 5% in weight of the additive, so called ignition activator, enabling self ignition of high ethanol fuel – table.

Table. E95 fuel content

Fuel component	*Mass content*
Ethanol 95% v/v	*92,2%*
Ignition activator	*5%*
Ether MTBE	*2,3%*
Isobuthanol	*0,5%*
Corrosion Inhibitor	*90 ppm*

Figures 1 – 4 show specific brake pollutants emission from the Scania DSI9E 01 and DSC9 11 engines in the type approval static test – ESC (European Stationary Cycle) together with EURO 4 and EURO 5 limits [17].

The engine meets the pollutants emission requirements of the EURO 4 level (obligatory since – 2005) without any additional exhaust purification devices, and apart from nitrogen oxides, even of the EURO 5 level (obligatory from – 2008). In the version with EGR (Exhaust Gas Recirculation) and particulate matter filter CRT (Continuously Regenerating Trap), the engine meets EURO 5 and EEV (Enhanced Environmentally Friendly Vehicle) requirements in the dynamic ETC (European Transient Cycle) test [18] – figures 5 – 7.

New Scania engine on E95 fuel, which is to be introduced to the market in the second half of 2007, is a design especially prepared to run on this fuel [18]. This is an in–line, five cylinder

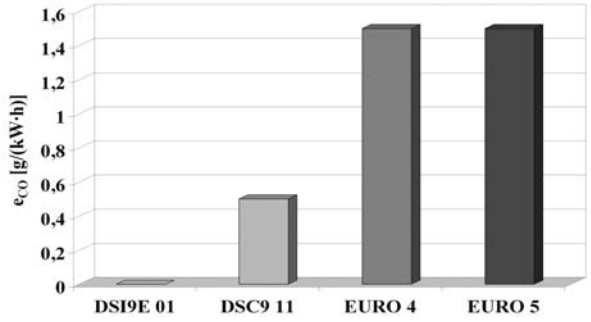

Fig. 1. Carbon monoxide (CO) specific brake emission – in the ESC test, from the DSC9E 01 and DSC9 11 engines with EURO 4 and EURO 5 limits

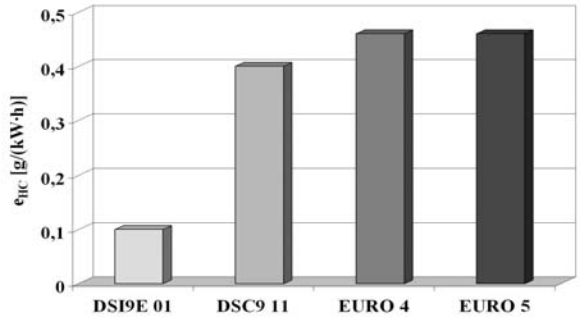

Fig. 2. Hydrocarbons (HC) specific brake emission – in the ESC test, from the DSC9E 01 and DSC9 11 engines with EURO 4 and EURO 5 limits

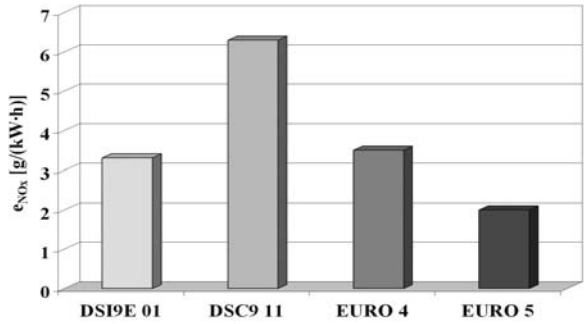

Fig. 3. Nitrogen oxides (NO_x) specific brake emission – in the ESC test from the DSC9E 01 and DSC9 11 engines with EURO 4 and EURO 5 limits

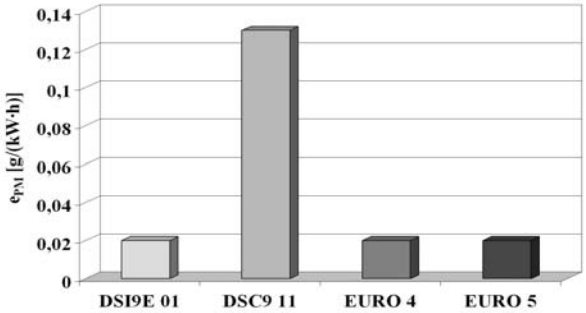

Fig. 4. Particulate matter (PM) specific brake emission – in the ESC test from the DSC9E 01 and DSC9 11 engines with EURO 4 and EURO 5 limits

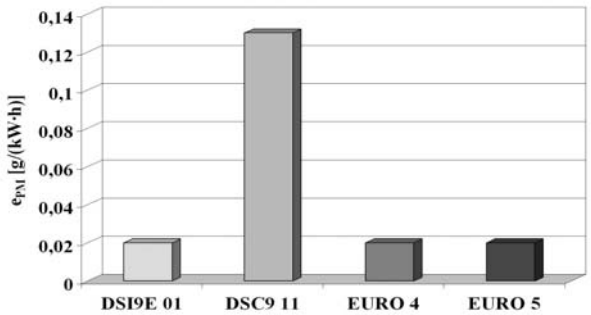

Fig. 5. Non methane hydrocarbons (NMHC) specific brake emission – in the ETC test, from the DSC9E 01 engine with EURO 4, EURO 5 and EEV limits

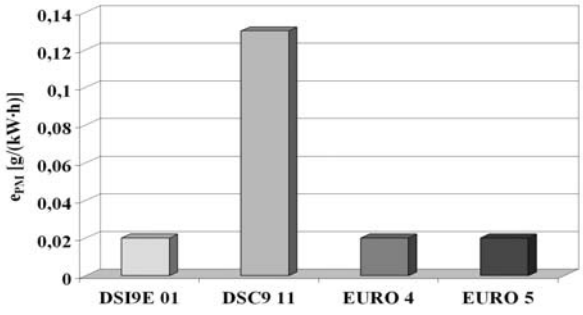

Fig. 6. Nitrogen oxides (NO_x) specific brake emission – in the ETC test, from the DSC9E 01 engine with EURO 4, EURO 5 and EEV limits

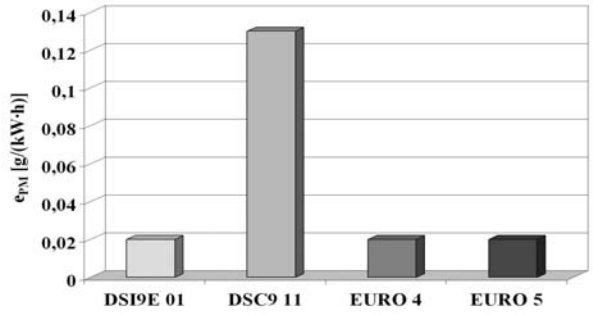

Fig. 7. Particulate matter (PM) specific brake emission – in the ETC test, from the DSC9E 01 engine with EURO 4, EURO 5 and EEV limits

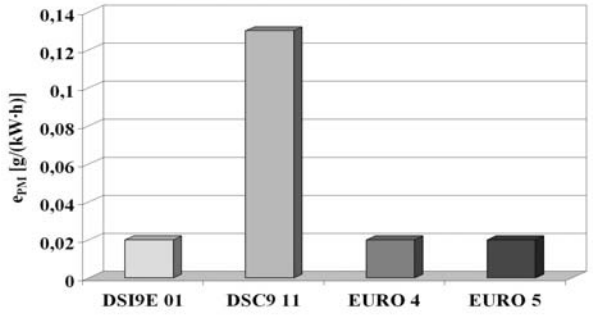

Fig. 8. Relative difference between EURO 4 limits and specific pollutants emission of: carbon monoxide – CO, hydrocarbons – HC, nitrogen oxides – NO_x and particulate matter – PM in the ESC test of a new Scania engine

unit of 8,9 dm^3 capacity and compression ratio ε = 28. The engine develops nominal useful power N_{eN} = 199 kW (270 KM) at n_N = 1900 RPM. There are four valves per cylinder. The engine has EGR system (Exhaust Gas Recirculation), but no catalytic converters have been used. The engine comfortably meets and even accedes the EURO 5 and EEV requirements – Figure 8.

Very good ecological characteristics of the engines running on biofuels with high bioethanol content, justify hopes connected with these fuels. Based on the data presented above and contained in the literature as well as Scania materials [11, 12, 18], it is possible to compare ecological characteristics of self ignition engines running on the following fuels:

- diesel oil,
- B20 fuel, being a mixture of diesel oil and 20% rape oil methyl esters,
- B100 fuel, – rape oil methyl esters,
- bioethanol E95 fuel.

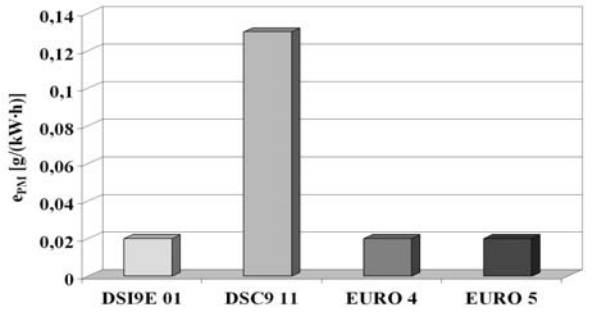

Fig. 9. Relative specific carbon monoxide brake emission – CO in the ESC test

Figures 9 – 12 show the specific brake pollutants emission in the ESC test for the engines running on biofuels against specific brake pollutants emission for pure diesel oil.

Pollutants emission analysis, presented in figures 9 – 12, clearly shows ecological benefits from using E95 fuel to power self ignition engines.

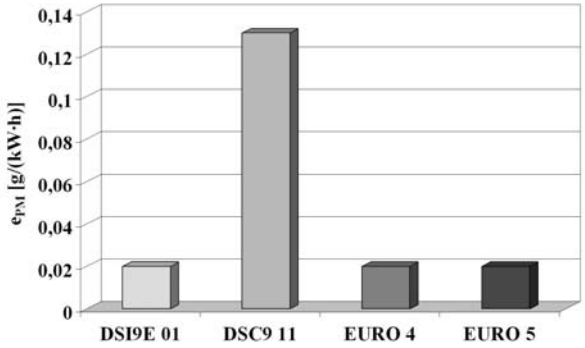

Fig. 10. Relative specific hydrocarbons emission – HC in the ESC test

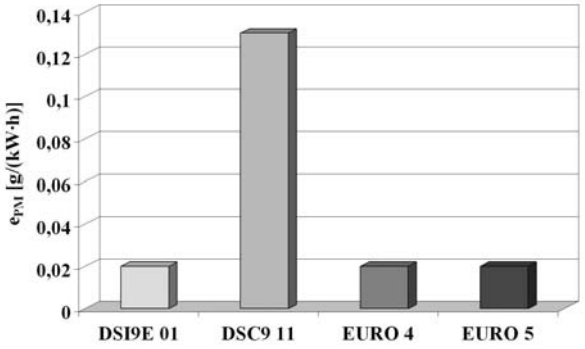

Fig. 11. Relative specific nitrogen oxides brake emission – NO_x in the ESC test

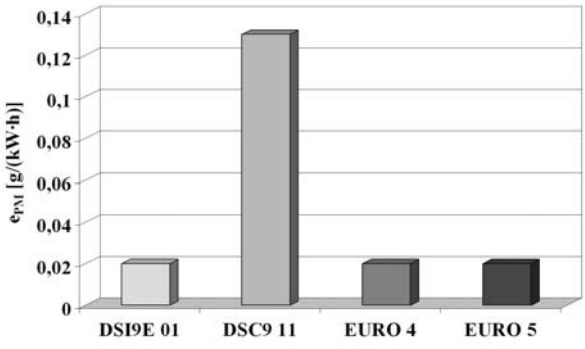

Fig. 12. Relative specific particulate matter brake emission – PM in the ESC test

3. Summary

The use of bioethanol based fuels requires – in case of high bio component content – specially prepared engines. Spark ignition engines are developed as multi–fuel ones, enabling running on the mixture of bioethanol fuel and petrol in any proportion, while self ignition engines are adapted to run only on E95 fuel. Thus, possibilities of propagating bioethanol fuels are smaller

than in case of vegetable oil esters. Also costs of propagating bioethanol fuels are higher. However, there are very serious arguments in favour of developing bioethanol fuels.

The most important being the fact that popularising bioethanol fuels, requiring the use of new designs, is a professional solution advocating modernity. It is impossible to use bioethanol fuels for the old designs, as it is the case with fuels based on vegetable oil esters. This fact thus favours natural forcing of modernity, although entails higher costs.

The second argument is – exceptionally beneficial ecological effects of using bioethanol fuels, particularly possibilities of lowering – unlike in the case of vegetable oil esters – nitrogen oxides emission.

The third one is – significantly more advantageous operating properties of bioethanol fuels in relation to fuels with added vegetable oil esters. Particularly better starting properties in low temperatures and better resistance to induction system contamination in connection with possible growth of biological flora in the fuel.

4. References

[1] Brusstar M.: *Ethanol–Gasoline Blends: Fuel Economy and Emissions Benefits*. The SAE Government and Industry Meeting. Washington D.C., May 13, 2003.

[2] Carstedt P.: *End of Oil! Future of What? Just Do It! Bioethanol and the road to sustainable transport*. Imperial College. London March 22, 2006. BAFF – BioAlcohol Fuel Foundation.http://www.baff.info/Filer/BioEthanolLondon/.

[3] Chłopek Z.: *A simulation researches of a pollution emission in a vehicle traffic*. 3rd International Conference Maintenance 2004. Praha 2004.

[4] Chłopek Z.: *Motor vehicles. Natural environment protection*. WKŁ. Warsaw 2002.

[5] Chłopek Z.: *Pollutants emission tests of the compression ignition engine powered by ethanol fuel E95*. Combustion Engines Nr 2007–SC3.

[6] Chłopek Z.: *Development problems of urban buses' engines*. Zeszyty Naukowe Wyższej Szkoły Ekonomii i Innowacji. Nr 2. Lublin 2005.

[7] Chłopek Z.: *Urban buses' engines development solutions*. Road Transport. 3 – 2005. 29 – 46.

[8] Chłopek Z.: *Development tendencies in urban buses' power plants*. Eksploatacja i Niezawodność Nr 1/2006. 3 – 9.

[9] Chłopek Z.: *Tendencies of urban buses' engines development*. Konferencja Komisji Autobusowej Izby Gospodarczej Komunikacji Miejskiej. Szklarska Poręba 2005.

[10] Chłopek Z.: *The use of ethanol fuel to power self ignition engines*. Zeszyty Naukowe Instytutu Pojazdów Politechniki Warszawskiej. (Praca w druku).

[11] Chłopek Z., Bardziński W., Jarczewski M, Sar H.: *The influence of FAME vegetable oil methyl ester additive to the diesel oil, on ecology, fuel consumption and car dynamic properties*. Journal of KONES 2006.

[12] Chłopek Z., Bardziński W., Jarczewski M., Sar H.: *Pollutants emission from the engine powered by fuel with the vegetable oil methyl ester, in the dynamic tests*. Journal of KONES 2005.

[13] Cole R.L., Poola R.B., Sekar R., Schaus J.E., McPartlin P.: *Effects of Ethanol Additives on Diesel Particulate and NOx Emissions*. SAE 2001–01–1937.

[14] Guerrieri D.A., Caffrey P. J., Rao V.: *Investigation into the Vehicle Exhaust Emissions of High Percentage Ethanol Blends*. SAE 950777.

[15] Hygrell L.: *BioEthanol…The Saab Way*. Bioethanol and the road to sustainable transport. Imperial College. London March 22, 2006. BAFF – BioAlcohol Fuel Foundation. http://www.baff.info/Filer/BioEthanolLondon/.

[16] Johansson U.: *Ethanol Buses – experiences and prospects for sustainable urban transport*. Bioethanol and the road to sustainable transport. Imperial College. London March 22, 2006. BAFF – BioAlcohol Fuel Foundation. http://www.baff.info/Filer/BioEthanolLondon/.

[17] Kelly K.J., Beiley B.K., Coburn T.C., Clark W., Lissiuk P.: *Federal Test Procedure Emissions Test Results from Ethanol Variable–Fuel Vehicle Chevrolet Luminas*. SAE 961092.

[18] Scania AB – internal materials not published.

[19] SEBAB AB – internal materials not published.

[20] Strömberg J.: *Towards Sustainable Travel in Stockholm's Public Transport*. Bioethanol and the road to sustainable transport. Imperial College. London March 22, 2006. BAFF – BioAlcohol Fuel Foundation. http://www.baff.info/Filer/BioEthanolLondon/.

[21] Taylor A.: *Bio–ethanol: an Environmental Opportunity for UK?!* Bioethanol and the road to sustainable transport. Imperial College. London March 22, 2006. BAFF – BioAlcohol Fuel Foundation. http://www.baff.info/Filer/BioEthanolLondon/.

Prof. Ph. D. Eng. Zdzisław Chłopek
Warsaw University of Technology
02–524 Warsaw, 84 Narbutta Str., Poland
E–mail: zchlopek@simr.pw.edu.pl

Henryk TOMASZEK
Józef ŻUREK
Michał JASZTAL

A METHOD OF EVALUATING FATIGUE LIFE OF SOME SELECTED STRUCTURAL COMPONENTS AT A GIVEN SPECTRUM OF LOADS – AN OUTLINE

The paper has been intended to introduce a method of evaluating the damage hazard and fatigue life of a structural component of an aircraft for: a given spectrum of loading the component; the Paris formula with the range of values of the material constant – differentiated.
Fatigue crack growth while the aircraft is operated shows random nature. To describe the dynamics of the crack propagation as a random process, a difference equation was used to arrive at a partial differential equation of the Fokker-Planck type. Having solved this equation enables the density function of growth in the crack length to be found. With the density function of the crack length and the boundary value thereof, probability of exceeding the boundary condition has been determined. The function obtained in this way enables estimations of fatigue life of a structural component.

Keywords*: damage hazard, fatigue life, density function, stress intensity factor, probability, cyclic loading.*

1. Introduction

In many papers one could find a method to evaluate fatigue life of a structural component for some selected notations of the Paris formula and a simplified fatigue loading pattern.

An attempt has been made in this paper to present a method of evaluating fatigue life of a structural component of an aircraft, assuming that:

- fatigue loading of the component is determined with some spectrum of loads, set up using a pattern of loading in the course of aircraft operation,
- the crack growth process, approached in a deterministic way, has been described with the Paris formula in the following form:

$$\frac{da}{dN_z} = C \quad M_k^m \quad E[(\sigma_{max})^m]\pi^{\frac{m}{2}} \quad a^{\frac{m}{2}} \tag{1}$$

where: C, m – material constants, a – crack length, N_z – the number of fatigue cycles, M_k – coefficient of the finiteness of the component's dimensions and position of the crack $E[(\sigma_{max})^m]$ – the expected value determined on the spectrum of loads, found in the following way:

$$E[(\sigma_{max})^m] = P_1(\sigma_1^{max})^m + P_2[(\sigma_2^{max})^m + ... + P_L[(\sigma_L^{max})^m \tag{2}$$

$$\sigma_i^{max} = \frac{\sigma_i^{max} + \sigma_i^{min}}{2} + \sigma_i^a \qquad i=1,2,...,L \tag{3}$$

σ_i^{max} – maximum value of cyclic loading within the i-th value interval (discrete loading value), σ_i^{min} – minimum value of cyclic loading within the i-th value interval, σ_i^a – amplitude of cyclic loading within the i-th value interval, P_i – frequency of threshold values of loading, determined with the following dependence:

$$P_i = \frac{n_i}{N_c} \qquad N_c = \sum_{i=1}^{L} n_i \tag{4}$$

n – the number of repetitions of specific threshold values of loading, using a single aircraft flight (standard flight), N_c – the total number of cycles in the course of aircraft standard flight.

Relationship (1) can be expressed against time, i.e. – in more detail – against flying time of the aircraft. Hence, the following assumption is made:

$$N_z = \lambda t \tag{5}$$

where: λ – intensity of the occurrence of cycles of fatigue loading of the structural component, t – flying time of the aircraft.

In our case, $\lambda = \frac{1}{\Delta t}$, where Δt – loading-cycle duration. A provisional formula to determine Δt could be accepted in the following form:

$$\Delta t = \frac{T}{N_c} \tag{6}$$

where: T – time of a standard aircraft flight.

Using assumptions and notifications made earlier, one can set to describing – in probabilistic terms – the dynamics of crack growth in the component.

In [1], the following difference equation has been used:

$$U_{a,t+\Delta t} = P_1 U_{a-\Delta a_1,\,t} + P_2 U_{a-\Delta a_2,\,t} + ... + P_L U_{a-\Delta a_L,\,t} \tag{7}$$

where: $U_{a,t}$ – probability that for the flying time equal to "t", the crack length was "a", Δa_i – crack length increment in time interval "Δt" for the stress σ_i^{max} $(i = 1,2,...,L)$.

The following differential equation of the Fokker-Planck type has been obtained from equation (7) in [3]:

$$\frac{\partial u(a,t)}{\partial t} = -\alpha(a)\frac{\partial u(a,t)}{\partial a} + \frac{1}{2}\beta(a)\frac{\partial^2 u(a,t)}{\partial a^2} \tag{8}$$

where: $u(a,t)$ – a crack-length density function that depends on the flying time of the aircraft, $\alpha(a)$ – coefficient that determines average crack-length increment per time unit, defined with the following dependence:

$$\alpha(a) = \lambda \sum_{i=1}^{L} P_i \Delta \quad a_i \tag{9}$$

$\beta(a)$ – square of the crack-length increment as referred to time unit, determined with the following dependence:

$$\beta(a) = \lambda \sum_{i=1}^{L} P_i(\Delta\ a_i)^2 \tag{10}$$

Δa_i– crack-length increment determined with the following dependence:

$$\Delta\ a_i = C_m(\sigma_i^{max})^m a^{\frac{m}{2}} \tag{11}$$

$$C_m = C\ \ M_k^m\ \ \pi^{\frac{m}{2}} \tag{12}$$

2. How to find a crack-length density function for m ≠ 2

With the accepted notification applied, eq (1) could be presented in the following form:

$$\frac{da}{dt} = \lambda\ \ C\ \ M_k^m E[(\sigma_{max})^m]\pi^{\frac{m}{2}} a^{\frac{m}{2}} \tag{13}$$

The following dependence is a solution of eq (13):

$$a = (a_o^{\frac{2-m}{2}} + \frac{2-m}{2}\lambda\ \ C\ \ M_k^m E[(\sigma_{max})^m]\pi^{\frac{m}{2}} t)^{\frac{2}{2-m}} \tag{14}$$

With eq (14) applied, coefficients α(a) and β(a) could be developed to take then the following forms:

$$\alpha(t) = \lambda\ \ C\ \ M_k^m \pi^{\frac{m}{2}} E[(\sigma^{max})^m] \cdot \cdot [a_o^{\frac{2-m}{2}} + \frac{2-m}{2}\lambda\ \ C\ \ M_k^m E[(\sigma_{max})^m]\pi^{\frac{m}{2}} t]^{\frac{m}{2-m}} \tag{15}$$

$$\beta(t) = \lambda\ \ C^2\ \ M_k^{2m}\pi^m E[(\sigma^{max})^{2m}] \cdot \cdot \{[a_o^{\frac{2-m}{2}} + \frac{2-m}{2}\lambda\ \ C\ \ M_k^m E[(\sigma_{max})^m]\pi^{\frac{m}{2}}]^{\frac{2}{2-m}}\}^m \tag{16}$$

Taking eqs (15) and (16) into account, eq (8) takes the form:

$$\frac{u(a,t)}{\partial t} = -\ \ \alpha(t)\frac{\partial u(a,t)}{\partial a} + \frac{1}{2}\beta(t)\frac{\partial^2 u(a,t)}{\partial a^2} \tag{17}$$

Solution of eq (17) is the requested crack-length function that depends on the flying time:

$$u(a,t) = \frac{1}{\sqrt{2\pi\ \ A(t)}}\ e^{-\frac{(a-B(t))^2}{2A(t)}} \tag{18}$$

where: $B(t)$ – an average value of crack length for the flying time equal to "t", whereas $A(t)$ – a variance of crack length for the flying time equal to "t".

Computational formulae take the following forms:

$$B(t) = \int_0^t \alpha(z)dz \tag{19}$$

$$A(t) = \int_0^t \beta(z)dz \tag{20}$$

Having calculated the integrals, we arrive at:

$$B(t) = [a_o^{\frac{2-m}{2}} + \frac{2-m}{2}\lambda\ \ C\ \ M_k^m \pi^{\frac{m}{2}} E[(\sigma^{max})^m]t]^{\frac{2}{2-m}} - a_o \tag{21}$$

$$A(t) = \frac{2}{2+m}\ C\ M_k^m\ \pi^{\frac{m}{2}} \cdot \frac{E[(\sigma^{max})^{2m}]}{E[(\sigma^{max})^m]} \cdot \cdot [(a_o^{\frac{2-m}{2}} + \frac{2-m}{2}\ \lambda\ C\ M_k^m\ \pi^{\frac{m}{2}} E[(\sigma^{max})^m]t)^{\frac{2+m}{2-m}} - a_o^{\frac{2+m}{2}}] \tag{22}$$

Notations:

$$\_= CM_k^m \pi^{\frac{m}{2}} E[(\sigma^{max})^m] \tag{23}$$

$$\omega = \frac{E[(\sigma^{max})^{2m}]}{(E[(\sigma_{max})^m])^2} \tag{24}$$

With account taken of (23) and (24), eqs (21) and (22) take the following forms:

$$B(t) = [a_o^{\frac{2-m}{2}} + \frac{2-m}{2}\ \_\lambda t]^{\frac{2}{2-m}} - a_o \tag{25}$$

$$A(t) = \frac{2}{2+m}\ \_\omega\ \ [(a_o^{\frac{2-m}{2}} + \frac{2-m}{2}\_\lambda t)^{\frac{2+m}{2-m}} - a_o^{\frac{2+m}{2}}] \tag{26}$$

3. How to find a crack-length density function for m = 2

When the material constant takes value equal to two (m = 2), the crack-length density function takes the following form [3]:

$$u(a,t) = \frac{1}{\sqrt{2\pi\ \ \hat{A}(t)}}\ e^{-\frac{(a-\hat{B}(t))^2}{2\hat{A}(t)}} \tag{27}$$

where:

$$\hat{B}(t) = a_o(e^{\lambda\bar{C}t} - 1) \tag{28}$$

$$\hat{A}(t) = \frac{1}{2}a_o^2\bar{C}\bar{\omega}(e^{2\bar{C}\lambda t} - 1) \tag{29}$$

$$\bar{C} = CM_k^2\pi\ \ E\ \ [(\sigma^{max})^2] \tag{30}$$

$$\bar{\omega} = \frac{E[(\sigma^{max})^4]}{(E[(\sigma_{max})^2])^2} \tag{31}$$

4. How to determine the hazard of a catastrophic damage to a structural component of an aircraft, from the point of view of fatigue and fatigue life

To determine some critical value of the crack length, the stress intensity factor in the following form could be used:

$$K = M_k\sigma\sqrt{\pi\ \ a} \tag{32}$$

where: M_k – correlation factor that comprises geometric characteristics of the finiteness of dimensions of the component and the crack shape, σ – the loading that affects the component.

The stress intensity factor, determined with dependence (32), becomes a quantity of a critical value K_c when the crack length and the stress take critical values a_{kr} and σ_{kr}, respectively. Then it is called 'resistance of the material to cracking':

$$K_c = M_k\sigma_{kr}\sqrt{\pi\ \ a_{kr}} \tag{33}$$

With eq (33) applied, the critical value of the crack length can be defined:

$$a_{kr} = \frac{K_c^2}{M_k^2\sigma_{kr}^2\ \pi} \tag{34}$$

Having exceeded the critical value of the crack length usually leads to a catastrophic damage to the component.

If the factor of safety is introduced, one can find the admissible value of the crack.

The computational formula takes then the following form:

$$a_d = \frac{K_c^2}{k\ \ M_k^2\sigma_{kr}^2\ \pi} \tag{35}$$

where: k – factor of safety, σ_{kr} – maximum value of service stress affecting the aircraft component.

With the crack-length density function (18) and formula (34), one can determine a given dependence to estimate the hazard of a catastrophic crack of the component for the flying time equal to *t*:

$$Q(t) = \int_{a_{kr}}^{\infty} u(a,t)da \tag{36}$$

The hazard of damaging the component will be determined in the following way, with the factor of safety taken into account:

$$\bar{Q}(t) = \int_{a_d}^{\infty} u(a,t)da \tag{37}$$

Applying one of dependences, i.e. (36) or (37), one could estimate fatigue life of the component for the assumed level of damage hazard.

The computational formula will be then as follows:

$$\bar{Q}(t)_{dop} = \int_{a_d}^{\infty} \frac{1}{\sqrt{2\pi\ A(t)}}\ e^{-\frac{(a-B(t))^2}{2A(t)}}\ da \tag{38}$$

To normalise the crack-length density function, the following dependence could be used:

$$Z_t = \frac{a - B(t)}{\sqrt{A(t)}} \tag{39}$$

The computational formula (38) after normalisation takes the following form:

$$\bar{Q}(t)_{dop} = \frac{1}{\sqrt{2\pi}} \int_{\frac{a_d - B(t)}{\sqrt{A(t)}}}^{\infty} e^{-\frac{1}{2} z_t^2}\ dz \tag{40}$$

The right side of dependence (40) can be found using tables of normal distribution.

When the (required) $\bar{Q}(t)^*_{dop}$ is determined, some value of time should be found – such as to make the left side of eq (40) equal the right one.

The value of "*t*" found in this way will be the searched for "life" for the assumed level of $\bar{Q}(t)_{dop}$.

Eq (40) could be converted into a form convenient enough to use tables of normal distribution.

With the following notifications introduced:

$$\frac{a_d - B(t)}{\sqrt{A(t)}} = \gamma(t) \tag{41}$$

$$\Phi(t) = \int_0^t \frac{1}{\sqrt{2\pi}}\ e^{-\frac{1}{2} z^2}\ dz \tag{42}$$

the computational formula (40) can be reduced to take the following form:

$$\bar{Q}(t)_{dop} = \frac{1}{2} - \Phi(\gamma(t)) \qquad \text{for } \gamma(t) > 0 \tag{43}$$

$$\bar{Q}(t)_{dop} = \frac{1}{2} + \Phi(\gamma(t)) \qquad \text{for } \gamma(t) < 0 \tag{44}$$

While computing either the damage hazard or fatigue life of the structural component, one should take value of the m coefficient into account and select a suitable function.

5. Final remarks

Presented density function of fatigue crack length and function enabled to calculate damage hazard and fatigue life of selected structural components are very important in research about reliability and durability of aviation technology.

The main advantage of the presented method is: fact that the method takes into consideration random value of stress and can be use for material with "*m*" coefficient not equal two. Authors are going to carry out further verification the method with use real maintenance data.

****

This research was made with the financial support of the Ministry of Science and Higher Education as a working project in 2006-2008 years.

****

6. References

[1] Kocańda S.: *Zmęczeniowe pękanie metali*. WNT, Warszawa, 1985 r.

[2] Kocańda S., Tomaszek H.: *Probabilistyczna ocena trwałości zmęczeniowej elementów konstrukcyjnych w warunkach rozwoju pęknięć*. Zeszyty Naukowe Politechniki Świętokrzyskiej, Mechanika nr 50, Kielce 1993, s. 259-272.

[3] Szczepanik R., Tomaszek H., Jasztal M.: *Zarys metody określania rozkładu czasu narastania pęknięcia elementu do wartości granicznej w warunkach zmęczenia w procesie eksploatacji statku powietrznego*. ZEM Zeszyt 3(147), 2006, s.81-89.

[4] Szczepanik R., Tomaszek H.: *Metoda określania rozkładu czasu do przekroczenia stanu granicznego*. ZEM Zeszyt 4(144), 2005, s.35-44.

Prof. dr hab. inż. Henryk TOMASZEK
Prof. dr hab. inż. Józef ŻUREK
Air Force Institute of Technology
ul. Księcia Bolesława 6, 01-494 Warszawa 46, Poland

Dr inż. Michał JASZTAL
Military University of Technology
ul. Gen. Kaliskiego 2, 00-908 Warszawa 49, Poland
E-mail: Michal.Jasztaj@wat.edu.pl

Przemysław DROŻYNER
Paweł MIKOŁAJCZAK

ASSESSMENT OF THE EFFECTIVENESS OF MACHINE AND DEVICE OPERATION

In effectively managed companies, the answer to the question of whether employees should be perceived as cost or as investment, is obvious. Investment should be made in human resources as this allows for reducing the cost of company's activities, increasing its effectiveness, efficiency, etc. A similar question can be put for machine operation, but here the answer is not so straightforward. The conflict between production managers and machine maintenance managers still exists; it is usually settled with the production side winning. This paper is an attempt to assess the effectiveness of machine operation and the effectiveness of the whole company based on an analysis of so called OEE (Overall Equipment Effectiveness) index, calculated from a timekeeping study of a big food producing company.

***Keywords**: vehicle operation, effectiveness.*

1. Introduction

Machine maintenance in a production company is a key issue; however, in a process approach it is usually classified as an auxiliary process for the production. Meanwhile, the process can have a fundamental effect on the amount and cost of production, quality of the final product, safety of people and the environment. The effectiveness of any actions, including machine maintenance, will be limited without a precise goal and measures used to monitor the degree in which the goals have been achieved. In general, two principles of rational management are correct: the principle of the maximum effect, where the degree of the goal achievement with given resources should be maximized, and the principle of minimum resources, where for an assumed degree of the goal achievement, the resources are minimized. These principles clearly indicate that it is not possible to achieve increasing values of readiness or reliability indexes with simultaneous reduction of sums spent on machine maintenance, inspections, repairs, etc. This truth is frequently missed, which is shown in the so-called conflict of operation managers. The conflict stems from the fact that technical objects participate in two different activities: in their use, oriented towards the product, and their operation, oriented towards the object itself and its value. Therefore, the use of a machine is directly linked to performing a production task, while operation is regarded as an auxiliary process; this is often expressed as "I use the machine (i.e. I produce) while you repair it (you generate costs)". An analysis of Fig. 1 leads to the conclusion that operation decisions should be based on cost calculation which includes the cost of machine operation and the cost of production loss being the result of machine stoppages [11].

An increase in the expenses for machine maintenance beyond the basic actions, including oil and filter replacement and surveys, reduces the loss resulting from unexpected stoppages and reduces the considered cost. The tendency is apparent only until the moment, beyond which the production loss starts to grow, it being the result of excessive stoppages in the operation sub-system. However, it is very important to consider all the operation-related costs, both the direct costs, which are easily measurable, related to labour and material related expenses, and those less obvious, resulting from reducing working speeds as a result of the machine's technical condition. The issue can be visualized as an iceberg (Fig. 2).

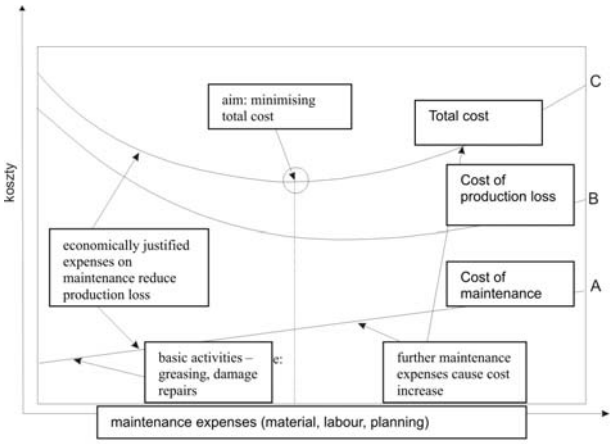

Fig. 1. The relationship between the cost of machine maintenance, cost of production loss and total cost

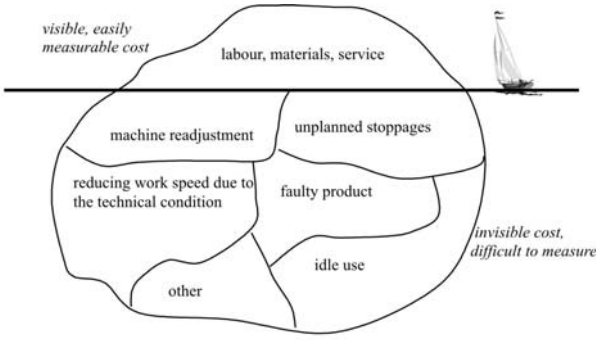

Fig. 2. Maintenance costs as an iceberg

2. OEE

Ideally, machines and devices could work for 100% of assumed work time, with 100% efficiency and with the final product in 100% conformity with the requirements. In reality, there are three categories of losses, which, according to the TPM idea, make up six big losses (Table 1).

Tab. 1. Six big losses according to TPM [11]

category of losses	*Loss*
LOSS IN READINESS (machine switch-off)	*Machine breakdown*
	Adjustments, regulations, replacement the working tool, etc.
LOSS OF EFFECTIVENESS (loss of working speed)	*Idle speed, minor stoppages*
	Reduced working speeds
LOSS OF QUALITY (defects of final products)	*Product defects and their repair*
	Loss (product defects) during the machine start-up

Now that the ISO 9001 series standards have become common (which indicates the need for constant improvement) and modern methods of management are widely applied, it seems that it would be appropriate to adopt an index to show potential for improvement of machine and device maintenance process. Such an index could be the so-called Overall Equipment Effectiveness *(OEE*), whose value embraces all the categories of loss encountered during the process of machine and device use as compared to the ideal conditions. The index is obtained by multiplying three elements:

- the readiness index, which is the percentage of use of the general time of change K_G;
- the productivity index, which is the percentage of the machine productivity during a time unit in relation to the rated value K_W;
- the quality index, which the percentage of the number of products in conformity with the requirements in relation to the overall number of manufactured products K_J.

The *OEE* index can be expressed as the general formula:

$$OEE = K_G K_W K_J \quad (1)$$

Table 2 shows the diagram of calculating the OEE index value.

An example of calculating the *OEE*: work for 65% of the planned time, the productivity of 80% of the rated value, 98% conformity of the final product with the requirements; then *OEE* = 0.65 x 0.8 x 0.99 = 0.51.

3. Examining the possibility of applying the OEE index in a production company

The aim of the study was to assess a possibility of applying the *OEE* index in assessment of the effectiveness of a machine maintenance system in a production company [2].

The study object was a production line for vacuum packing of foodstuff – a Multivac R 7000 roll machine.

The timekeeping study was conducted during five days in the first shift lasting from 6.00 a.m. to 2.00 p.m. The adopted duration of the shift was t_z = 8 h – 30 min = 7 h 30 min = 27000 s. The total shift duration should always be reduced by the time which decreases the effective work time fund and are not included in the OEE index. In this example, it is the duration of the planned morning break – 30 minutes. Table 3 shows the forms of the components of the OEE index.

Data for the calculation of the OEE value for the CRAYOWAC VR 8620 packing machine and the calculation results are shown in table 4.

Graphic presentation of the OEE index and its components values as well as the results of the Pareto analysis for the portion of the stoppage times is shown in Fig. 3.

An analysis of the results of timekeeping studies and the calculated values of the productivity, readiness and quality indexes reveals that that the values of productivity and quality indexes are constantly high, while the value of the readiness index is low, which results from a long "no production" time. The length of the time depends on the marketing department, which determines the amount of the packed product. The value is not pre-planned and depends on the orders from customers.

Tab. 2. The diagram of calculating the OEE index value

<table>
<tr><td colspan="5">Total work time</td></tr>
<tr><td rowspan="2">readiness</td><td colspan="3">A work time</td><td>Planned lack of manufacture</td></tr>
<tr><td colspan="2">B manufacture time</td><td>defects, adjustments, tool replacement</td><td rowspan="4"></td></tr>
<tr><td rowspan="2">efficiency</td><td colspan="2">C planned productivity</td><td rowspan="2"></td></tr>
<tr><td>D actual productivity</td><td>minor stoppages, reduced speed</td></tr>
<tr><td rowspan="2">quality</td><td>E number of product</td><td rowspan="2"></td><td rowspan="2">LOSS OF THE EFFECTIVENESS OF A MACHINE USE</td></tr>
<tr><td>F number of conforming products</td><td>product defects, their repair, loss during start-up</td></tr>
<tr><td colspan="5">OEE = B/A × D/C × F/E</td></tr>
</table>

Tab. 3. The indexes adopted for calculating the OEE value

Readiness index K_G	*Productivity index* K_W	*Quality index* K_J
$K_G = \frac{t_z - p}{t_z}$	$K_W = \frac{l_C - l_0}{l_C}$	$K_J = \frac{l_D - l_N}{l_D}$
t_z – *shift duration (27000s)* p – *breaks [s], time of: product preparation, container preparation, change of product range, production stoppage, failure.*	l_c – *total number of produced packages,* l_o – *number of idle movements of the machine – it is the number of unfilled vacuum chambers, with which the machine is equipped.*	l_D – *the number of produced conforming packages,* l_N – *the number of non-conforming packages (not airtight)*

Tab. 4. Timekeeping data and determined values of the index for CRAYOWAC VR 8620

	day1	*day2*	*day3*	*day4*	*day5*	*mean x*	*standard deviation*
Time of product preparation	1740	2940	2580	3480	1800	2508	746.2
Time of container preparation	0	0	0	0	660	132	295.1
Time of product range change	840	1260	0	1560	1080	948	591.5
Time of production stoppage	9000	16980	13380	16620	8280	12852	4100.5
Time of failure	120	0	0	0	360	96	156.4
Number of idle movements of the machine (l_O)	324	164	294	136	289	241.4	85
Number of non- air-tight packages (l_N)	144	16	18	12	78	53.6	57.4
Number of good packages (l_D)	2244	1276	1885	1180	2385	1794	548.9
Readiness index	0.56	0.22	0.41	0.2	0.55	0.388	0.173
Productivity index	0.88	0.94	0.86	0.9	0.89	0.894	0.0296
Quality index	0.93	0.99	0.99	0.99	0.97	0.974	0.02607681
OEE	0.45	0.20	0.35	0.18	0.47	0.33	0.135830777

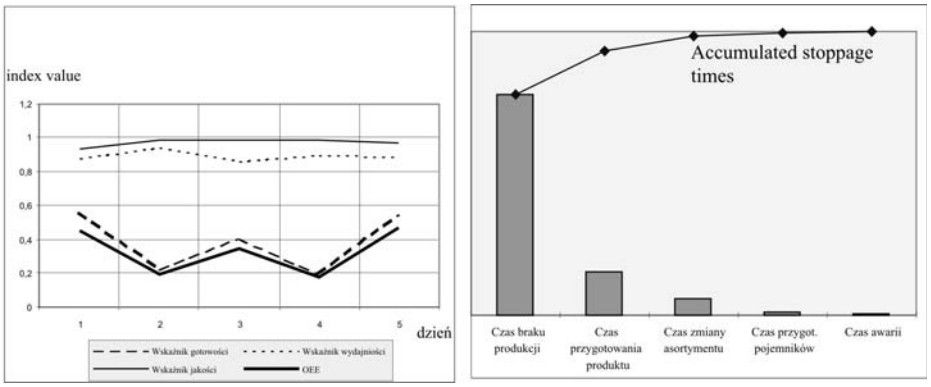

Fig. 3. The values of K_G, K_W, K_J indexes and OEE as well as the Pareto analysis of the CRAYOWAC VR 8620 machine stoppages

The Pareto analysis indicates that the value of the *OEE* index is most affected (due to the effect of the readiness index) by the "no production" time, product preparation time, product range change time, etc., i.e. the times which are not related to the process maintenance.

4. Summary

1. *OEE* is a general measure of the effectiveness of machine use, taking into account the effectiveness of all the parties concerned: machine maintenance department, production department, planning department, marketing and other departments.
2. *OEE* "measures" all the aspects concerning the effectiveness of use of machines and devices, both in terms of quality (performing work correctly) and quantity (performing correct work).
3. *OEE* seems a simple and convenient tool to monitor the processes of machine maintenance and production upkeep and to compare the effectiveness of machine use. The comparisons can be internal and external. The former are conducted in a company in certain intervals for the same machine, device or production line. The aim of the latter is to compare the effectiveness of use of machines in various companies (benchmarking), but in that case it is of particular importance to strictly establish the principles of calculation of the *OEE* values.
4. The *OEE* index should be used with caution. Assuming, for example, that the values of the readiness, productivity and quality indexes for a certain period are equal to 0.95%, 85% and 98%, respectively, and for another - 98%, 85% and 90%, the *OEE* value calculated in each case is the same: 0.79. Analysis of the index only in terms of its total value does not provide a warning about the productivity increasing at the cost of product quality.

5. References

[1] Drożyner P., Veith E.: *Risk Based Inspection Methodology Overview*, Diagnostyka nr 27, 2002.
[2] Kłobukowski M.: *Analiza efektywności systemu utrzymania maszyn w przedsiębiorstwie Indykpol z wykorzystaniem wskaźnika OEE (Całkowita Efektywność Eksploatacji)*, praca magisterska zrealizowana na Wydziale Nauk Technicznych UWM, Olsztyn 2004.
[3] Niziński S.: *Eksploatacja obiektów technicznych.* ITE Radom 2000.
[4] Niziński S.: *Elementy eksploatacji obiektów technicznych*, UWM. Olsztyn 2000.
[5] Niziński S.: Michalski R.: *Diagnostyka obiektów technicznych*. ITE, Radom 2002.
[6] Niziński S.: Żółtowski B.: *Modelowanie procesów eksploatacji maszyn*. MARKAR – BZ, Bydgoszcz- Sulejówek, 2002.
[7] Niziński S.: Żółtowski B.: *Zarządzanie eksploatacją obiektów technicznych za pomocą rachunku kosztów*. ATR , Bydgoszcz, 2003.
[8] PN-EN ISO 9001:2001, Systemy zarządzania jakością - Wymagania.
[9] Żółtowski B.: *Podstawy diagnostyki technicznej*. ATR, Bydgoszcz 1996.
[10] Maintenance – Key Performance Index, dokument TC 319 WI WG6.50 przygotowywany przez Technical Committee CEN/TC 319 "Maintenance" (w przygotowaniu).
[11] Pod red. Nizińskiego S. i Michalskiego R.: *Utrzymanie maszyn i pojazdów*. ITE Radom 2007 – w druku.
[12] Internet websites:
http://www.oeetoolkit.nl/
http://www.udt.gov.pl/
http://www.barringer1.com/
http://www.plant-maintenance.com/

Dr inż. Przemysław DROŻYNER
Dr inż. Paweł MIKOŁAJCZAK

Department of Vehicle and Machine Construction and Maintenance
University of Warmia and Mazury in Olsztyn
Ul. Oczapowskiego nr 11 10-900 Olsztyn, Poland
E-mail: przemyslaw.drozyner@uwm.edu.pl, pawel.mikolajczak@uwm.edu.pl

Konstantin N. NECHVAL
Nicholas A. NECHVAL
Gundars BERZINS
Maris PURGAILIS

PLANNING INSPECTIONS IN SERVICE OF FATIGUE-SENSITIVE AIRCRAFT STRUCTURE COMPONENTS FOR INITIAL CRACK DETECTION

Based on a random sample from the Weibull distribution with unknown shape and scale parameters, lower and upper prediction limits on a set of m future observations from the same distribution are constructed. The procedures, which arise from considering the distribution of future observations given the observed value of an ancillary statistic, do not require the construction of any tables, and are applicable whether the data are complete or Type II censored. The results have direct application in reliability theory, where the time until the first failure in a group of m items in service provides a measure regarding the operation of the items, as well as in service of fatigue-sensitive aircraft structures to construct strategies of inspections of these structures; examples of applications are given. Keywords: Aircraft structure, fatigue crack, Weibull distribution, prediction limit, inspection strategy

Keywords*: Aircraft structure, fatigue crack, Weibull distribution, prediction limit, inspection strategy.*

1. Introduction

The Weibull distribution is a powerful modelling tool used in reliability analyses to predict failure rates and to provide a description of the failure of parts and equipment. The Weibull distribution has been widely used in the empirical modelling of economic models. Applications include the modelling of unemployment spells, strike durations, income distributions, the length of a firm's innovation period, and the size of research and development budgets. Depending on the particular problem, the variable under consideration may not be fully observed, requiring censoring procedures for estimation.

Based on engineering and macroscopic viewpoints, the mechanical properties of metallic materials are often considered homogeneous. However, a considerable amount of scatter has been observed in fatigue data even under the same loading condition. It may be attributed to the inhomogeneous material properties. As a result, probabilistic approaches for the fatigue crack growth have received great attention in recent years. Along with the development of fracture mechanics for the past three decades and the need of reliability or risk assessment for some important structures or components such as:

- Transportation Systems and Vehicles – aircraft, space vehicles, trains, ships;
- Civil Structures – bridges, dams, tunnels;
- Power Generation – nuclear, fossil fuel and hydroelectric plants;
- High-Value Manufactured Products – launch systems, satellites, semiconductor and electronic equipment;
- Industrial Equipment – oil and gas exploration, production and processing equipment, chemical process facilities, pulp and paper;

the so-called 'probabilistic fracture mechanics' has thus arisen [1]. One of the important issues in the probabilistic fracture mechanics analysis lies in the probabilistic modeling of fatigue crack growth phenomenon. Many probabilistic models have been proposed to capture the scatter of the fatigue crack growth data. Some of these models are based on the two-parameter Weibull distribution. It exhibits a wide range of shapes for the density and hazard functions that makes this distribution suitable for modelling complex failure data sets. Many authors have considered the problem of constructing prediction limits for the extreme value and Weibull distributions. References [3] and [4] contain good discussions of available procedures. As a rule, the better procedures involve the use of tables generated by Monte Carlo methods.

In this paper our focus is on prediction limits for future samples of observations from the two-parameter Weibull distribution and the purpose is to present a technique for constructing the prediction limits which can be used very generally, for Type II censored as well as complete data. The procedures should in particular be useful in situations not handled by the tables in the aforementioned references.

The proposed technique may be useful when we consider, for example, the reliability problem associated with fatigue damage that arises from the initiation of fatigue cracks originating from rivet holes along the top longitudinal row of the outer skin of the fuselage (Fig. 1).

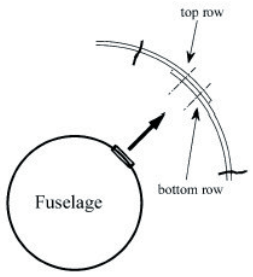

Fig. 1. Rivet row in consideration

It is assumed that a fatigue crack can initiate randomly at either side of a hole with diameter d. Experiments show that the number of flight cycles at which an initial crack will appear at one side with respect to a particular rivet follows the two-parameter Weibull distribution.

A post-failure photograph of one of the F-16 479 bulkhead test components (Fig. 2) indicates the location of fatigue crack initiation at the radius between the bulkhead and one of the two vertical tail attach pads.

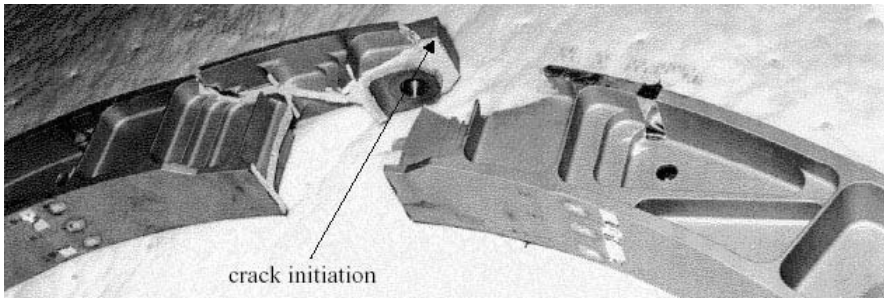

Fig. 2. F-16 479-bulkhead test specimen number -7B, post-failure crack initiation

The probability density function for the random variable X of the two-parameter Weibull distribution is given by:

$$f(x;\sigma,\delta) = \frac{\delta}{\beta}\left(\frac{x}{\beta}\right)^{\delta-1} exp\left[-\left(\frac{x}{\beta}\right)^{\delta}\right] \quad (x>0) \tag{1}$$

where δ>0 and β>0 are the shape and scale parameters, respectively. Writing:

$$S = \mu + \sigma Z \tag{2}$$

where Z is a random variable with standardized extreme value density,

$$f(z) = exp(z - e^{z}), \quad -\infty < z < \infty \tag{3}$$

then the density of S can be obtained as

$$f(u;\mu,\sigma) = \frac{1}{\sigma} exp\left(\frac{s-\mu}{\sigma} - exp\left(\frac{s-\mu}{\sigma}\right)\right), \quad -\infty < s < \infty \tag{4}$$

The distribution of S is known as the smallest extreme value distribution (SEV). If $S=lnX$, so that, $X=e^{S}$, then:

$$f(x;\mu,\sigma) = \frac{1}{x}\frac{1}{\sigma}(xe^{-\mu})^{1/\sigma} exp[-(xe^{-\mu})^{1/\sigma}] \tag{5}$$

With $\sigma=1/\delta$ and $\mu=ln\beta$, X is distributed as Weibull with shape parameter δ and scale parameter β. Given this, for analytical and computational convenience, this paper works in the $S=lnX$ scale, the results, however, are reported directly for the Weibull observations.

2. Lower prediction limit

Theorem 1. Let $X_1 < \ldots < X_r$ be the first r ordered past observations from a sample of size n from the distribution (1). Then a lower conditional (1–α) prediction limit y_1 on the minimum Y_1 of a set of m future ordered observations $Y_1 < \ldots < Y_m$ is given by:

$$Pr\{Y_1 > y_l;\mathbf{z}\} = Pr\left\{\hat{\delta}\, ln\left(\frac{Y_1}{\hat{\beta}}\right) > \hat{\delta}\, ln\left(\frac{y_l}{\hat{\beta}}\right);\mathbf{z}\right\} = Pr\{W_1 > w_l;\mathbf{z}\}$$

$$= \frac{\int_0^{\infty} v^{r-2} e^{v\hat{\delta}\sum_{i=1}^{r} ln(x_i/\hat{\beta})}\left(me^{vw_l} + \sum_{i=1}^{r} e^{v\hat{\delta}\, ln(x_i/\hat{\beta})} + (n-r)e^{v\hat{\delta}\, ln(x_r/\hat{\beta})}\right)^{-r} dv}{\int_0^{\infty} v^{r-2} e^{v\hat{\delta}\sum_{i=1}^{r} ln(x_i/\hat{\beta})}\left(\sum_{i=1}^{r} e^{v\hat{\delta}\, ln(x_i/\hat{\beta})} + (n-r)e^{v\hat{\delta}\, ln(x_r/\hat{\beta})}\right)^{-r} dv} = 1-\alpha \tag{6}$$

where $\hat{\beta}$ and $\hat{\delta}$ are the maximum likelihood estimators of β and δ based on the first r ordered past observations ($X_1, \ldots, X_r$) from a sample of size n from the Weibull distribution, which can be found from solution of

$$\hat{\beta} = \left(\frac{\sum_{i=1}^{r} x_i^{\hat{\delta}} + (n-r)x_r^{\hat{\delta}}}{r}\right)^{1/\hat{\delta}} \tag{7}$$

and

$$\hat{\delta} = \left[\left(\sum_{i=1}^{r} x_i^{\hat{\delta}} ln\, x_i + (n-r)x_r^{\hat{\delta}} ln\, x_r\right)\left(\sum_{i=1}^{r} x_i^{\hat{\delta}} + (n-r)x_r^{\hat{\delta}}\right)^{-1} - \frac{1}{r}\sum_{i=1}^{r} ln\, x_i\right]^{-1} \tag{8}$$

$$\mathbf{z} = (z_1, z_2, \ldots, z_{r-2}) \tag{9}$$

$$Z_i = \hat{\delta}\, ln\left(\frac{X_i}{\hat{\beta}}\right), \quad i = 1, \ldots, r-2 \tag{10}$$

$$W_1 = \hat{\delta}\, ln\left(\frac{Y_1}{\hat{\beta}}\right), \quad w_l = \hat{\delta}\, ln\left(\frac{y_l}{\hat{\beta}}\right) \tag{11}$$

Proof. The joint density of $S_1=ln(X_1), \ldots, S_r=ln(X_r)$ is given by:

$$f(s_1, \ldots, s_r;\mu,\sigma) = \frac{n!}{(n-r)!}\prod_{i=1}^{r}\frac{1}{\sigma} exp\left(\frac{s_i-\mu}{\sigma} - exp\left(\frac{s_i-\mu}{\sigma}\right)\right) exp\left(-(n-r)exp\left(\frac{s_r-\mu}{\sigma}\right)\right) \tag{12}$$

Let $\hat{\mu}$, $\hat{\sigma}$ be the maximum likelihood estimators (estimates) of μ, σ based on $S_1, \ldots, S_r$ and let:

$$V_l = \frac{\hat{\mu}-\mu}{\hat{\sigma}} \tag{13}$$

$$V = \frac{\hat{\sigma}}{\sigma} \tag{14}$$

and

$$Z_i = \frac{S_i - \hat{\mu}}{\hat{\sigma}} \qquad i = 1(1)r \tag{15}$$

Parameters μ and σ in (12) are location and scale parameters, respectively, and it is well known that if $\hat{\mu}$ and $\hat{\sigma}$ are estimates of μ and σ, possessing certain invariance properties, then the quantities V_1 and V are parameter-free. Most, if not all, proposed estimates of μ and σ possess the necessary properties; these include the maximum likelihood estimates and various linear estimates. Z_i, i=1(1)r, are ancillary statistics, any r-2 of which form a functionally independent set. We then find in a straightforward manner that the joint density of V_1, V, conditional on fixed $z=(z_1, z_2, \ldots, z_{r-2})$, is:

$$v_1 \in (-\infty, \infty), \quad v \in (0, \infty) \tag{16}$$

where:

$$\vartheta(\mathbf{z}) = \left(\int_{0}^{\infty} \int_{-\infty}^{\infty} v^{r-1} exp\left(\sum_{i=1}^{r} (z_i + v_1)v - \sum_{i=1}^{r} exp[(z_i + v_1)v] - (n-r)exp[(z_r + v_1)v] \right) dv_1 dv \right)^{-1} \quad (17)$$

is the normalizing constant. For notational convenience we include all of $z_1, \ldots, z_r$ in (15); z_{r-1} and z_r can be expressed as function of $z_1, \ldots, z_r$ only.

Writing:

$$W = \frac{ln Y_1 - \mu}{\sigma} \quad (18)$$

where Y_1 is the smallest observation from an independent second sample of m observations also from the distribution (1), and noting that exp(W) is the smallest observation in a sample of m observations from the standard exponential distribution, we have the density of W as:

$$f(w) = me^{w} exp(-me^{w}) \quad w \in (-\infty, \infty) \quad (19)$$

Since W is distributed independently of v_1, v we find the joint density of w, v_1, v, conditional on z, as the product of (16) and (19),

$$f(w, v_1, v; \mathbf{z}) = f(w) f(v_1, v; \mathbf{z}) \quad (20)$$

Note that $$W_1 = \frac{ln Y_1 - \hat{\mu}}{\hat{\sigma}} = \frac{W - V_1 V}{V} \quad (21)$$

making the transformation $w_1=(w-v_1v)/v$, $v_1=v_1$, $v=v$ we find the joint density of w_1, v_1, v, conditional on z, as:

$$f(w_1, v_1, v; \mathbf{z}) = m\vartheta(\mathbf{z}) v^{r} exp\left((r+1)v_1 v + \left(w_1 + \sum_{i=1}^{r} z_i \right) v \right) \times exp\left(-m exp[(w_1 + v_1)v] \right) \times exp\left(-exp[v_1 v] \left(\sum_{i=1}^{r} exp[z_i v] + (n-r)exp[z_r v] \right) \right)$$

$$w_1 \in (-\infty, \infty), \quad v_1 \in (-\infty, \infty), \quad v \in (0, \infty) \quad (22)$$

Now v_1 can be integrated out of (22) in a straightforward way to give:

$$f(w_1, v; \mathbf{z}) = \frac{\Gamma(r+1)\vartheta(\mathbf{z}) v^{r-2} exp\left(v \sum_{i=1}^{r} z_i \right) mv exp[w_1 v]}{\left(m exp[w_1 v] + \sum_{i=1}^{r} exp[z_i v] + (n-r)exp[z_r v] \right)^{r+1}} =$$

$$= \frac{r v^{r-2} exp\left(v \sum_{i=1}^{r} z_i \right) mv exp[w_1 v]}{\left(m exp[w_1 v] + \sum_{i=1}^{r} exp[z_i v] + (n-r)exp[z_r v] \right)^{r+1}} = \frac{\int_{0}^{\infty} v^{r-2} exp\left(v \sum_{i=1}^{r} z_i \right) \left(m exp[w_1 v] + \sum_{i=1}^{r} exp[z_i v] + (n-r)exp[z_r v] \right)^{-r} dv}{\int_{0}^{\infty} v^{r-2} exp\left(v \sum_{i=1}^{r} z_i \right) \left(\sum_{i=1}^{r} exp[z_i v] + (n-r)exp[z_r v] \right)^{-r} dv}$$

$$= \frac{\int_{0}^{\infty} v^{r-2} e^{v\delta \sum_{i=1}^{r} ln(x_i/\hat{\beta})} \left(m e^{v w_1} + \sum_{i=1}^{r} e^{v\delta ln(x_i/\hat{\beta})} + (n-r) e^{v\delta ln(x_r/\hat{\beta})} \right)^{-r} dv}{\int_{0}^{\infty} v^{r-2} e^{v\delta \sum_{i=1}^{r} ln(x_i/\hat{\beta})} \left(\sum_{i=1}^{r} e^{v\delta ln(x_i/\hat{\beta})} + (n-r) e^{v\delta ln(x_r/\hat{\beta})} \right)^{-r} dv} \quad (24)$$

$$w_1 \in (-\infty, \infty), \quad v \in (0, \infty) \quad (23)$$

Thus, for fixed w_1 ($-\infty < w_1 < \infty$),

$$Pr\{W_1 > w_l; \mathbf{z}\} = \int_{0}^{\infty} \int_{w_l}^{\infty} f(w_1, v; \mathbf{z}) dw_1 dv$$

This completes the proof.

Corollary 1.1. If $r=n$ and n is large, (24) should be more or less independent of Z. Also, $Z_1, \ldots, Z_n$ will be nearly independent and approximately distributed as standard extreme values, with pdf

$$f_o(\bullet w) = e^{\bullet w} exp(-e^{\bullet w}) \quad \bullet w \in (-\infty, \infty) \quad (25)$$

Our first step is to replace $z_1, \ldots, z_n$ in the numerator of (24) by $n\mathrm{E}\{\bullet W\} = -n\gamma$, where $\gamma=0.577215\ldots$ is the Euler constant. We now suppose that $(1/n) \sum_{i=1}^{n} exp[z_i v]$ will be approximately equal to the moment generating function for (25), with dummy variable v. Since $\mathrm{E}\{exp[\bullet w\eta]\} = \Gamma(1+\eta)$, we approximate the above sum in the denominator of (24) by $n\Gamma(1+v)$. We thus arrive at the following approximation to (6), where $r=n$,

$$Pr\{Y_1 > y_l\} = Pr\left\{ ln\left(\frac{Y_1}{\hat{\sigma}}\right)^{\delta} > ln\left(\frac{y_l}{\hat{\sigma}}\right)^{\delta} \right\} = Pr\{W_1 > w_l\} = \frac{\int_{0}^{\infty} v^{n-2} e^{-n\gamma v} \left[(m/n) e^{v w_l} + \Gamma(1+v) \right]^{-n} dv}{\int_{0}^{\infty} v^{n-2} e^{-n\gamma v} \left[\Gamma(1+v) \right]^{-n} dv} = 1 - \alpha \quad (26)$$

3. Upper prediction limit

Theorem 2. Let $X_1 < \ldots < X_r$ be the first r ordered past observations from a sample of size n from the distribution (1). Then an upper conditional $(1-\alpha)$ prediction limit y_u on the maximum Y_m of a set of m future ordered observations $Y_1 < \ldots < Y_m$ is given by:

$$Pr\{Y_m < y_u; \mathbf{z}\} = Pr\left\{ \hat{\delta} ln\left(\frac{Y_m}{\hat{\beta}}\right) < \hat{\delta} ln\left(\frac{y_u}{\hat{\beta}}\right); \mathbf{z} \right\} = Pr\{W_m < w_u; \mathbf{z}\}$$

$$= 1 - \left[-\sum_{j=0}^{m-1} \binom{m-1}{j} (-1)^j \int_{0}^{\infty} v^{r-2} e^{v\delta \sum_{i=1}^{r} ln(x_i/\hat{\beta})} (j+1)^{-1} \left((j+1) e^{v w_u} + \sum_{i=1}^{r} e^{v\delta ln(x_i/\hat{\beta})} + (n-r) e^{v\delta ln(x_r/\hat{\beta})} \right)^{-r} dv \right] \times$$

$$\times \left[\sum_{j=0}^{m-1} \binom{m-1}{j} (-1)^j \int_{0}^{\infty} v^{r-2} e^{v\delta \sum_{i=1}^{r} ln(x_i/\hat{\beta})} (j+1)^{-1} \left(\sum_{i=1}^{r} e^{v\delta ln(x_i/\hat{\beta})} + (n-r) e^{v\delta ln(x_r/\hat{\beta})} \right)^{-r} dv \right]^{-1} = 1 - \alpha \quad (27)$$

Prof. The proof is carried out in the same manner as the proof of Theorem 1, with the exception of that:

$$W = \frac{ln Y_m - \mu}{\sigma} \quad (28)$$

where Y_m is the largest observation from an independent second sample of m observations also from the distribution (1), and noting that $\exp(W)$ is the largest observation in a sample of m observations from the standard exponential distribution, we have the density of W as:

$$f(w) = me^{w} exp(-e^{w})[1-exp(-e^{w})]^{m-1} =$$
$$= me^{w}\sum_{j=0}^{m-1}\binom{m-1}{j}(-1)^{j} exp[-(j+1)e^{w}] \qquad w\in(-\infty,\infty) \quad (29)$$

Corollary 2.1. If $r=n$ and n is large, in the same manner as in Theorem 1 we arrive at the following approximation to (27):

$$Pr\{Y_m < y_u\} = Pr\left\{ln\left(\frac{Y_m}{\hat{\sigma}}\right)^{\hat{\delta}} < ln\left(\frac{y_u}{\hat{\sigma}}\right)^{\hat{\delta}}\right\} = Pr\{W_m < w_u\}$$
$$= 1-\left[\sum_{j=0}^{m-1}\binom{m-1}{j}(-1)^{j}\int_0^{\infty}\frac{v^{n-2}e^{-n\gamma v}(j+1)^{-1}}{\left[(j+1)(m/n)e^{vw_u}+\Gamma(1+v)\right]^{n}}dv\right]$$
$$\left[\sum_{j=0}^{m-1}\binom{m-1}{j}(-1)^{j}\int_0^{\infty}\frac{v^{n-2}e^{-n\gamma v}(j+1)^{-1}}{\left[\Gamma(1+v)\right]^{n}}dv\right]^{-1} = 1-\alpha \quad (30)$$

4. Examples of applications

4.1. Estimation of warranty period

For instance, consider the data of fatigue tests on a particular type of structural components (stringer) of aircraft IL-86. The data are for a complete sample of size $r = n = 5$, with observations (Table 1).

Tab. 1. The data of fatigue tests

Observations	*Time to crack initiation (in number of 10^4 flight hours)*
x_1	5
x_2	6.25
x_3	7.5
x_4	7.9
x_5	8.1

and results being expressed here in number of 10^4 flight-hours. On the basis of these data it is wished to estimate a lower 0.95 prediction limit on Y_1 in a group of $m = 5$ identical components (for a fleet of k=1 aircraft IL-86) which are to be put into service.

Goodness-of-fit testing. We assess the statistical significance of departures from the Weibull model by performing empirical distribution function goodness-of-fit test. We use the K statistic [2]. For censoring (or complete) datasets, the K statistic is given by:

$$K = \frac{\sum_{i=[r/2]+1}^{r-1}\left(\frac{ln(x_{i+1}/x_i)}{M_i}\right)}{\sum_{i=1}^{r-1}\left(\frac{ln(x_{i+1}/x_i)}{M_i}\right)} = \frac{\sum_{i=3}^{4}\left(\frac{ln(x_{i+1}/x_i)}{M_i}\right)}{\sum_{i=1}^{4}\left(\frac{ln(x_{i+1}/x_i)}{M_i}\right)} = 0.184 \quad (31)$$

where $[r/2]$ is a largest integer $\le r/2$, the values of M_i are given in Table 13 [2]. The reject region for the α level of significance is $\{K>K_{n;1-\alpha}\}$. The percentage points for $K_{n;1-\alpha}$ were given by Kapur and Lamberson [2]. For this example,

$$K=0.184 < K_{n=5;\,1-\alpha=0.95}=0.86 \quad (32)$$

Thus, there is not evidence to rule out the Weibull model.

The maximum likelihood estimates of unknown parameters β and δ are $\hat{\beta} = 7.42603$ and $\hat{\delta} = 7.9081$, respectively. It follows from (6) that:

$$Pr\{Y_1 > y_l;\mathbf{z}\} = Pr\left\{\hat{\delta}\,ln\left(\frac{Y_1}{\hat{\beta}}\right) > \hat{\delta}\,ln\left(\frac{y_l}{\hat{\beta}}\right);\mathbf{z}\right\} = Pr\{W_1 > w_l;\mathbf{z}\} =$$
$$= Pr\{W_1 > -8.4378;\mathbf{z}\} = \frac{0.0000141389}{0.0000148830} = 0.95 \quad (33)$$

and a lower 0.95 prediction limit for Y_1 is y_l=2.5549 ($\times 10^4$) flight hours, i.e., we have obtained the warranty period (or the time to the first inspection) equal to 25549 flight hours with confidence level $\gamma=1-\alpha=0.95$.

4.2. Planning in-service inspections

Let us assume that in a fleet of k aircraft there are km of the same individual structure components, operating independently. Suppose an inspection is carried out at time τ_j, and this shows that initial crack (which may be detected) has not yet occurred. We now have to schedule the next inspection. Let Y_1 be the minimum time to crack initiation in the above components. In other words, let Y_1 be the smallest observation from an independent second sample of km observations also from the distribution (1). Then the inspection times can be calculated recursively as:

$$\tau_{j+1} = \hat{\beta}\,exp(w_{j+1}/\hat{\delta}) \quad j\ge 1, \quad (34)$$

where τ_1 is a time of the first inspection, w_{j+1} is determined from:

$$Pr\{W_1 > w_{j+1}; W_1 > w_j, \mathbf{z}\} = \frac{Pr\{W_1 > w_{j+1};\mathbf{z}\}}{Pr\{W_1 > w_j;\mathbf{z}\}} = \frac{Pr\left\{\hat{\delta}\,ln\left(\frac{Y_1}{\hat{\beta}}\right) > w_{j+1};\mathbf{z}\right\}}{Pr\left\{\hat{\delta}\,ln\left(\frac{Y_1}{\hat{\beta}}\right) > w_j;\mathbf{z}\right\}}$$
$$= \left(\int_0^{\infty} v^{r-2}e^{v\hat{\delta}\sum_{i=1}^{r}ln(x_i/\hat{\beta})}\left(kme^{vw_{j+1}}+\sum_{i=1}^{r}e^{v\hat{\delta}\,ln(x_i/\hat{\beta})}+(n-r)e^{v\hat{\delta}\,ln(x_r/\hat{\beta})}\right)^{-r}dv\right) \quad (35)$$
$$\times\left(\int_0^{\infty} v^{r-2}e^{v\hat{\delta}\sum_{i=1}^{r}ln(x_i/\hat{\beta})}\left(kme^{vw_j}+\sum_{i=1}^{r}e^{v\hat{\delta}\,ln(x_i/\hat{\beta})}+(n-r)e^{v\hat{\delta}\,ln(x_r/\hat{\beta})}\right)^{-r}dv\right)^{-1} = 1-\alpha \quad j\ge 1$$

where:

$$Pr\{W_1 > w;\mathbf{z}\} = Pr\left\{\hat{\delta}\,ln\left(\frac{Y_1}{\hat{\beta}}\right) > w;\mathbf{z}\right\}$$
$$= \left(\int_0^{\infty} v^{r-2}e^{v\hat{\delta}\sum_{i=1}^{r}ln(x_i/\hat{\beta})}\left(kme^{vw}+\sum_{i=1}^{r}e^{v\hat{\delta}\,ln(x_i/\hat{\beta})}+(n-r)e^{v\hat{\delta}\,ln(x_r/\hat{\beta})}\right)^{-r}dv\right)$$
$$\times\left(\int_0^{\infty} v^{r-2}e^{v\hat{\delta}\sum_{i=1}^{r}ln(x_i/\hat{\beta})}\left(\sum_{i=1}^{r}e^{v\hat{\delta}\,ln(x_i/\hat{\beta})}+(n-r)e^{v\hat{\delta}\,ln(x_r/\hat{\beta})}\right)^{-r}dv\right)^{-1} \quad (36)$$

$\hat{\beta}$ and $\hat{\delta}$ are the MLE's of β and δ, respectively, and can be found from solution of (7) and (8), respectively.

But again, for instance, consider the data of fatigue tests on a particular type of structural components of aircraft IL-86: x_1=5, x_2=6.25, x_3=7.5, x_4=7.9, x_5=8.1 (in number of 10^4 flight hours) given in Table I, where $r=n=5$ and the maximum likelihood estimates of unknown parameters β and δ are $\hat{\beta} = 7.42603$ and

$\hat{\delta}$ = 7.9081, respectively. Thus, using (35) with τ_1=2.5549 ($\times 10^4$ flight hours) (the time of the first inspection), we have obtained the following inspection time sequence (see Table 2).

Tab. 2. The inspection time sequence

w_j	*Inspection time* τ_j *(×10⁴ flight hours)*	*Interval* $\tau_{j+1}-\tau_j$ *(flight hours)*
–	$\tau_0 = 0$	–
$w_1 = -8.4378$	$\tau_1 = 2.5549$	25549
$w_2 = -6.5181$	$\tau_2 = 3.2569$	7020
$w_3 = -5.5145$	$\tau_3 = 3.6975$	4406
$w_4 = -4.8509$	$\tau_4 = 4.0212$	3237
$w_5 = -4.3623$	$\tau_5 = 4.2775$	2563
$w_6 = -3.9793$	$\tau_6 = 4.4898$	2123
$w_7 = -3.6666$	$\tau_7 = 4.6708$	1810
$w_8 = -3.4038$	$\tau_8 = 4.8287$	1579
$w_9 = -3.1780$	$\tau_9 = 4.9685$	1398
⋮	⋮	⋮

5. Conclusions

The method of constructing prediction limits for future samples from a Weibull distribution introduced in this paper utilizes all the information in a sample, but since it involves the use of numerical integration, many may prefer to use this technique only in situations not readily handled by other of the methods described earlier. With modern computing, however, the conditional prediction limits are not difficult to calculate and should be recommended when the ability to do computations is available.

****

This research was supported in part by Grant Nr 06.1936 and Grant Nr 07.2036 from the Latvian Council of Science and the National Institute of Mathematics and Informatics of Latvia.

****

6. References

[1] Blischke W.R., Murthy D.N.P.: *Reliability*. New York: Wiley, 2000.

[2] Kapur K.C., Lamberson L.R.: *Reliability in Engineering Design*. New York: John Wiley and Sons, 1977.

[3] Mann N.R., Fertig K.W.: *Tables for obtaining Weibull confidence bounds and tolerance bounds based on best linear invariant estimates of parameters of extreme-value distribution*. Technometrics vol. 15, 1973, p. 87-101.

[4] Mann N.R., Schafer R.E., Singpurwalla N.D.: *Methods for Statistical Analysis of Reliability and Life Data*. New York: John Wiley and Sons, 1974.

Dr. sc. Konstantin N. NECHVAL
Applied Mathematics Department
Transport and Telecommunication Institute
Lomonosov Street 1, LV-1019 Riga, Latvia
konstan@tsi.lv

Dr. habil. sc. Nicholas A. NECHVAL
Dr. sc. Gundars BERZINS
Dr. sc. Maris PURGAILIS
Mathematical Statistics Department
University of Latvia
Raina Blvd 19, LV-1050 Riga, Latvia
nechval@junik.lv

Ewa MARECKA–CHŁOPEK
Zdzisław CHŁOPEK

POLLUTANTS EMISSION PROBLEMS FROM THE COMBUSTION ENGINES OF OTHER APPLICATIONS THAN MOTOR CARS

Following motor car combustion engines, more and more significance is being attached to the pollutants emissions from the engines other than used in motor cars. The scale and variety of applications of such engines are considerable. At present these engines are less modern than those from motor cars, and requirements posed for them are not as restrictive with regards environmental protection, as in the case of motorism. This paper analyzes assessment procedures for the pollutant emissions from the combustion engines of other applications than in motor cars. Influence of the engine operating conditions on the pollutants emission has been evaluated.

Keywords*: construction machines, combustion engines, pollutants emission.*

1. Introduction

The requirements posed for the combustion engines by the environmental protection are at present becoming their quality factors. Particular importance is being attached to the emission of the pollutants harmful for humans and the environment. Following the achievements in limiting pollutants emission from the motor cars engines, there is growing interest in the improvement of the ecological characteristics of the engines in other applications than motorcars. This practically concerns all types of applications of combustion engines, amongst them: ships, aircraft, diesel locomotives, construction, agricultural and forestry machines, as well as gardening and utility devices [1, 2, 5, 9 – 14].

Knowledge of combustion engines ecological characteristics with respect to their pollutants emission is required for three basic reasons.

First reason is the necessity to qualify the combustion engines to be introduced to commercial trading and into operation, from their environmental impact characteristics point of view. To this end there are type approval procedures being used, enabling to establish compatibility of the product with the formal requirements [3, 5].

Second reason for testing combustion engines pollutants emissions is the necessity to know their environmental characteristics in the conditions equivalent to the real operating ones. This is necessary to evaluate the combustion engines environmental impact and in particular to record pollutants emission from various civilisation sources. Numerous counties, including Poland are obliged, upon international agreements, to record pollutants emissions, amongst them: European Program CORINAIR (Coordinated Information on the Environment in the European Community) [3, 5].

The third reason is connected with the ability to objectively evaluate methods to improve combustion engines characteristics regarding pollutants emission. It is necessary therefore to work out methods of testing pollutants emission from the combustion engines in the conditions reflecting the real operating ones. This enables to evaluate these engines characteristics in the specific conditions they work in. [1 – 3, 4, 6 – 7, 9, 11 – 14].

At present, there are well developed methods of testing motor cars combustion engines [3, 5]. These methods have been verified as a result of testing programs such extended, that it is possible to formulate conclusions of a statistic nature. In the case of the engines of applications other than in the motor cars, as well as in the motor cars, but very specific, (such as urban buses), the methods of car engine testing often turn out however to be ineffective. Which justifies the interest in the topic, being the subject of this paper.

2. Methods of testing pollutants emissions from the combustion engines of applications other than in motorcars.

Pollutants emission from the combustion engines is closely dependent on conditions these engines are in [3, 8]. Engines operating conditions can be characterised by the following processes: thermal state, revolutions and values characterising load, most often the torque [3, 4, 6, 8 – 14]. Pollutants emission from the combustion engines strongly depends on the static work states, defined by the torque value and engine revolutions [3, 4, 6, 10, 11], as well as on the dynamic states occurring in the engine operating conditions [3, 8]. For those reasons, there are combustion engines testing methods being developed with regards the pollutants emission, both static and dynamic.

Static tests are easier methods of testing combustion. Engines technical requirements with respect of testing equipment, used with the engine test bench, are lower in this case [5, 8, 11]. For those reasons, in the earlier period of testing, practically only static methods were being developed. These tests were used for motor car engines. The thirteen phase test has been developed according to Regulation 49 UN–EEC (Economic Commission for Europe), known as ECE R 49 [3, 5]. As time went by, using experiences from testing car engines, there have been static tests developed to test combustion engines of other applications. Static tests for combustion engines are defined by giving value of phase coordinates in various points on the plane: Engine revolutions against torque and proportions (weight ratios) of those phases in the whole test [3, 5, 9, 11 – 13]. Tests are carried out for the thermally stabilised state of the engine.

Dynamic tests are defined by the revolutions – torque curve. To conduct them, there is engine test bench equipment needed, which enables loading the engine in the dynamic conditions. Additionally, the dynamic tests often include states of negative torque, reflecting braking with the engine, which requires propelling the engine. This poses additional demands for a bench

brake and its control system. For those reasons dynamic engine tests have been developed within the last few years: first dynamic tests were carried out in the United States in 1985. (HDDTT – Heavy Duty Diesel Transient Test and HDGTT – Heavy Duty Gasoline Transient Test) [3, 5, 11]. In Europe, first dynamic test of combustion engines was introduced in 2000. (ETC – European Transient Cycle), but it has been used for type approval processes only since 2005. [11]. For the engines of construction machines, first dynamic tests were developed only at the end of XX century by US EPA – United States Environment Protection Agency) [14]. The universal dynamic test have also been proposed for testing non–road machines, called NRTC (Non–road Transient Cycle). This test was also accepted by the European Union and introduced into testing procedures after 2005 [11].

Combustion engines' tests are defined in relative coordinates, related to values on the engine characteristics.

Relative speed is [4, 6, 11 – 13]:

$$n_w = \frac{n - n_{bj}}{n_N - n_{bj}} \tag{1}$$

where: n – speed, n_{bj} – minimal idling speed, n_N – nominal speed.

Relative torque for the engine n speed is being related to the torque on the engine characteristics for the same revs. [4, 6, 11 – 13]:

$$M_{ew} = \frac{M_e(n)}{M_{ez}(n)} \tag{2}$$

where: $M_e(n)$ – torque for the n speed, $M_{ez}(n)$ – torque on the engine characteristics for the n speed.

Relative useful power for the n speed. is defined as a ratio [11 – 13]:

$$N_{ew} = \frac{N_e(n)}{N_{ez}(n)} \tag{3}$$

where: $N_e(n)$ – useful power for the n speed, $N_{ez}(n)$ – useful power on the engine characteristics for the n speed.

Figure 1 shows ECE R 49 static test complying with Regulation 49.02 UN ECE. In the static tests presented on the diagrams, the areas of the circles are proportional to the share of each phase in the test.

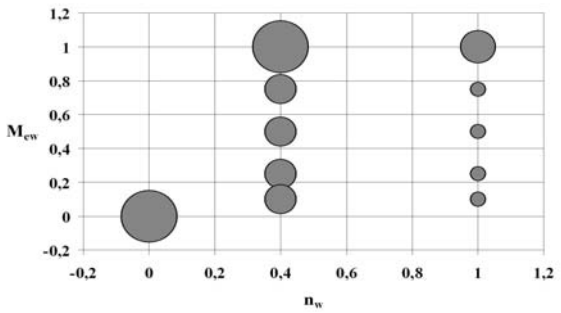

Fig. 1. Test ECE R 49

Test ECE R 49, being for years a standard one for testing pollutants emission from the motor car self ignition engines as well as engines powered by gas fuels, has become, (according to the ISO 8178–4 Standard), a basis for the synthesis of the static tests for the engines of other applications than motorcars [3, 5, 8, 11 – 13]. Points of this test define, so called universal test, marked as B test – Figure 2.

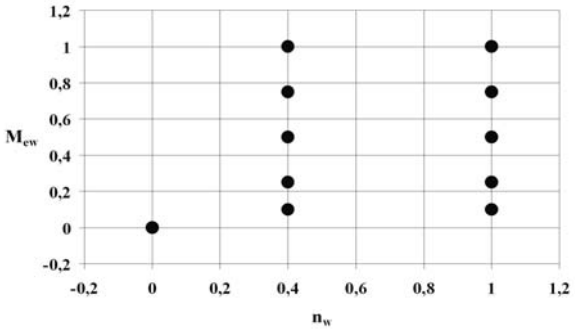

Fig. 2. Type B universal test according to ISO 8178–4 standard

In the universal test, the coordinates of measuring points are taken [3, 5, 8, 12, 13]:

- idling with minimal revolutions;
- nominal relative revolutions with loads of relative torque : 0,1; 0,25; 0,5; 0,75 and 1;
- intermediate relative revolutions with loads of relative torque : 0,1; 0,25; 0,5; 0,75 and 1; while the intermediate revolutions – n_p meets conditions:

$$\begin{aligned} &n_P = n_M, \quad \text{when} \quad n_M \in (0{,}6 \div 0{,}75)\, n_N \\ &\text{or} \quad n_P = 0{,}6\, n_N, \quad \text{if} \quad n_M < 0{,}6 \\ &\text{or} \quad n_P = 0{,}75\, n_N, \quad \text{if} \quad n_M > 0{,}75 \end{aligned} \tag{4}$$

Figures 3 and 4 show examples of static tests acc. to ISO 8178–4 standard. C1 test is designed for off road vehicles and self propelled off road machines powered by by self ignition engines. This test uses points from the universal test. E3 test is adapted for ships powered by highly loaded engines. Due to specifics of the ships main power plants operating conditions, the points of E3 test do not coincide (agree) with the universal test points, but are placed on the engine propeller characteristics.

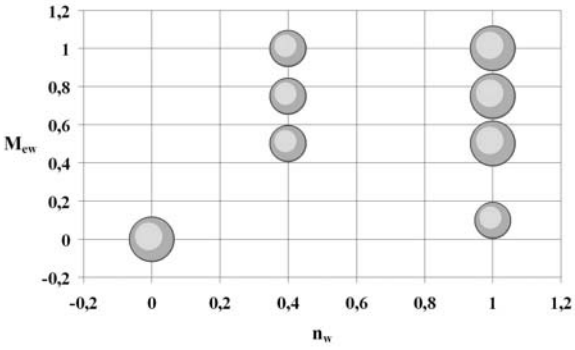

Fig. 3. C1 type test for off road vehicles and self propelled off road machines powered by self ignition engines

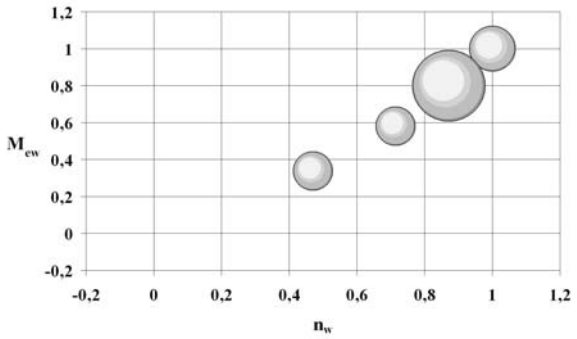

Fig. 4. E3 type test for ships powered by highly loaded engines

Dynamic tests are defined as time functions of relative revolutions and relative torque [3, 11, 14].

Figure 5 shows dynamic test – Agricultural Tractor Cycle (ATR) for testing agricultural tractor engines, developed in US EPA (Environment Protection Agency) [11, 14].

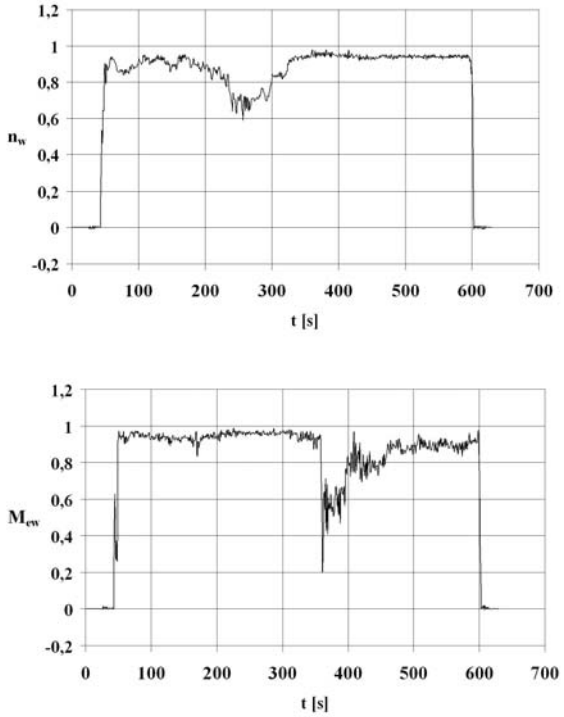

Fig. 5. Test Agricultural Tractor Cycle (ATR)

Figure 6 shows universal dynamic test – NRTC, for testing engines of none road machines.

Criterial values of assessing pollutants emission from the engines of the applications other than motorcars are specific brake pollutants emissions – "*e*", averaged in the tests [3, 5, 11 – 13]. Pollutants emission from the combustion engine is described by its mass – *m*. Specific brake pollutants emission is defined as a pollutants emission derivative of useful work – L_e [3, 5]:

$$e = \frac{dm}{dL_e} \tag{5}$$

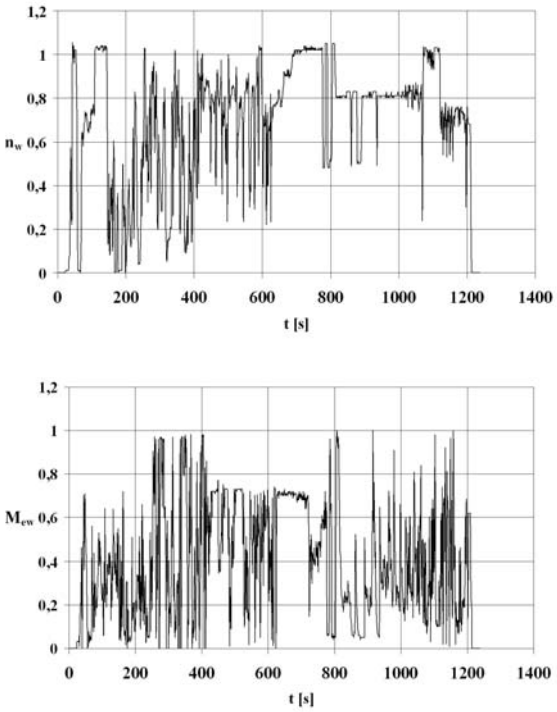

Fig. 6. NRTC test

Usually specific brake pollutants emission is obtained as an emission intensity derivative – *E* of useful power – N_e [3, 5]:

$$e = \frac{dE}{dN_e} \tag{6}$$

where: pollutant emission intensity is emission derivative of time – *t* [3, 5]:

$$E = \frac{dm}{dt} \tag{7}$$

Average specific brake pollutant emission, in the static tests, is defined using each test phase – u as [3, 5, 11]:

$$e = \frac{\sum_{i=1}^{K} E_i \cdot u_i}{\sum_{i=1}^{K} N_{ei} \cdot u_i} \tag{8}$$

where: *K* – number of test phases.

In the dynamic tests, average specific brake pollutants emission is calculated as [3, 5, 11]:

$$e = \frac{\int_0^{t_T} E \; dt}{\int_0^{t_T} N_e \; dt} \frac{1}{2} \tag{9}$$

where: t_T – test duration.

It has been accepted that the specific brake pollutants emission value is expressed in traditional measuring units, inconsistent with SI system, namely, grams per kilowatt, times an hour, written

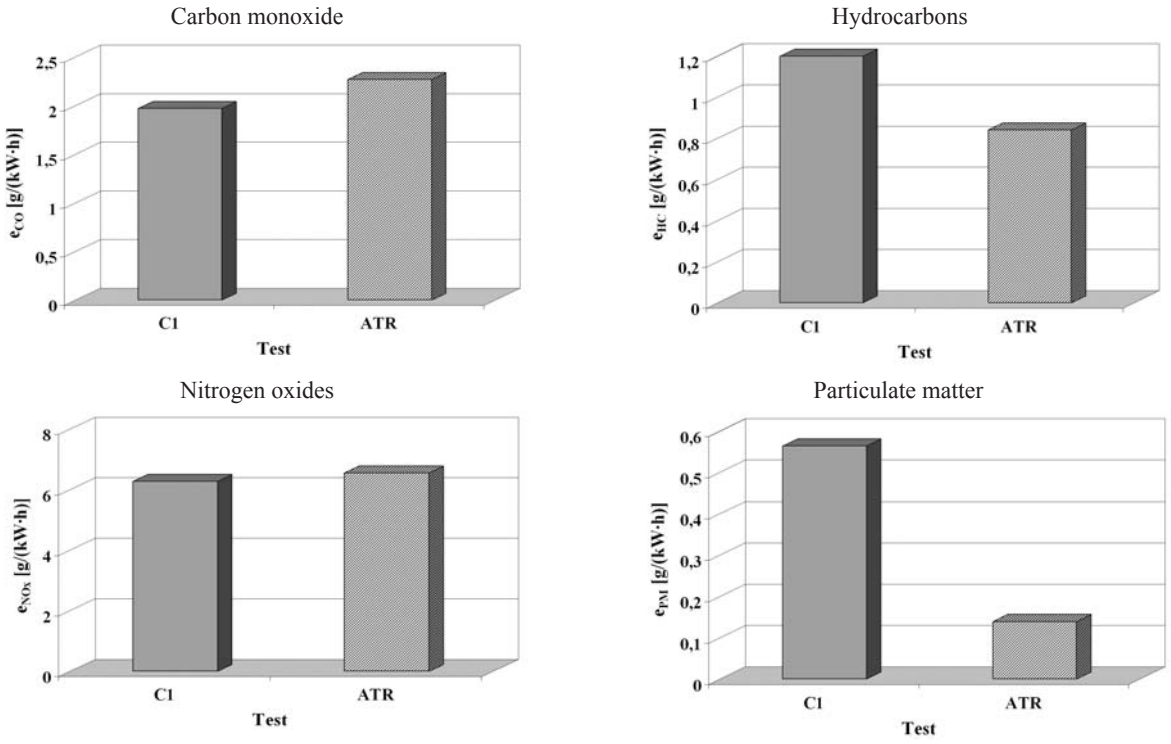

Fig. 7. Specific brake pollutants emissions in the tests: static C1 and dynamic ATR

correctly as – „g/(kW·h)", while in the legal acts and specialist literature, it usually appears in an incorrect form as – „g/kWh" [3, 5].

3. Results of pollutants emission simulation studies in the research tests

It has been accepted that pollutants emission simulation studies in research tests use mathematical model of a self ignition engine in a form of a vector function of pollutants intensity [7, 11]

$$\mathbf{c} = \mathbf{f}\left(n, M_e\right) \tag{10}$$

Vector "c" contains intensities of each pollutant in the exhaust gasses

$$c = \left[c_{CO}, c_{HC}, c_{NOx}, c_{PM}\right]^T \tag{11}$$

where: c_{CO} – carbon monoxide volumetric intensity in the exhaust gasses, c_{HC} – hydrocarbons volumetric intensity in the exhaust gasses, c_{NOx} – nitrogen oxides volumetric intensity in the exhaust gasses, c_{PM} – hydrocarbons mass intensity in the exhaust gasses.

Identification of the model parameters has been done as a result of empirical tests in the static conditions, according to the Box–Bekhen plan [11].

Procedures used to test agricultural tractors have been selected here as an example research tests: static C1 test acc. to ISO 8178 as well as dynamic – ATR. Values from the model (10) have been accepted for pollutants emission intensity simulation in both static and dynamic conditions.

Figure 5 shows specific brake pollutants emissions in the tests: static C1 and dynamic ATR.

Although tests C1 and ATR are envisaged for the same category of combustion engines, the results obtained differ significantly. This confirms great sensitivity of the pollutants emission to the engine static operating conditions. In the case of taking into account the differences in the pollutants emission form the engine in the dynamic conditions; even more distinct differences are to be expected [8].

4. Summary

The pollutants emissions matters from the combustion engines of various applications are becoming – like in the case of motor car applications – a priority subject, determining development of various machines and devices power plants. Existing testing methods refer usually to the type approval procedures and can – in case of engine applications, different than typical motor cars operation – be little effective to objectively evaluate the engine characteristics. This stems, first of all, from significant sensitivity of the ecological characteristics of engines to their operating conditions, with regards both static and dynamic states in their working environments. For those reasons, it is necessary – first of all to evaluate environmental impact – to test engine working conditions in the machines and devices, not limiting it to the qualifying test methods.

5. Bibliography

[1] California Air Resources Board: Off–Road Emissions Inventory Program. http://www.arb.ca.gov/.
[2] California Air Resources Board: On–Road Emissions Inventory Program. http://www.arb. ca.gov/msei/nonroad/.
[3] Chłopek Z.: *Modelling exhaust emission processes in the road vehicles combustion engines' operating conditions*. Scientific work. Seria „Mechanika" z. 173. Oficyna Wydawnicza Politechniki Warszawskiej. Warsaw 1999.
[4] Chłopek Z.: *About the equivalence criteria of the operating conditions and conditions of combustion engines testing*. Fourth International Symposium on Combustion Engines in Military Applications. Jurata 1999.
[5] Chłopek Z.: *Motor vehicles – Natural environment protection*. WKŁ. Warsaw 2002.
[6] Chłopek Z.: *Synthesis of the combustion engines static research tests*. PAN Oddział w Krakowie. Teka Komisji Naukowo–Problemowej Motoryzacji. Zeszyt 18. Kraków 1999.
[7] Chłopek Z., Piaseczny L.: *Application of experience planning theory in the ecological studies of the combustion engines characteristics*. Archiwum Motoryzacji 2–3/2002. 69 – 94.
[8] ISO 08178: „Reciprocating internal combustion engines – Exhaust emission measurement – Part 4: Test cycles for different engine applications".
[9] Chłopek Z., Rostkowski J.: *Analysis of the pollutants emission from the self ignition engines in the dynamic conditions*. Archiwum Motoryzacji 3/2003. 119 – 140.
[10] Kniaziewicz T., Merkisz J., Piaseczny L.: *Simulation of the ship engines real loads in their exhaust toxicity research tests*. PAN Oddział w Krakowie, Teka Komisji Naukowo–Problemowej Motoryzacji. Kraków 1999.
[11] Marecka–Chłopek E., Chłopek Z.: *Evaluation of the construction machines' combustion engines characteristics with regards the pollutants emission*. Przegląd Mechaniczny 6'07. 20 – 26.
[12] Marecka–Chłopek E., Chłopek Z.: *Synthesis of the combustion engines static research tests in the applications other than motor cars, with regards pollutants emission and fuel consumption*. Przegląd Mechaniczny 7'07.
[13] Marecka–Chłopek E.: *Analysis of the combustion engines static pollutants emission tests in the applications other than motor cars*. Przegląd Mechaniczny 8'07.
[14] US EPA Nonregulatory Nonroad Duty Cycles. August 1999.

Eng. Ewa Marecka–Chłopek
Institute of Mechanised Construction and Rock Mining
02–673 Warsaw, 6/8 Racjonalizacji Str., Poland
E–mail: e.marecka–chlopek@imbigs.org.pl

Prof. Ph. D. Eng. Zdzisław Chłopek
Warsaw University of Technology
02–524 Warsaw, 84 Narbutta Str., Poland
E–mail: zchlopek@simr.pw.edu.pl